Available online at www.sciencedirect.com
SCIENCE DIRECT®
Plant Physiology and Biochemistry 42 (2004) 49–55
Plant Physiology and Biochemistry
www.elsevier.com/locate/plaphy

Original article

Expression of the fission yeast cell cycle regulator *cdc25* induces de novo shoot formation in tobacco: evidence of a cytokinin-like effect by this mitotic activator

Petra Suchomelová [a,*], Denisa Velgová [a], Tomáš Mašek [b], Dennis Francis [c], Hilary J. Rogers [c], Angela M. Marchbank [c], Helena Lipavská [a]

[a] *Department of Plant Physiology, Faculty of Science, Charles University, Viničná 5, 128 44 Prague 2, Czech Republic*
[b] *Department of Genetics and Microbiology, Faculty of Science, Charles University, Viničná 5, 128 44 Prague 2, Czech Republic*
[c] *School of Biosciences, Cardiff University, P.O. Box 915, Cardiff CF10 3TL, UK*

Received 5 May 2003; accepted 14 October 2003

Abstract

During the last decade, the cell cycle and its control by cyclin-dependent kinases (CDKs) has been extensively studied in eukaryotes. The regulation of CDK activity includes, among others, its activation by Cdc25 phosphatase at G_2/M. However, within the plant kingdom studies of this regulation have lagged behind and a plant *cdc25* homologue has not been identified yet. Here, we report on the effects of transformation of tobacco (*Nicotiana tabacum* L., cv. Samsun) with fission yeast (*Schizosaccharomyces pombe*) *cdc25* (*Spcdc25*) on de novo plant organ formation, a process dependent on rate and orientation of cell division. On shoot-inducing medium (low 1-naphthylacetic acid (NAA), high 6-benzylaminopurine (BAP)) the number of shoots formed on internode segments cultured from transgenic plants was substantially higher than in the non-transformed controls. Anatomical observations indicated that the shoot formation process was accelerated but with no changes in the quality and sequence of shoot development. Surprisingly, and in contrast to the controls, when on root-inducing medium (high NAA, low BAP) cultured segments from transgenic plants failed to initiate hardly any roots. Instead, they continued to form shoots at low frequencies. Moreover, in marked contrast to the controls, stem segments from transgenic plants were able to form shoots even without the addition of exogenous growth regulators to the medium. The results indicate that *Spcdc25* expression in cultured tobacco stem segments mimicked the developmental effects caused by an exogenous hormone balance shifted towards cytokinins. The observed cytokinin-like effects of *Spcdc25* transformation are consistent with the concept of an interaction between cell cycle regulators and phytohormones during plant development.

Keywords: Auxin; *cdc25*; Cell cycle; Cytokinin; *Nicotiana tabacum*; Organogenesis; *Schizosaccharomyces pombe*

1. Introduction

Primordium initiation could be driven by a local increase in the rate of cell division or by a reorientation of the plane of cell division, followed by expansion and differentiation processes in the proliferating tissue [21,32]. Alternatively, bulging could be driven by local expansion of primordium initials [6,24], followed by division of expanded cells. Progression of dividing cells through the cell cycle is controlled by key enzymes: cyclin-dependent kinases (CDKs), the products of *cdc2*-like genes. There are at least three classes of CDK in plants, distinguished on the basis of their nucleotide sequences and timing of expression [3,11,16]. The expression of *cdc2*-like genes (such as *Arath;CDC2A;1*) can be influenced by many factors including plant growth regulators, mainly auxins and cytokinins. For example, the application of different cytokinins to intact *Arabidopsis* plants caused an increase in *Arath;CDC2A;1* expression in root pericycle and vascular parenchyma [10] and in the shoot apical meristem [3]. Prolonged exposure of intact roots to auxin and cytokinin resulted in an increase in cell number. Nevertheless, culti-

Abbreviations: BAP, 6-benzylaminopurine; CDK, cyclin-dependent kinase; IAA, 3-indolylacetic acid; ICK, cyclin-dependent kinase inhibitor; NAA, 1-naphthylacetic acid; PCR, polymerase chain reaction; RIM, root-inducing medium; RT-PCR, reverse transcriptase polymerase chain reaction; SIM, shoot-inducing medium.

* Corresponding author.
E-mail address: suchomel@natur.cuni.cz (P. Suchomelová).

doi:10.1016/j.plaphy.2003.10.010

vation with either cytokinin or auxin alone enhanced *Arath;CDC2A;1* expression without increased DNA synthesis and cell division [10] indicating that the acquisition of competence to divide requires triggering by both growth regulators.

The CDK activity is strictly dependent on the presence of a cyclin subunit. A number of cyclin classes have been identified in plants with the peaks of expression and degradation in different cell cycle phases. Like plant CDK, plant cyclin expression can be modulated by phytohormones (e.g. [3,7]).

In yeasts and animals, the CDK–cyclin complex activity is reversibly modulated by the presence of CDK inhibitors and by the action of specific inhibitory protein kinases (e.g. Wee1), activating protein kinases (cyclin-dependent activating kinases) and phosphatases (e.g. Cdc25) (e.g. [4,5,8,26]). In plants, CDK inhibitors (e.g. ICKs from *Arabidopsis* [12,33]) as well as CDK activating kinases (rice [9] and *Arabidopsis* [35]) and inactivating kinases (*wee 1*, maize [31] and *Arabidopsis* [29]) have already been cloned. However, a homologue to *cdc25*—in eukaryotes a universally present activating phosphatase—has not been fully identified in plants yet (e.g. [15,18,20]), despite the existence of a fragment of putative *cdc25* that has been amplified by PCR from maize and barley [27]. Nevertheless, plant mitotic CDKs contain tyrosine 15 that can be dephosphorylated by fission yeast Cdc25 and by cytokinin treatment [36], providing evidence of phosphoregulatory mechanisms operating on plant CDK complexes (for details see review of Mironov et al. [22]). The mechanism is further supported by identification of an antagonistic plant wee1 kinase [31].

In the absence of a plant homologue to *cdc25*, Bell et al. [1] raised questions about the regulation of the cell cycle and development by expressing the fission yeast version (*Spcdc25*) in tobacco (*Nicotiana tabacum* L., cv. Samsun) under the control of the 35S CaMV promotor. Nine independent transformants were obtained and *Spcdc25* expression was verified. Under in vivo, the transgenic plants showed changes in leaf morphology and in the onset and intensity of flowering and mitotic cells in the root meristems were smaller than wild type [1].

Clearly, both cytokinin treatment and Spcdc25 can dephosphorylate plant Cdc2 [36], and this transgene can induce changes in the development of tobacco plants [1,19,34]. In order to understand more fully the cross-talk between this cell cycle regulator and development, we intended to discover the extent to which *Spcdc25* could influence the classic hormone-dependent organogenic response of cultured tobacco explants.

Here, we present evidence that in tobacco *Spcdc25* does indeed stimulate shoot development not only in a treatment that favours shoot formation (high cytokinin-to-low auxin) but also under root-stimulating conditions (high auxin-to-low cytokinin) and most remarkably even without exogenous growth regulator treatment.

2. Results

Bell et al. [1] reported that tobacco transformed with fission yeast *Spcdc25* exhibited altered morphology and development compared with wild type. Here, we used four of those *Spcdc25* expressing lines and compared them with wild type under in vitro conditions. We confirmed the gross morphological differences compared to the control reported earlier: changed leaf morphology, restricted rooting and increased tendency to flower formation. However, more extensive appraisal of the transgenic plants proved to be difficult because of the complexity of the system. To overcome this difficulty we used a simplified system of de novo organ regeneration on stem internode segments enabling separate root or shoot formation to be examined on appropriate growth regulator treatments [28].

2.1. Enhanced shoot formation in the transformants on shoot-inducing medium

Organogenesis on shoot-inducing medium (SIM) was significantly different in cultured internode segments of the four independent *Spcdc25* expressing lines A, B, C and F compared with wild type. Clearly, the SIM induced shoot formation both in the wild type and the segments from transgenic plants but the latter exhibited a significantly greater number of buds (Fig. 1A, B). The frequency of shoots and shoot primordia was roughly three times higher on segments cultured from transgenic plants compared to the non-transformed wild type (Fig. 2).

2.2. Earlier formation of meristemoids in segments from transgenic plants

The initial morphological screening of shoot formation on SIM was carried out on internode segments that had been cultured for 21 days. A time course of shoot formation was obtained in a separate experiment by analysing cultures every 3 days from day 10 to day 21. This study indicated earlier shoot formation on the segments of transformed lines A and C compared with the controls (Fig. 3). On the 10 day of cultivation meristemoids were observed in transgenics A and C while virtually no such structures were observed in the controls at that time (Fig. 3).

The data on the total amount of meristematic structures support the results of morphological study, as the structure formation was more abundant in transformants during the whole period studied (Fig. 3). The evaluation of shoot primordium structure revealed no changes in quality and developmental sequence of shoot formation (data not shown).

2.3. Shoot formation is favoured in the transformants on RIM

Given the significant increase in the number of shoots that formed in transgenic segments on SIM, we wondered how

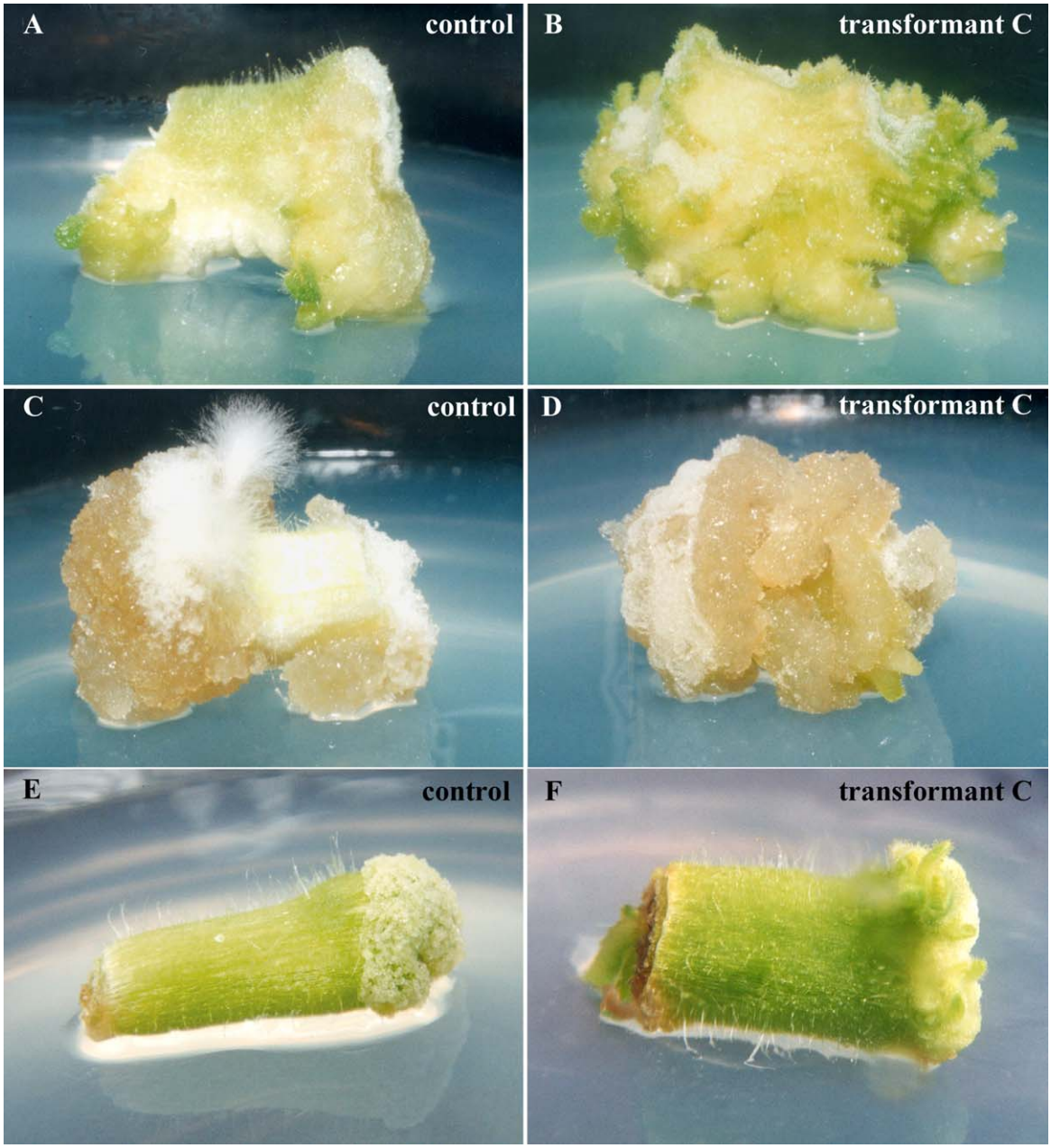

Fig. 1. Organ formation on tobacco internode stem segments of control and transformant C. Twenty-one days after the transfer to: A + B, SIM (MS medium with 0.1 mg l^{-1} NAA and 2.0 mg l^{-1} BAP); A, control; B, transformant C; C + D, RIM (MS medium with 3.0 mg l^{-1} NAA and 0.1 mg l^{-1} BAP); C, control; D, transformant C; E + F, basal MS (MS medium without growth regulators); E, control; F, transformant C.

morphogenesis would be affected in these transgenic segments when cultured on root-inducing medium (RIM). This treatment resulted in a predictable pattern of root morphogenesis in non-transformed controls. However, in the transformants a remarkable shift in the morphogenetic response was observed (Fig. 1C, D). There was a persistent formation of shoots albeit in low frequency in transgenics A, B, C and F accompanied by an extremely rare occurrence of root primordia (Fig. 4). Neither increasing the auxin concentration in the medium nor substituting 1-naphthylacetic acid (NAA) for 3-indolylacetic acid (IAA) resulted in a significant rise in root formation in the segments cultured from the transgenic plants (data not shown).

2.4. Shoots form in the absence of added cytokinins

Clearly, strengthened shoot formation was the prevalent phenotype exhibited by the cultured segments from the *Spcdc25* plants either on SIM or RIM. The next question was whether shoot formation could occur in the absence of exogenous cytokinin. Stem segments of all tested transgenic lines (A, B, C and F) did indeed exhibit shoot formation on the basal MS medium while shoot primordia were not observed in non-transformed control (Figs. 1E, F and 5).

The results were further supported by experiments of the same design using transformant Tx—the transgenics with *Spcdc25* under the tetracycline-inducible promotor (transfor-

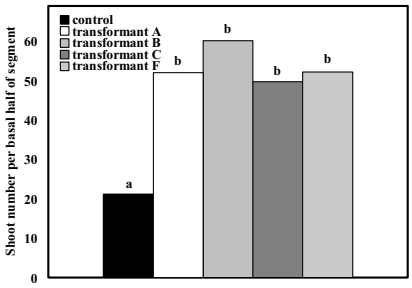

Fig. 2. Number of shoots and shoot primordia on segments of tobacco, SIM. Analysis was carried out on the basal halves of internode stem segments 21 days after the transfer to SIM. For each organ type significant differences are indicated by different letters ($n = 10$, $P < 0.05$). Averages and standard deviations: control, 21.2 ± 8.9; transformant A, B, C, F, 52.4 ± 7.7, 60.2 ± 13.3, 49.8 ± 12.0, 52.8 ± 14.2, respectively.

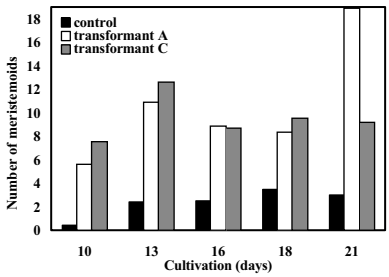

Fig. 3. Time course of shoot primordium formation on segments of tobacco, SIM. Analysis was carried out on the basal halves of internode stem segments cultivated on SIM. Number of meristemoids per 1-mm thick segment slice was counted.

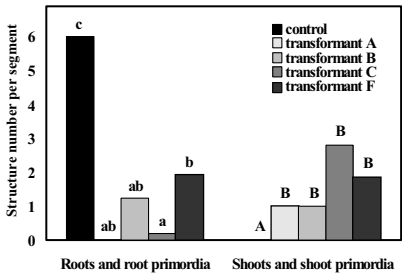

Fig. 4. Number of organogenic structures on segments of tobacco, RIM. Analysis was carried out on whole internode stem segments 21 days after the transfer to RIM. For each organ type significant differences are indicated by different letters ($n = 10$, $P < 0.05$); the small letters and the capital letters are used for statistical comparison of the numbers of root structures and shoot structures, respectively. Averages and standard deviations (roots): control, 6.0 ± 1.8; transformant A, B, C, F, 0.0 ± 0.0, 1.2 ± 0.3, 0.2 ± 0.3, 1.9 ± 0.8, respectively. Standard deviations (shoots): control 0.0 ± 0.0; transformant A, B, C, F, 1.0 ± 0.2, 1.0 ± 0.4, 2.8 ± 2.0, 1.8 ± 1.4, respectively.

mants were generated by McKibbin et al. [19]). On basal MS, the tetracycline application at the start of cultivation resulted 10 times higher shoot production in tetracycline-inducible segments compared to non-induced ones (Fig. 6). There were no significant differences among the controls including segments of wild type and inducible transformant on non-inducing (tetracycline-free) media and wild type on tetracycline-supplemented medium. The shoot number of controls was very low, 0–1 per segment in average (Fig. 6).

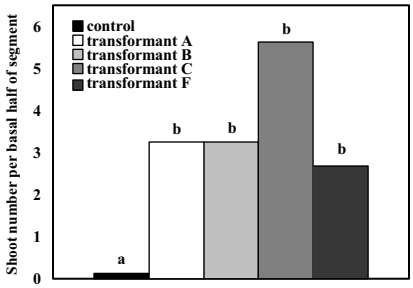

Fig. 5. Number of shoots and shoot primordia on segments of tobacco, basal MS medium. Analysis was carried out on the basal halves of internode stem segments 21 days after the transfer to the medium without growth regulators. For each organ type significant differences are indicated by different letters ($n = 10$, $P < 0.05$). Averages and standard deviations: control, 0.1 ± 0.1; transformant A, B, C, F, 3.2 ± 1.5, 3.2 ± 1.8, 5.6 ± 0.9, 2.7 ± 1.9, respectively.

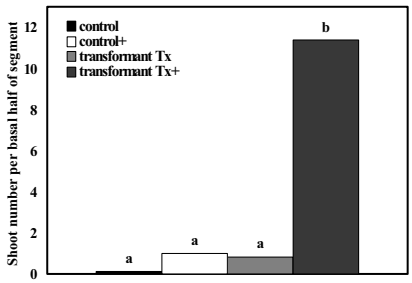

Fig. 6. Number of shoots and shoot primordia on segments of tobacco, basal MS medium. Analysis was carried out on the basal halves of internode stem segments 21 days after the transfer to the medium without growth regulators. Control, wild type non-treated with tetracycline and control+, wild type treated with tetracycline; transformant Tx, inducible transformant non-treated with tetracycline and transformant Tx+, inducible transformant treated with tetracycline. For each organ type significant differences are indicated by different letters ($n = 8$, $P < 0.05$). Averages and standard deviations: control, 0.1 ± 0.3; control+, 1.0 ± 0.7; transformant Tx, 0.8 ± 0.6; transformant Tx+, 11.3 ± 3.7.

Repeated transfer to a fresh medium containing tetracycline (every 3 days throughout the cultivation period) did not enhance the organogenic response in inducible transformed segments (data not shown).

In order to determine the timing of *Spcdc25* transcript accumulation in tetracycline-inducible transformants total RNA was isolated from internode stem segments of transformant Tx cultivated for 3, 7, 14 and 21 days on tetracycline-supplemented basal MS medium. As a non-induced control we used total RNA from segments cultivated 21 days on tetracycline-free medium. RT-PCR analyses were carried out using the modified protocol of McKibbin et al. [19]. *Spcdc25* transcripts were found in segments cultivated 3–14 days on tetracycline-supplemented medium (Fig. 7). No *Spcdc25* transcripts were detected in segments cultivated 21 days on tetracycline-supplemented medium as well as in segments cultivated 21 days on tetracycline-free medium (Fig. 7). The *Spcdc25* mRNA levels in tetracycline-induced segments were comparable to transcripts levels in *Spcdc25* constitutively expressing transformants A and C (data not shown). The results show that *Spcdc25* expression in trans-

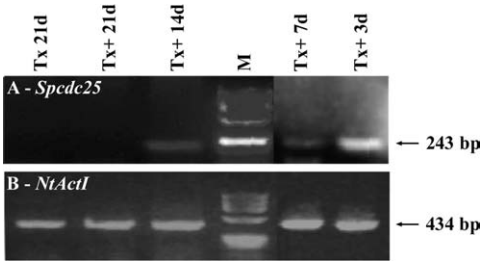

Fig. 7. Detection of *Spcdc25* transcript in transformant Tx segments. Electrophoretic separation of RT-PCR products of *Spcdc25* (A) and tobacco actin (*NtActI*) (B) transcripts. RNA was isolated from internode stem segments cultivated 3, 7, 14 and 21 days on tetracycline-supplemented basal MS medium. Non-induced control RNA was isolated from internode stem segments cultivated on tetracycline-free medium. Tx+ 3, 7, 14, 21 days, transformant Tx cultivated on tetracycline-supplemented medium for 3, 7, 14 and 21 days, respectively; Tx 21 days, transformant Tx cultivated on tetracycline-free medium for 21 days; M, DNA molecular weight marker IX (Roche).

formant Tx precedes organogenic response observed on the 21st day of cultivation on tetracycline-supplemented medium.

3. Discussion

Plant organ formation is known to be dependent on the rate, frequency and plane of cell division [21]. Hence, any interference with cell cycle regulation might result in changes in organogenic processes. This was confirmed when *Spcdc25* expression in tobacco resulted in a small cell size at division, and alterations in development [1,19]. Given the established links between cytokinins, *Spcdc25* and the cell cycle [36], and cytokinins and de novo shoot formation (see Section 1) we have explored the extent to which *Spcd25* could mimic the shoot-induction effect of cytokinins. The data presented here on the morphogenetic response of cultured internode segments of tobacco show, for the first time, that *Spcdc25* can induce shoot formation, over and above that in wild type on SIM, persistently on RIM where root initiation would be predicted, and most notably in a basal medium that lacked exogenous cytokinin and could not normally promote shoot initiation.

Clearly, the presence of Spcdc25 in tobacco results in a response, which is characteristic of a treatment where the exogenous hormone balance has been shifted towards cytokinins, thus creating a cytokinin-like effect. Could this be a cell cycle-related phenomenon? Riou-Khamlichi et al. [25] reported cytokinin-like effects of constitutive expression of G1/S cyclin (CycD3) in cell cultures of *Arabidopsis*. In CycD3 transgenics healthy calli can be induced and maintained for extended periods in the absence of exogenous cytokinin. These calli, however, were unable to regenerate shoots. As mentioned in Section 1, both Spcdc25 and cytokinin treatment resulted in dephosphorylation of plant CDK in suspension cultures of *Nicotiana plumbaginifolia* [36]. This led to the hypothesis that "plant-like" cdc25 may be regulated by a cytokinin-mediated signalling pathway [14]. Notably, when zeatin synthesis is partially inhibited by lovastatin (an inhibitor of mevalonic acid synthesis) in tobacco BY-2 cultures, cells are prevented from undergoing mitosis [17] but tobacco BY-2 cells expressing *Spcdc25* can overcome this block (C.B. Orchard et al., unpublished data). In relation to the results reported here on shoot formation in the absence of added cytokinins, perhaps *Spcdc25* compensates for the absence of a cytokinin-mediated regulation of the cell cycle, which then predisposes the formation of shoots. However, there was no apparent effect of *Spcdc25* on cell size in meristematic cells in the culture explants (data not shown). This is similar to the effect of ectopic expression of *Spcdc25* in leaves of tobacco; there were alterations in the number of cell layers in the leaf margin but there was not a pronounced effect on cell size [34]. In previous studies, mitotic cell size was characteristically smaller in *Spcdc25* transformants in: tobacco plants [1,19], tobacco BY-2 cells (Orchard et al., unpublished data) and *Arabidopsis* plants (Francis et al., unpublished data). Hence, *Spcdc25* can activate plant cells into mitosis at a reduced cell size, and clearly, it has been long known cytokinin treatment can promote the cell cycle progression (e.g. [36]). In our view, there is tangible, albeit circumstantial evidence, that links the cell cycle to a change in development in the cultured internode segments reported on here. Note that a reduced cell size effect was observed in roots of the original transgenic lines upon which the current work is based [1].

Given the hypothesised link between cell cycle activation, cytokinins and de novo shoot formation, we fully recognise that other interpretations are possible. Clearly, *Spcdc25* may be interacting with the tobacco genome in an unspecified way that indirectly shifts endogenous cytokinin biosynthesis in the cultured explants that leads to de novo organogenesis. Measurements of endogenous cytokinins in the *Spcdc25* transformants compared with wild type did not reveal any consistent trends (data not shown). This is perhaps unsurprising as the most recent models of cell cycle regulation feature cytokinin as active upstream of the plant cdc25-like phosphatase in CDK dephosphorylation.

Clearly, in the absence of a definitive plant homologue to *Spcdc25*, the possibility of a random transgene effect cannot be ignored but the presence of the phosphoregulatory residues T14 and Y15 in plant CDKs and the existence of the inhibitory Wee1 kinase (see Section 1) both strongly argue for a plant-like cdc25 phosphatase. Hence, despite some reservations, we favour a link between *Spcdc25*, the cell cycle, cytokinins and the induction of de novo shoot formation.

In conclusion, the recent models of plant cell cycle regulation propose direct cytokinin interaction with a hypothetical plant *cdc25* homologue in the G_2/M transition [30]. This concept corresponds well with the results presented here showing that transformation of tobacco with fission yeast *Spcdc25* can substitute for the cytokinin treatment in de novo organ formation. Nevertheless, other interactions, including

indirect ones must be taken into consideration that might involve spatially and temporarily restricted modifications of the endogenous hormone balance in favour of cytokinins, altered sensitivity of transformed material to auxin/cytokinin balance or alterations in other signal transduction pathway(s) leading to CDK activation.

4. Methods

4.1. Plant material

The experiments described here were undertaken on *N. tabacum* L., cv. Samsun, wild type, and four independent lines transformed with *cdc25* cDNA from *Schizosaccharomyces pombe* (*Spcdc25*) under the 35S CaMV promotor (originally designated lines A, B, C and F [1]) and tetracycline-inducible line designated here as transformant Tx (*tetR*$^+$ plants transformed with *cdc25* cDNA from *S. pombe* under the control of Tx promotor, for details see [19]).

4.2. Plant propagation

Both wild type and transgenic tobacco seeds were surface-sterilised and germinated on solid Murashige–Skoog (MS) medium [23] at 25 °C, 16 h photoperiod and at irradiance 240 μmol m^{-2} s^{-1}. The plant material was propagated using stem node segments with 6-week subcultivation intervals. One centimeter long stem internode segments were cut from the 6-week-old plants and transferred to MS media: with 0.1 mg l^{-1} NAA and 2.0 mg l^{-1} 6-benzylaminopurine (BAP) (SIM), with 3.0 mg l^{-1} NAA and 0.1 mg l^{-1} BAP (Sigma Aldrich) (RIM) or without plant growth regulators (basal MS). Tetracycline-treated segments were cultivated on basal MS medium modified to contain 5 mg l^{-1} tetracycline–HCl (Sigma Aldrich).

4.3. Morphological analysis

Samples were collected after 21 days and under a dissecting stereomicroscope the type and number of organs that formed were counted. Quantification was done on whole segments for material cultivated on RIM and on the basal halves of segments in all other cases. The term shoot primordium was used for a swelling on the internode segment that goes onto form a shoot apical meristem and vegetative leaves. A one-way ANOVA was used as the statistical analysis (Tukey–Kramer and Kruskal–Wallis tests, $P < 0.05$).

4.4. Time course of shoot formation on SIM

Segments cultivated on SIM were collected after 10, 13, 16, 18 and 21 days of cultivation. The samples were fixed in 50% FAA (50% ethanol/acetic acid/formaldehyde—18/1/1, v/v/v) and then serial longitudinal paraffin sections were prepared according to Johansen [13] and consecutively stained by nuclear fast red and alcian blue [2]. The number of morphogenetic structures was determined by plain estimation on basal halves of 70 sections (12.5 μm thickness) using a binocular stereomicroscope.

4.5. RT-PCR analysis of Spcdc25 expression

Total RNA was isolated from internode stem segments using the TRI-Reagent isolation protocol (Sigma Aldrich). The RNA integrity was checked by RNA denaturing agarose gel electrophoresis and quantified at OD_{260}. Fifteen micrograms of total RNA was treated with DNase I using a DNA-free kit (Ambion) in order to eliminate the genomic DNA contamination. Five micrograms of purified RNA was reverse transcribed by SuperScriptII RNAseH$^-$ Reverse Transcriptase (Invitrogen) according to the manufacturer's instructions. OligodT primer was used for cDNA synthesis. One to three microlitres of RT reaction was subjected to PCR amplification of *Spcdc25* templates using gene-specific primers (forward primer: 5′-TTAGGTCCCCTTCTCCG-ATG-3′; reverse primer: 5′-TCAATGAGTCCTCCTT-CACG-3′). PCR was carried out using High Fidelity PCR Master system according to Roche instructions. After 40 cycles of amplification (initial template denaturation, 94 °C 2 min, denaturation 94 °C 20 s, primer annealing, 53 °C 30 s, extension, 68 °C 1 min, final extension, 72 °C, 7 min), aliquots of the PCR samples were run on 2.5% TAE agarose gels and visualised by ethidium bromide staining. For comparison of cDNA synthesis efficiency, constitutively expressed transcripts of tobacco actin gene *NtActI* (accession number X63603) were detected in independent PCR reactions from RT samples using the same amplification conditions as for *Spcdc25* (forward primer: 5′-AAGCACC-TCTTAACCCGAAGG-3′; reverse primer: 5′-CACCGAT-GGTAATCACTTGACC-3′). In order to exclude the possibility that detected PCR products arose from DNA contamination, every experiment was supplemented by RT-PCR controls carried out in the same way but without the addition of reverse transcriptase. The identity of *Spcdc25* amplification products was checked by restriction fragment analysis.

Acknowledgements

We thank to Dr. Jana Albrechtová for the advice regarding the anatomical study, Dr. Luboš Daněk for photo-documentation, Dr. Martin Pospíšek for assistance in molecular analyses and Dr. Ivana Macháčková for preliminary measurements of cytokinin levels. The work was supported by the grants 88/1998/B and 149/2003/B of the Grant Agency of Charles University and by the grant LN A0081 of the Ministry of Education, Youth and Sports of the Czech Republic.

References

[1] M.H. Bell, N.G. Halford, J.C. Ormrod, D. Francis, Tobacco plants transformed with *cdc25*, a mitotic inducer gene from fission yeast, Plant Mol. Biol 23 (1993) 445–451.

[2] K. Beneš, M. Kamínek, The use of aluminium lake of nuclear fast red in plant material successively with alcian blue, Biol. Plant 15 (1973) 294–297.

[3] S. Burssens, M. VanMontagu, D. Inzé, The cell cycle in *Arabidopsis*, Plant Physiol. Biochem 36 (1998) 9–19.

[4] J. Correabordes, P. Nurse, p25 (Rum1) orders S-phase and mitosis by acting as an inhibitor of the p34 (Cdc2) mitotic kinase, Cell 83 (1995) 1001–1009.

[5] C. Featherstone, P. Russell, Fission yeast p107^{wee1} mitotic inhibitor is a tyrosine/serine kinase, Nature 349 (1991) 808–811.

[6] A.J. Fleming, S. McQueen-Mason, T. Mandel, C. Kuhlemeier, Induction of leaf primordial by the cell wall protein expansin, Science 276 (1997) 1415–1418.

[7] D. Francis, D.A. Sorrell, The interface between the cell cycle and plant growth regulators: a mini review, Plant Growth Develop 33 (2001) 1–12.

[8] K.L. Gould, S. Moreno, D.J. Owen, S. Sazer, P. Nurse, Phosphorylation at Thr 167 is required for *Schizosaccharomyces pombe* p34^{cdc2} function, EMBO J 10 (1991) 3297–3309.

[9] S. Hata, H. Kouchi, I. Suzuka, T. Ishii, Isolation and characterisation of cDNA clones for plant cyclins, EMBO J 10 (1991) 2681–2688.

[10] A.S. Hemerly, P. Ferreira, J. deAlmeida Engler, M. VanMontagu, G. Engler, D. Inzé, Cdc2a expression in *Arabidopsis* is linked with competence for cell division, Plant Cell 5 (1993) 1711–1723.

[11] A.S. Hemerly, P.C.G. Ferreira, M. VanMontagu, D. Inzé, Cell cycle control and plant morphogenesis: is there an essential link? Bioessays 21 (1999) 29–37.

[12] S. Jasinski, C. Riou-Khamlichi, O. Roche, C. Perennes, C. Bergounioux, N. Glab, The CDK inhibitor NtKIS1 is involved in plant development, endoreduplication and restores normal development of cyclin D3;1-overexpressing plants, J. Cell Sci 115 (2002) 973–982.

[13] D.A. Johansen, Plant Microtechnique, McGraw-Hill Book Co. Inc., New York, 1940.

[14] P.C.L. John, The plant cell cycle: conserved and unique features in mitotic control, in: L. Meijer, S. Guidet, L. Vogel (Eds.), Progress in Cell Cycle Research, vol. 2, Plenum Press, New York, 1996, pp. 59–72.

[15] P.C.L. John, K. Zhang, Cytokinin control of cell proliferation in plant development, in: D. Francis (Ed.), The Plant Cell Cycle and its Interfaces, Sheffield Academic Press, UK, 2001, pp. 190–211.

[16] J. Joubes, C. Chevalier, D. Dudits, E. Heberle-Bors, D. Inze, M. Umeda, J.P. Renaudin, CDK-related protein kinases in plants, Plant Mol. Biol 43 (2000) 607–620.

[17] F. Laureys, W. Dewitte, E. Witters, M. Van Montagu, D. Inzé, H. Van Onckelen, Zeatin in indispensable for the G2-M transition in tobacco BY-2 cells, FEBS Lett 426 (1998) 29–32.

[18] S. Laurie, N.G. Halford, The role of protein kinases in the regulation of plant growth and development, Plant Growth Develop 34 (2001) 253–265.

[19] R.S. McKibbin, N.G. Halford, D. Francis, Expression of fission yeast *cdc25* alters the frequency of lateral root formation in transgenic tobacco, Plant Mol. Biol 36 (1998) 601–612.

[20] T. Mészáros, P. Miskolczi, F. Ayaydin, A. Pettkó-Szandter, A. Peres, Z. Magyar, G.V. Horváth, L. Bakó, A. Fehér, D. Dudits, Multiple cyclin-dependent kinase complexes and phosphatases control G_2/M progression in alfalfa cells, Plant Mol. Biol 43 (2000) 595–605.

[21] E.M. Meyerowitz, Genetic control of cell division patterns in developing plants, Cell 88 (1997) 299–308.

[22] V. Mironov, L. De Veylder, M. Van Montagu, D. Inzé, Cyclin-dependent kinases and cell division in plants—the nexus, Plant Cell 11 (1999) 509–522.

[23] T. Murashige, F. Skoog, A revised medium for rapid growth and bioassays with tobacco tissue cultures, Physiol. Plant 15 (1962) 473–497.

[24] D. Reinhardt, F. Wittwer, T. Mandel, C. Kuhlemeier, Localized upregulation of a new expansin gene predicts the site of leaf formation in the tomato meristem, Plant Cell 10 (1998) 1427–1437.

[25] C. Riou-Khamlichi, R. Huntley, A. Jacqmard, J.A.H. Murray, Cytokinin activation of *Arabidopsis* cell division through a D-type cyclin, Science 283 (1999) 1541–1544.

[26] P. Russell, P. Nurse, *Cdc^{25+} functions as an inducer in the mitotic control of fission yeast, Cell 45 (1986) 145–153.*

[27] P. Sabelli, S.R. Burgess, A.K. Kush, P.R. Shewry, DNA replication initiation and mitosis induction in eukaryotes: the role of MCM and Cdc25 proteins, in: D. Francis, D. Dudits, D. Inzé (Eds.), Plant Cell Division, Portland Press, Colchester, UK, 1998, pp. 243–268.

[28] F. Skoog, C.O. Miller, Chemical regulation of growth and organ formation in plant tissues cultured in vitro, Symp. Soc. Exp. Biol 11 (1957) 118–131.

[29] D.A. Sorrell, A. Marchbank, K. McMahon, J.R. Dickinson, H.J. Rogers, D. Francis, A *WEE1* homologue from *Arabidopsis thaliana*, Planta 215 (2002) 518–522.

[30] H. Stals, P. Casteels, M. Van Montagu, D. Inzé, Regulation of cyclin-dependent kinases in *Arabidopsis thaliana*, Plant Mol. Biol 43 (2000) 583–593.

[31] Y. Sun, B.P. Dilkes, C. Zhang, R.A. Dante, N.P. Carneiro, K.S. Lowe, R. Jung, W.J. Gordon-Kamm, B.A. Larkins, Characterisation of maize (*Zea mays* L.) Wee1 and its activity in developing endosperm, Proc. Natl. Acad. Sci. USA 96 (1999) 4180–4185.

[32] T. Vernoux, D. Autran, J. Traas, Developmental control of cell division patterns in the shoot apex, Plant Mol. Biol 43 (2000) 569–581.

[33] H. Wang, L.C. Fowke, W.L. Crosby, A plant cyclin-dependent kinase inhibitor gene, Nature 386 (1997) 451–452.

[34] J. Wyrzykowska, S. Pien, W.H. Shen, A.J. Fleming, Manipulation of leaf shape by modulation of cell division, Development 129 (2002) 957–964.

[35] M. Yamaguchi, M. Umeda, H. Uchimiya, A rice homolog of Cdk7/MO15 phosphorylates both cyclin-dependent protein kinase and the carboxy-terminal domain of RNA polymerase II, Plant J 16 (1998) 613–619.

[36] K. Zhang, D.S. Letham, P.C.L. John, Cytokinin controls the cell cycle at mitosis by stimulating the tyrosine dephosphorylation and activation of p34cdc2-like H1 histone kinase, Planta 200 (1996) 2–12.

Available online at www.sciencedirect.com
SCIENCE DIRECT®
Analytical Biochemistry 336 (2005) 46–50
ANALYTICAL BIOCHEMISTRY
www.elsevier.com/locate/yabio

Denaturing RNA electrophoresis in TAE agarose gels

Tomas Masek[a], Vaclav Vopalensky[a], Petra Suchomelova[b], Martin Pospisek[a,*]

[a] Department of Genetics and Microbiology, Faculty of Science, Charles University in Prague, Viničná 5, 128 44, Prague, Czech Republic
[b] Department of Plant Physiology, Faculty of Science, Charles University in Prague, Viničná 5, 128 44, Prague, Czech Republic

Received 23 June 2004
Available online 5 November 2004

Abstract

Current methods of analytical RNA electrophoresis are based on the utilization of either complicated laboratory instrumentation or toxic, carcinogenic, or expensive chemicals. We suggest here the use of classical Tris–acetate–ethylenediamine tetraacetic acid (TAE) agarose gels combined with prior denaturation of RNA samples in hot formamide for the electrophoretic separation of RNA species. We present a brief comparison of the proposed TAE/formamide method with the most common 3-(*N*-morpholino)propanesulfonic acid/formaldehyde agarose gel protocol and show that both methods produce comparable results for size determination of RNA molecules and subsequent Northern blotting of gels. In addition to purified RNA samples, the robustness of the TAE/formamide protocol is demonstrated by its suitability for the analysis of RNA quality in crude yeast cell lysates containing large amounts of proteins, DNA, and other contaminating molecules. We therefore propose the TAE/formamide agarose electrophoresis as a rapid, simple, and cheaper alternative to current methods of RNA electrophoresis. Additionally, another benefit is the reduced exposure of laboratory personnel to hazardous chemicals.

Keywords: RNA; Electrophoresis; Northern blotting; Formamide

Detection and precise sizing of specific mRNAs continues to be a centrally important technique in molecular biology. Major improvements in RNA molecular weight determination were introduced by electrophoretic techniques that make use of gel matrixes such as polyacrylamide or purified agarose and advances in the understanding of the effects of secondary RNA structure and base pairing on RNA electrophoretic mobility. A number of different approaches have been used to establish a fully denaturing environment during electrophoresis with the aim of disrupting hydrogen bond formation to prevent imprecise estimation of RNA molecular weights. Many of these methods require complicated instrumentation or utilize toxic, carcinogenic, or expensive chemicals. An example of the former is the glyoxal/dimethyl sulfoxide gel technique, which requires a buffer recirculation system or frequent buffer changes due to the low buffering capacity of the running buffer [1–3]. The most powerful but the most expensive and the most toxic denaturing reagent used for RNA electrophoretic separations is methyl mercury hydroxide [4,5]. Among other denaturants employed for this purpose are urea [6,7], guanidine thiocyanate [8], formamide [9,10], DMSO[1] [11], and the most frequently used formaldehyde [12,13].

Each of these methods has some disadvantages. Urea and formamide are not suitable for use in agarose gels. Gels containing toxic and carcinogenic formaldehyde require extensive washing in a large excess of RNase-free

* Corresponding author. Fax: +420 221951724.
E-mail address: martin@natur.cuni.cz (M. Pospisek).

[1] *Abbreviations used:* TAE, Tris–acetate–EDTA buffer; Mops, 3-(*N*-morpholino)propanesulfonic acid; DMSO, dimethyl sulfoxide; Tris, Tris-[hydroxymethyl]aminomethane; EDTA, ethylenediamine tetraacetic acid; SDS, sodium dodecylsulfate; SSC, sodium saline citrate.

0003-2697/$ - see front matter © 2004 Elsevier Inc. All rights reserved.
doi:10.1016/j.ab.2004.09.010

water before staining with ethidium bromide and especially before subsequent Northern blotting. Moreover, formaldehyde influences the electrophoretic mobility of RNA molecules, and broadening and tilting of RNA bands has been described in cases when, in an attempt to lower the use of toxic reagents, different concentrations of formaldehyde in the gel and running buffers were used [14]. Difficulties of staining formaldehyde gels can be overcome by addition of ethidium bromide into the sample prior to electrophoresis, but this experimental approach causes a decrease of signal intensity after RNA transfer to nylon membranes and hybridization with specific probes [15].

We describe here a simple method employing the Tris–acetate–EDTA buffer (TAE) commonly used for DNA electrophoresis with denaturation of the sample in formamide prior to electrophoresis, thus minimizing exposure of the investigator to hazardous chemicals. We also suggest the use of this protocol as a rapid and inexpensive approach for checking the quality of RNA preparations before subsequent methods such as cDNA probe preparation for microarray hybridization, subtractive hybridization, or other methods and as an alternative approach to other rapid protocols for RNA quality control, replacing methods that require expensive or complicated equipment [16]. In addition to these kinds of applications, we also tested our method for its applicability in Northern blotting and RNA molecular weight determination in comparison to the most widespread method, which makes use of Mops/formaldehyde gel electrophoresis.

Methods

Total RNA was extracted from *Saccharomyces cerevisiae* W303 strain by the hot acid–phenol method [17] and from leaves of *Nicotiana tabacum* cv. Samsun using TRI reagent (Sigma) [18]. RNA samples were dissolved in RNase-free water and their concentration and purity were determined spectrophotometrically. Yeast cell lysates were prepared from *S. cerevisiae* W303 strain according to the protocol described by Kuhn et al. [19].

TAE/formamide electrophoresis was performed in 1.2% agarose gels containing 1× TAE buffer (0.04 M Tris–acetate, 1 mM EDTA) [20], which was also used as a running buffer. Immediately before electrophoresis, the RNA samples were successively mixed with deionized formamide in the amount giving a final concentration of at least 60% (v/v) formamide, with 1/10 sample volume of 10× loading dye (50 mM Tris–HCl, pH 7.6, 0.25% bromphenol blue, 60% glycerol) [20] and 1 μl of ethidium bromide water stock solution (1 mg/ml) (for sample volume ranging from 10 to 30 μl). The samples were then denatured by heating for 5 min at 65 °C, immediately chilled on ice for 5 min, and loaded on the gel. Electrophoresis was performed at a voltage gradient of 5 V/cm. Analysis of crude cell lysate samples was carried out by essentially the same method with exception that the 10× loading dye solution was supplemented with 1% SDS. RNA Ladder, High Range (Fermentas, SM0421) was used for the estimation of mobility of RNAs of known molecular weights. TAE buffer retains sufficient buffering capacity during the course of electrophoretic separation so that buffer exchange or recirculation is not required.

For comparison, electrophoresis was carried out in Mops/formaldehyde gels containing 2.2 M formaldehyde both in the gel and in the 1× Mops running buffer, essentially as described in [13,20]. The voltage gradient was also 5 V/cm. Other parameters of electrophoretic separation were as shown in individual experiments (see legends to figures). Photographs were taken and electrophoretic mobilities were estimated with help of 1D Image Analysis Software, version 3.6.1 (Kodak). Capillary transfer of the electrophoresed RNA samples to a positively charged nylon membrane (Roche) was performed in either 10× SSC [20] or in 8 mM NaOH according to the Chomczynski [21] protocol, except that 3 M NaCl was omitted from the blotting solution. ^{32}P-labeled probe of the yeast actin gene was prepared by random primer synthesis. Blotting and hybridization were carried out essentially according to Sambrook et al. [20].

Results and discussion

The analysis of gene expression by the estimation of particular RNA levels has become a widely spread method in the current postgenomic era. An increasing number of samples to be analyzed in high-throughput types of experiments together with increased attention paid to the safety of laboratory personnel compels researchers to develop faster, safer, less expensive, and more reliable methods.

Storage of RNA preparations in formamide has been described as a method of choice to ensure high RNA stability and protection against ribonucleases [22]. We tested the possibility of using such samples directly for electrophoretic separation and have found that the quality of RNA preparations can be reliably analyzed after high-temperature denaturation in agarose gels containing the commonly used TAE buffer without additional denaturing reagents. Although the resuspension of RNA samples in formamide is an excellent technique for storage purposes, such samples are not suitable for further enzymatic manipulations without purification. To be able to employ the present method for aqueous RNA suspensions, we examined the influence of increasing the in-sample formamide concentration on RNA separation in TAE agarose gel electrophoresis. Yeast total RNA preparations dissolved in water were mixed either with RNase-free water

or with an increasing amount of deionized formamide, giving final formamide concentrations of 0, 25, 50, 75, and 96%. We have found that additional rRNA bands, caused by incomplete denaturation of RNA, disappeared at formamide concentrations higher than 50% (Fig. 1A). Therefore we used at least 60% (v/v) formamide in samples in all subsequent experiments.

The resolving power of the TAE/formamide method, compared to that of the most commonly used Mops/formaldehyde protocol, can be seen in the results of electrophoretic separation of whole RNA preparations from tobacco leaves. It is clear that, even in the case of the more complicated sample from photosynthetically active plant tissue containing some additional bands of more abundant transcripts (Fig. 1B), both methods (TAE/formamide and Mops/formaldehyde) give comparably good resolution, sharp bands, and similar electrophoretic mobilities.

As documented in Fig. 1C, the slightly modified TAE/formamide protocol is also suitable for analyses of RNA in crude cell lysates containing large amounts of proteins, DNA, and other contaminating molecules. DNA is well separated under these conditions as well. We use this feature of the TAE/formamide method routinely for rapid checking of the quality of yeast cell lysates for polysomal profile analyses, but the present approach might be also useful for other applications such as testing of the quality of translation lysates, analysis of cross-linked protein–RNA complexes, or other techniques.

Frequently, the evaluation of RNA integrity by electrophoresis is not informative enough and blotting of separated RNAs with subsequent hybridization using specific probes is often used as an analytic tool. For that reason, we also tested the suitability of the TAE/formamide protocol for Northern blotting and hybridization by comparison of the compatibility of the TAE/formamide method and the Mops/formaldehyde protocol with two of the most frequently used blotting procedures: capillary transfer to a positively charged nylon membrane in SSC buffer or in a solution of NaOH. Our previous experiences indicate that the use of SSC buffer in a final concentration of 10× (instead of 20×) does not affect quality of capillary blotting. The apparent efficiency of transfer, which was estimated on blotted gels and membranes by visualization of ethidium bromide-labeled fluorescent RNA bands under UV light, was equal in all variants (results not shown). Fig. 2 shows an example of hybridization detection of actin mRNA in a total yeast RNA preparation. We have found the TAE/formamide method suitable for Northern blotting and compatible with capillary transfer both in 10× SSC and in 8 mM NaOH; it also gives results comparable to those of the Mops/formaldehyde protocol. The present results of actin mRNA detection agree well with our previous experience with Northern blotting and hybridization using the TAE/formamide protocol, which has been used in our laboratory with a variety of probes without any observed incomplete denaturation

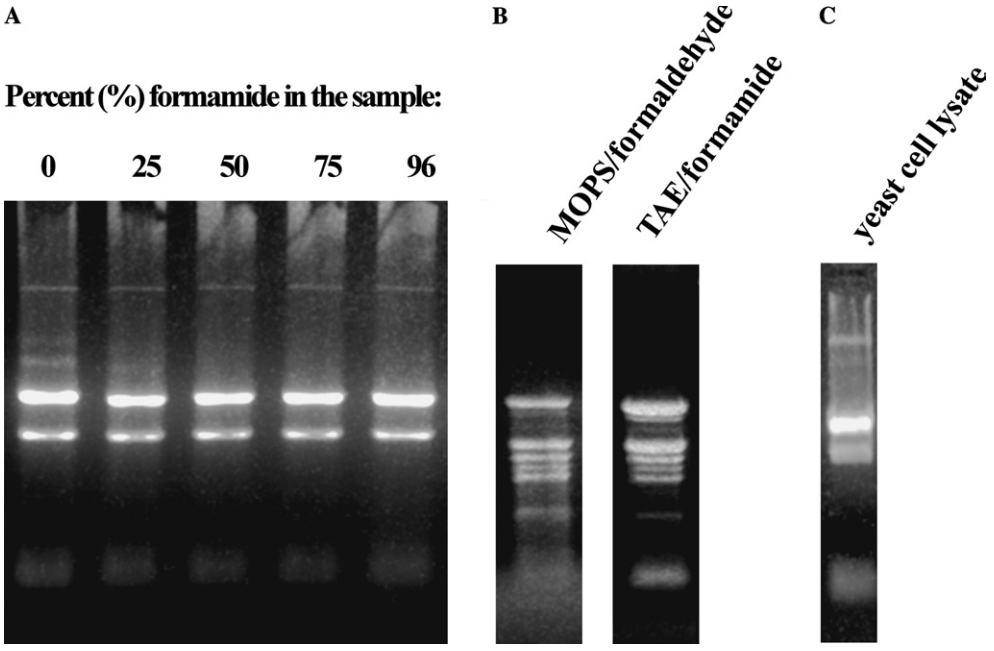

Fig. 1. RNA electrophoresis in 1× TAE buffer. (A) Influence of the in-sample formamide concentration on RNA denaturation. Yeast RNA dissolved in water (5 μg/μl) was mixed with deionized formamide to achieve a final concentration of formamide (v/v) of 0, 25, 50, 75, and 96%. (B) Tobacco leaf total RNA (6 μg) was separated using either TAE/formamide or Mops/formaldehyde electrophoresis. Concentration of denaturing agents in the sample was adjusted to 80% of formamide for the TAE/formamide protocol and to 60% of formamide and 25% of formaldehyde for the Mops/formaldehyde electrophoresis. (C) TAE/formamide method in crude cell lysates. Formamide was added to yeast cell lysate to achieve 60% of final concentration.

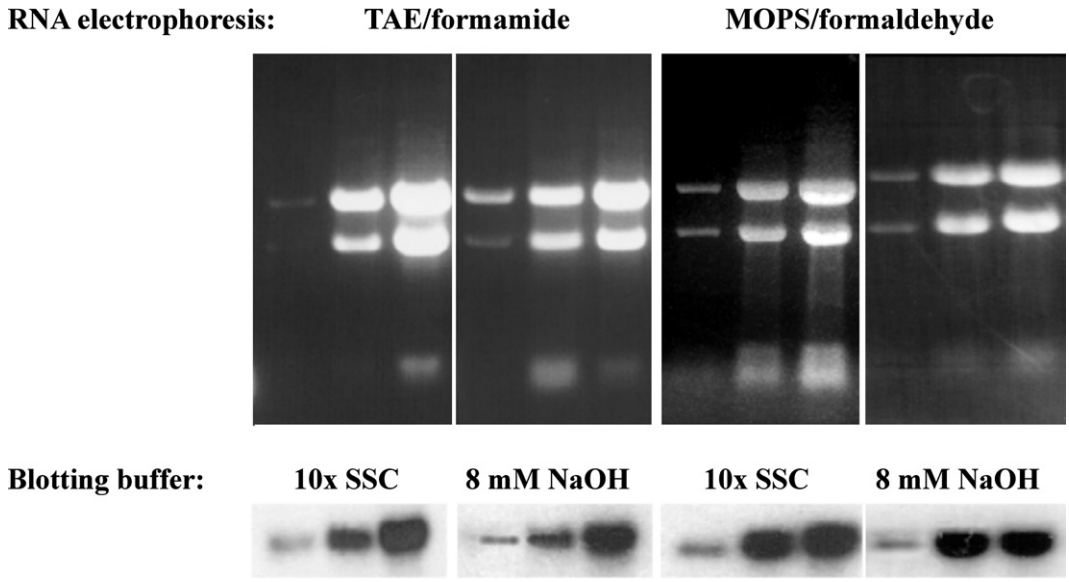

Fig. 2. Comparison of the efficiency of Northern blotting and the specificity of hybridization after TAE/formamide or Mops/formaldehyde agarose gel electrophoresis. Two, 10, and 20 μg of yeast RNA (5 μg/μl, in water) were loaded either on a 1× TAE gel (samples contained 0.4–4 μl of RNA, 18 μl of formamide, 1 μg of ethidium bromide, and 1× loading dye) or on a 1× Mops gel containing 2.2 M formaldehyde both in the gel and in the 1× Mops running buffer (samples contained 0.4–4 μl of RNA, 12.5 μl of formamide, 5 μl of formaldehyde, 1.25 μl of 20× Mops, 1 μg of ethidium bromide, and 1× loading dye). The efficiency of capillary transfer to positively charged nylon membrane was tested both in 10× SSC buffer and 8 mM NaOH. Hybridization was carried out with a ^{32}P-labeled probe of the yeast gene for actin.

of target RNA. Although we did not perform extensive studies on transfer and hybridization efficiency following both protocols of electrophoretic separation, the TAE/formamide protocol seemed to give more plausible results in Northern blotting of serial sample dilutions (Fig. 2). We suppose that, unlike the Mops/formaldehyde agarose gel electrophoresis, the TAE/formamide method does not suffer from an unequal lowering of hybridization signal intensity when smaller amounts of target mRNA are loaded on the gel. This phenomenon of a lowering of signal intensity in Northern blots has been described for Mops/formaldehyde gels when ethidium bromide is used for staining both before and after the electrophoresis [15].

We also analyzed the effect of the TAE/formamide protocol on RNA molecular weight determination (Fig. 3).

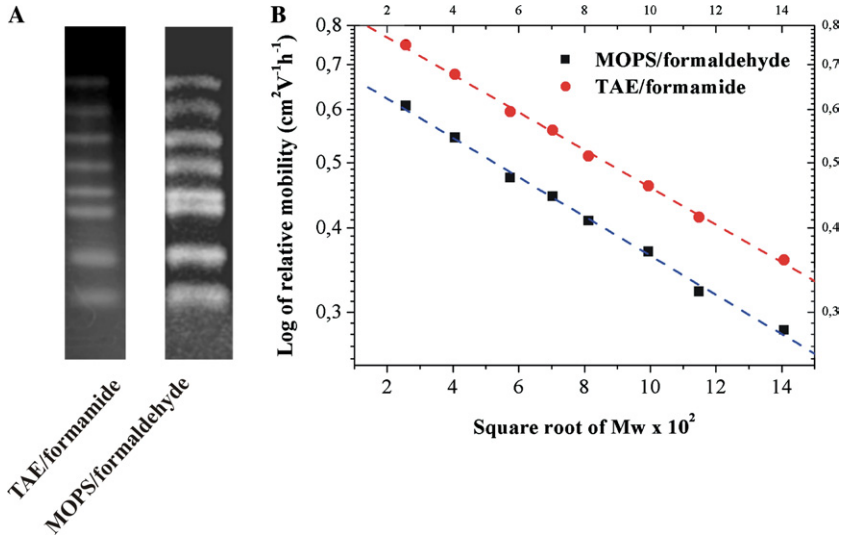

Fig. 3. Comparison of the influence of TAE/formamide and Mops/formaldehyde electrophoresis on molecular weight determination. (A) RNA ladder, (2 μg) (High range, Fermentas) containing eight discrete RNA species ranging from 200 to 6000 bp in length was loaded either on 1× TAE gel (75% formamide in the sample) or on Mops/formaldehyde gel (2.2 M formaldehyde both in the gel and in the running buffer, 50% of formamide and 25% of formaldehyde in the sample). Electrophoreses were run at the voltage gradient 5 V/cm. (B) Graph of dependence of log-relative mobility to square root of molecular weight.

We measured electrophoretic mobility of RNA species with known molecular weights ranging from 200 to 6000 nucleotides and observed that both electrophoretic systems (TAE/formamide and Mops/formaldehyde) produce RNA separation that demonstrates a linear dependence of log-relative mobility to the square root of molecular weights, confirming thus that the separated molecules are denatured to a similar extent in both systems and that the mobility of RNA molecules depends primarily on their molecular weights [12]. The observed slope of the lines and the differences in relative mobility of specific RNA species in the two gel systems demonstrate that while ensuring similar resolution to Mops/formaldehyde system, electrophoresis using the TAE/formamide method is more rapid under the same voltage gradient conditions (5 V/cm were used in both cases).

In summary, we have described here a method for analytical RNA electrophoretic separation in TAE agarose gels, which is useful for the rapid determination of quality of RNA preparations. The method can also be used for the detection and quantification of specific target RNA by Northern hybridization. The TAE/formamide protocol is more rapid, less expensive, more simple, and more compatible with chemicals and instrumentation generally used in DNA electrophoretical procedures than the majority of currently used protocols for denaturing RNA electrophoresis. The modified TAE/formamide protocol (Fig. 1C) can also be used for the detection of RNA integrity and analyses of RNA species in complex samples such as crude cell lysates containing proteins, DNA, and other contaminating molecules. Finally, the introduction of the TAE/formamide protocol minimizes the exposure of the investigator to hazardous chemicals: the use of formaldehyde is completely eliminated and formamide is used only in minute amounts.

Acknowledgments

We thank Vlasta Pelechova and Romana Puckova for technical assistance; K. Steven LaForge and Dana Hola for careful reading and editing of the manuscript; and the Czech Grant Agency (Grant No. 204/03/1487), the Grant Agency of Charles University (Grant No. 251/2004/B-BIO/PrF), and the Ministry of Education (Grant No. MSM 113100003) for financial support.

References

[1] J.M. Bantle, I.H. Maxwell, W.E. Hahn, Specifity of oligo(dT)-cellulose chromatography in the isolation of polyadenylated RNA, Anal. Biochem. 72 (1976) 413–427.

[2] G.K. McMaster, G.C. Carmichael, Analysis of single- and double-stranded nucleic acids on polyacrylamide and agarose gels by using glyoxal and acridine orange, Proc. Natl. Acad. Sci. USA 74 (1977) 4835–4838.

[3] P.S. Thomas, Hybridization of denatured RNA and small DNA fragments transferred to nitrocellulose, Proc. Natl. Acad. Sci. USA 77 (1980) 5201–5204.

[4] J.M. Baily, N. Davidson, Methylmercury as a reversible denaturing agent for agarose gel electrophoresis, Anal. Biochem. 70 (1976) 75–85.

[5] T.J. Sebo, J.C. Schmit, Analytical gel electrophoresis of high-molecular-weight RNA in acrylamide-agarose gels containing methylmercuric hydroxide, Anal. Biochem. 120 (1982) 136–145.

[6] R.W. Floyd, M.P. Stone, W.K. Joklik, Separation of single-stranded ribonucleic acids by acrylamide-agarose-urea gel electrophoresis, Anal. Biochem. 59 (1974) 599–609.

[7] G.W. Wertz, N.L. Davis, RNase III cleaves vesicular stomatitis virus genome-length RNAs but fails to cleave viral mRNAs, J. Virol. 30 (1979) 108–115.

[8] S.K. Goda, N.P. Minton, A simple procedure for gel electrophoresis and northern blotting of RNA, Nucleic Acids Res. 23 (1995) 3357–3358.

[9] J.C. Pinder, D.Z. Staynov, W.B. Gratzer, Electrophoresis of RNA in formamide, Biochemistry 13 (1974) 5373–5378.

[10] G. Spohr, M.-E. Mirault, T. Imaizumi, K. Scherrer, Molecular-weight determination of animal-cell RNA by electrophoresis in formamide under fully denaturing conditions on exponential polyacrylamide gels, Eur. J. Biochem. 62 (1976) 313–322.

[11] R.N. Skopp, L.C. Lane, Agarose gel electrophoresis of denatured RNA with silver staining, Anal. Biochem. 169 (1988) 132–137.

[12] H. Lehrach, D. Diamond, J.M. Wozney, H. Boedtker, RNA molecular weight determinations by gel electrophoresis under denaturing conditions, a critical reexamination, Biochemistry 16 (1977) 4743–4751.

[13] T. Maniatis, E.F. Fritsch, J. Sambrook, Molecular Cloning: A Laboratory Manual, Cold Spring Harbor Laboratory Press, Cold Spring Harbor, NY, 1982 pp. 202–203.

[14] S.S. Tsang, X. Yin, C. Guzzo-Arkuran, V.S. Jones, A.J. Davison, Loss of resolution in gel electrophoresis of RNA: a problem associated with the presence of formaldehyde gradients, BioTechniques 14 (1993) 380–381.

[15] B. Ogretmen, H. Ratajczak, A. Kats, B.C. Stark, Effects of staining of RNA with ethidium bromide before electrophoresis on performance of Northern blots, BioTechniques 14 (1993) 932–935.

[16] O. Mueller, S. Lightfoot, A. Schroeder, RNA integrity number (RIN)—standardization of RNA quality control, Agilent Application Note, Publication Number 5989- 1165EN, 2004, pp. 1–8.

[17] K. Köhrer, H. Domdey, in: Ch. Guthrie, G.R. Fink (Eds.), in: Guide to Yeast Genetics and Molecular Biology, Methods in Enzymology, vol. 194, Academic Press, San Diego, 1991, pp. 398–401.

[18] P. Chomczynski, N. Sacchi, Single-step method of RNA isolation by acid guanidinium thiocyanate phenol chloroform extraction, Anal. Biochem. 162 (1987) 159–159.

[19] K.M. Kuhn, J.L. DeRisi, P.O. Brown, P. Sarnow, Global and specific translational regulation in the genomic response of *Saccharomyces cerevisiae* to a rapid transfer from a fermentable to a nonfermentable carbon source, Mol. Cell. Biol. 21 (2001) 916–927.

[20] J. Sambrook, E.F. Fritsch, T. Maniatis, Molecular Cloning: A Laboratory Manual, Cold Spring Harbor Laboratory Press, Cold Spring Harbor, NY, 1989 pp. B23, 7.43–7.45, B13.

[21] P. Chomczynski, One-hour downward alkaline capillary transfer for blotting of DNA and RNA, Anal. Biochem. 201 (1992) 134–139.

[22] P. Chomczynski, Solubilization in formamide protects RNA from degradation, Nucleic Acids Res. 20 (1992) 3791–3791.

The fission yeast mitotic activator, *cdc25*, and sucrose induce early flowering synergistically in the day-neutral *Nicotiana tabacum* cv. Samsun

Martina Teichmanová[1], Petra Mašková[1], Petra Vojvodová[1], Jan Krekule[2], Dennis Francis[3], and Helena Lipavská[1]

[1] Department of Plant Physiology, Faculty of Science, Charles University, Viničná 5, 128 44, Prague 2, Czech Republic

[2] Institute of Experimental Botany, Academy of Sciences of the Czech Republic, Na Karlovce 1, 160 00, Prague 6, Czech Republic

[3]School of Biosciences, Cardiff University, PO Box 915, CF10, 3TL, UK

Author for correspondence*:* Helena Lipavská

Tel: +420 2 21951680, Fax: +420 2 21951704.

E-mail: lipavska@natur.cuni.cz

Total words count: 5908

Number of words:

Summary: 200

Introduction: 968

Material and Methods: 602

Results: 820

Discussion: 1280

Acknowledgements: 21

References: 1540

Tables and figure legends: 477

Summary

- The tobacco (*Nicotiana tabacum* L.) day-neutral (DN) cv. Samsun transformed with the *Schizosaccharomyces pombe* mitotic activator gene, *Spcdc25,* was used to study the onset of flowering.
- Wild type (WT) and cdc25 plants were grown from seeds *in vitro* until they were 20 cm high. Apical and basal nodes were then subcultured repeatedly and the regenerated plants were used to document time-to-flower and leaf number until flowering. Three sucrose treatments (3, 5 or 7% (w/v)) were used and measurements of leaf endogenous soluble carbohydrates were performed.
- In the 3% treatment, WT plants did not flower but cdc25 plants did. Also, the higher sucrose treatments enabled WT flowering; two thirds of the plants flowered at 5%, while all plants flowered at 7% sucrose. However, in all treatments, cdc25 plants exhibited significantly earlier flowering and yet further reductions in leaf number. Remarkably, a typical acropetal flowering gradient in WT plants did not occur in cdc25 plants. In cdc25 leaves, there were significantly higher amounts of endogenous sugars with a higher proportion of sucrose compared with WT.
- The data are consistent with a synergistic effect of exogenous sucrose and *Spcdc25* expression resulting in fewer leaves, and shortened flowering times.

Keywords: *cdc25* gene, cell cycle regulation, day neutral tobacco, flower induction, *Schizosaccharomyces pombe*, sucrose

Introduction

Many studies on flower initiation have made use of obligate photoperiodically sensitive plants offering the advantage of studying floral mechanism(s) with treatments that result in either 100% or zero flowering (Bernier, 1988; Machackova *et al.*, 1993; Lejeune *et al.*, 1994; Corbesier *et al.*, 2004). However, recently even more effort has been devoted to the facultative long day *Arabidopsis thaliana*. Here the disadvantage of a quantitative floral response is far out weighed by genetic approaches to the flowering problem using *Arabidopsis* as the model. Thus, much is now known about genes that regulate floral induction and about floral genes expressed in the shoot apical meristem (Boss *et al.*, 2004; Blazquez *et al.*, 2006). Meristem identity genes respond to the floral stimulus by switching the fate of the shoot apical meristem (SAM) from vegetative to floral. Among them, *LEAFY* (*LFY*) expression is necessary to specify a primordium as floral (Jack, 2004). These changes are followed by the expression of downstream organ identity genes that control the fate of the floral whorls.

Much less is known about the regulation of flowering in true day neutral plants (DN), that by definition, flower equally well under short day and long day conditions and in which *LFY* is expressed at similar levels in vegetative and floral meristems (Kelly *et al.*, 1995). Autonomous developmental events regulated by endogenous signals must prevail in this case (Bernier *et al.*, 1981; Mcdaniel, 1992; Bernier *et al.*, 1993). Pioneer work on day neutral plants established that flowering depended on the SAM acquiring floral competence as it passed from a juvenile to adult state. For example *Impatiens parviflora* flowered when the eighth leaf pair became vascularised (Hughes, 1965). Also, when juvenile scions of *Larix leptolepis* (Japanese larch) or *Larix decidua* (European larch), were grafted onto mature plants, and examined a year later,

only one out of 56 surviving scions flowered in Japanese larch but none of the European larch scions produced cones (Robinson & Wareing, 1969). Conversely, Lang (1965) argued that differences between juvenile and mature plants were due to the ability of a plant to attain the induced state and produce florigen. More detailed work established that DN tobacco flowered after initiating a specific number of leaves. If a SAM that had already produced 20 leaves, was cut at its stem base and replanted it made another 20 leaves before flowering, exactly the same number of leaves in plants that were left undisturbed (Dennin & Mcdaniel, 1985). Hence, the idea was that even if leaves of DN plants can make the floral stimulus regardless of day length, the SAM must become temporally competent to flower.

In DN plants, more apical leaves are more effective in inducing flowering than the basal ones near to the root system (Gebhardt & Mcdaniel, 1991). They hypothesised that a floral inhibitor produced by the root system was sufficient to prevent the SAM from making an inflorescence until further leaves were formed thereby displacing the SAM from the field of root inhibition (Gebhardt & Mcdaniel, 1991). So, the general picture is of a floral stimulus able to off set root-made inhibitors, by inducing flowering in developmentally competent SAMs.

Extensive grafting experiments in tobacco established that the floral stimulus is graft transmissible (Zeevaart, 1962; Chailakhyan & Khazakhyan, 1974b; Chailakhyan & Khazakhyan, 1974a; Lang, 1989). The continual failure to identify florigen led to the hypothesis that the floral stimulus is multicomponent and that sugars are one of important sub components (Bernier, 1988). In inducible plants, an inductive photoperiod can cause a rapid increase in sucrose levels in leaf exudates (Houssa *et al.*, 1991; Lejeune *et al.*, 1991) and in some cases, accumulation of sucrose in the SAM

97 (Bodson & Outlaw, 1985; Bernier *et al.*, 1993; Corbesier *et al.*, 1998). Interestingly, the
98 addition of sucrose can rescue the late flowering phenotype of several *Arabidopsis*
99 mutants (Roldan *et al.*, 1999). More recently discovered *FLOWERING LOCUS T (FT)*
100 encodes an mRNA that is transported from leaf to apex (Huang *et al.*, 2005). These data
101 are consistent with *FT* and sucrose as components of florigen (Aksenova *et al.*, 2006).
102 Floral SAMs become larger than vegetative SAMs, the increase being necessary
103 to accommodate all organs of each floral whorl (Nougarède *et al.*, 1987; Nougarède *et*
104 *al.*, 1991). This is achieved by cell division. For example, increase in the meristem size
105 upon receipt of the floral stimulus is the result of shorter cell cycles (Miller & Lyndon,
106 1976; Gegas & Doonan, 2006). Lang (1965) suggested that derepression of floral genes
107 in the SAM might require not only the arrival of the floral stimulus but also a
108 stimulation of DNA replication in the SAM. Moreover, in *Antirrhinum*, rapid bursts of
109 cell division in the floral meristem were suppressed in non-flowering *flo* mutants (*FLO*
110 is homologous to *Arabidopsis LFY*). It is suggested that developmental control genes
111 regulate cell division rates in the prefloral SAM (Vincent *et al.*, 1995; Doonan, 1998).
112 Previously, we showed that in tobacco, flowering occurred earlier (by about 30
113 days cf. WT) in T_0 tobacco plants expressing the *Schizosaccharomyces pombe* mitotic
114 inducer gene, *Spcdc25* (Bell *et al.*, 1993). However, this was not followed by a detailed
115 temporal study of time-to-flower in T_1 and their descendants. Our aim was to fill this
116 gap by undertaking a thorough analysis of flowering time in plants that developed from
117 cultured nodes of *Spcdc25* expressing plants (referred to from here on as cdc25 plants).
118 Also given several reports on sucrose as component of the floral stimulus, we examined
119 the effects of sucrose treatments on flowering and the levels of endogenous sucrose,
120 glucose and fructose in the leaves of WT and cdc25 plants.

The data reported here show that compared with WT, *Spcdc25* expression results in precocious flowering and a uniform floral response from both apical and basal nodes. Moreover, sucrose and *Spcdc25* expression shortened time-to-flower, synergistically.

Material and Methods

Plant material. *Nicotiana tabacum* L., cv. Samsun, wild type and transformed lines with *cdc25* cDNA from *Schizosaccharomyces pombe* under 35S CaMV promoter and nopaline synthase terminator (designated as line A and C) (Bell *et al.*, 1993).

Plant cultivation. Both WT and cdc25 seeds were surface sterilised and germinated on solid hormone-free MS medium (Murashige & Skoog, 1962) with 3% sucrose at 25°C, 16h photoperiod, irradiance 240 $\mu mol.m^{-2}.s^{-1}$. Three weeks after sowing *in vitro* on medium with 3% sucrose the young seedlings were transferred into large Erlenmeyer vessels with 3, 5, 7 or 9 % (w/v) sucrose concentrations. These plants were allowed to grow to a height of 20 cm. Two positionally different node segments (see diagram) now referred to as 1) basal - the second node without leaf, 2) apical segments - apex with leaves smaller than 2 cm - were then isolated and further cultivated on the MS medium with 3, 5, 7, or 9% sucrose. They were allowed to develop to the height of 20 cm again, then the basal segments (excised from plants derived from basal segments) and apical segments (excised from apical segment derived plants) were repeatedly subcultivated onto fresh medium. Time-to-flower was recorded as the time from transfer of 3-week-old seedlings weeks after sowing into large Erlenmeyer vessels until flower formation.

Root system evaluation. At the time of segment excision, which was carried out when the plants had grown to an approx. height of 20 cm, the whole root system was removed and weighed.

Non - structural saccharides (NSS) content determination. Samples of fully developed leaves from the 20-cm high plants of 60 mg fresh weight per sample were freeze-dried and homogenised, then they were boiled with 80% methanol, the solvent evaporated, and the residue dissolved in Milli-Q ultra-pure water (Millipore, Bedford, MA). The content of extracted soluble NSS was detected using high performance liquid chromatography (HPLC) with refractometric detection, column IEX Pb form (Watrex, Czech Republic). For details see (Lipavska *et al.*, 2000).

RT PCR analysis

Total RNA was isolated from one-month-old seedlings (control and transformant A and C) using the TRI-Reagent isolation protocol (Sigma Aldrich). The RNA integrity was checked by RNA denaturing agarose gel electrophoresis (Masek *et al.*, 2005) and quantified at λ=260 nm. 15 μg of total RNA was treated with DNaseI using a DNAfree kit (Ambion) in order to eliminate the genomic DNA contamination. 5 μg of purified RNA was reverse transcribed by SuperScriptII RNAseH$^-$ Reverse Transcriptase (Invitrogen) according to the manufacturer's instructions. Oligo dT primer was used for cDNA synthesis. 2 μl of RT reaction was subjected to PCR amplification of *Spcdc25* templates using gene-specific primers (forward primer: 5′-TTAGGTCCCCTTCTCCGATG-3′; reverse primer: 5′-TCAATGAGTCCTCCTTCACG-3′). PCR was carried out using High Fidelity PCR Master system according to Roche instructions. After 40 cycles of amplification (initial template denaturation, 94°C 2min, denaturation, 94°C 20s, primer annealing, 53°C 30s,

extension, 68°C 1min, final extension, 72°C 7min), aliquots of the PCR samples were run on 2,5% TAE agarose gels and visualised by ethidium bromide staining. For comparison of cDNA synthesis efficiency, constitutively expressed transcripts of tobacco actin gene *NtActI* (accession no. X63603) were detected in independent PCR reactions from RT samples using the same amplification conditions as for *Spcdc25* (forward primer: 5′-AAGCACCTCTTAACCCGAAGG-3′ reverse primer: 5′-CACCGATGGTAATCACTTGACC-3′). To exclude the possibility of DNA contamination, every experiment was supplemented by RT PCR controls without the addition of reverse transcriptase. The identity of *Spcdc25* amplification products was checked by restriction fragment analysis.

Statistical analysis. A one-way ANOVA was used for statistical comparison of data (Tukey-Kramer and Kruskal-Wallis tests, $P<0.05$). Different letters upon columns indicate statistically significant differences between means.

Results

Confirmation of Spcdc25 expression

We selected two independently transformed lines of cdc25 plants, A and C (Suchomelova *et al.*, 2004a; Suchomelova *et al.*, 2004b) and confirmed the expression of *Spcdc25* at the RNA level by RT-PCR. Line C exhibited a higher level of *Spcdc25* mRNA compared with line A (Fig. 1); this pattern of differential transcript levels was shown in several replicate experiments. The results are in accordance with more cytokinin-independent vegetative shoot formation in line C compared to line A (Suchomelova *et al.*, 2004b). Line C was used in subsequent experiments.

cdc25 plants flower precociously

When the experimental material was multiplicated *via* nodal segments, the flowering of cdc25 plants occurred and time to flower was progressively shorter with increasing number of subcultivations. Such a characteristic was found in both, A and C lines as well as in other two independently transformed lines (B, F) not used further in this study. In contrast, flowering has never been observed in control plants under the same conditions.

Thus the detail study of this phenomenon was performed with precisely defined plant segments. In the 3% sucrose treatment, cdc25 plants, regenerated from apical and basal segments, had time-to-flower of 233 and 208 days, and they initiated 65 and 53 leaves, respectively. However, WT did not flower on 3% sucrose even after 350 days, producing 155 and 233 leaves in basal and apical segments derived plants, respectively (Fig. 2 and 3). Both WT and cdc25 plants were subcultured repeatedly. After 350 days in culture, 20 cm high WT plants, that were the result of repeatedly subcultured apical or basal segments, were removed from the flasks. Remarkably, when grown in soil following acclimatisation, until flowering they formed the same number of leaves as WT plants grown naturally from seeds (Fig. 4).

***Spcdc25* and sucrose act synergistically**

In the 5% treatment, the plants derived from apical and basal segments of cdc25 plants, flowered after 182, and 174 days, respectively (Fig. 2) whilst mean leaf number decreased to 33.1 and 26.1, respectively (Fig. 3). Two thirds of WT flowered in the 5% treatment, with average times-to-flower of 231 and 303 days, respectively, while the total number of leaves was 60.8 and 91.3, respectively (Fig. 2 and 3). These flowering times were much longer compared with cdc25 plants in the 3 and 5% treatments.

Moreover, in cdc25 plants there was no significant difference between numbers of leaves formed and days-to-flowering in basal compared to apical nodes (Fig. 2 and 3). Hence an acropetal floral response in WT was abolished in the cdc25 plants.

In the 7% sucrose treatment, time-to-flower for cdc25 plants further decreased to 143 and 113 d whilst leaf number was only 22 and 19.2. WT derived from apical and basal segments flowered after 216.1 and 283.5 days, respectively (Fig. 2) and leaf number was 53.4 and 81.5 respectively (Fig. 3). Hence, in the 7% sucrose treatment, time-to-flowering was yet shorter in cdc25 plants compared with cdc25s at both 3 and 5% and was substantially shorter compared with WT in corresponding sucrose treatments. Increasing the sucrose from 5 to 7% had little impact on time-to-flower in WT. In WT, an acropetal flowering gradient was also evident under these conditions whilst cdc25 plants derived from apical and basal segments flowered equally well. Raising the sucrose concentration to 9% resulted in poor growth of plants, probably because of severe osmotic stress, which did not allow an evaluation of time-to-flower.

Overall, the data are consistent with a synergistic effect of *Spcdc25* expression and sucrose on the switch to flowering rather than a growth response that was simply proportional to increasing amounts of sucrose supplied to the SAM.

Root dry weight accumulation was lower in cdc25 plants.

In the 5% and 7% treatments, root dry weight was significantly lower in cdc25 plants compared with WT (Fig. 5). Repeated root removal, however, had no effect on flowering onset (our unpublished data). Hence, there was no correlation between inhibition of flowering and the presence of a root system.

Endogenous sugars were higher in cdc25 plants with higher sucrose/ hexoses ratio.

It was of further interest to assess the effect of increasing the concentration of exogenous sucrose on the endogenous levels of sucrose, glucose and fructose in the leaves (Fig. 6). Increasing exogenous sucrose from 3 to 5 % did not result in any significant difference in the levels of the water-soluble carbohydrates, sucrose, glucose and fructose either for WT or cdc25 plants. However in each treatment, the content of sugars was significantly higher in cdc25 plants with prevailing glucose and fructose in the spectrum. Also, whilst sucrose was detected in cdc25 plants at all three concentrations, it was barely detectable in WT. Preliminary data on WT and cdc25 cell suspension cultures, as well as greenhouse grown plants show similar changes in soluble carbohydrate characteristics (our unpublished data) and hence the results are not consistent with a simple correlation between sugar status and growth characteristics.

Discussion

Spcdc25 expression results in reduced time-to-flower, and a decreased rate of leaf initiation. Moreover *Spcdc25* expression and increasing exogenous sucrose had a synergistic effect in shortening time-to-flower as well as reducing the leaf number formed until flowering. In fission yeast, *Spcdc25* phosphatase dephosphorylates Cdc2 at G2/M enabling cells to enter mitosis (Nurse, 1990). Expression of *Spcdc25* induces a small cell size in the root meristems of tobacco plants (McKibbin *et al.*, 1998), in tobacco BY-2 cells (Orchard *et al.*, 2005) and in epidermal cells in root meristems of *Arabidopsis* plants (Francis D., unpublished data). In *Nicotiana plumbaginifolia*, *Spcdc25* can dephoshorylate plant CDK at G2/M (Zhang *et al.*, 2005). Moreover, *Spcdc25* expression shortens G2 phase of the BY-2 cell cycle through a premature peak

263 of CDKB-kinase activity and bypasses a cytokinin requirement at G2/M (Orchard *et al.*,
264 2005). Hence, *Spcdc25* functions as a mitotic inducer in the plant cell cycle and
265 recognises G2/M CDK(s) as substrates. Given this evidence, we do not propose that
266 *Spcdc25* is operating any differently in the cdc25 plants studied in the current work.
267 An increase in the rate of DNA replication and mitosis has long-been regarded
268 as a neat mechanism for an efficient transduction of the floral stimulus into SAM cells
269 (Zeevaart, 1962; Lang, 1965; Ormrod & Francis, 1986). Also, acceleration of cell
270 division in the shoot apical meristem is a very early event of the floral transition, which
271 proceeds by many hours the earliest growth changes affecting the initiation of the first
272 reproductive structures (Bernier, 1988; Jacqmard *et al.*, 2003). We suggest that *Spcdc25*
273 induces more cells to enter the mitosis in DN tobacco SAMs.
274 Nutritionally, localised synthesis of cytokinins can turn leaves from source to
275 sink (Hartig & Beck, 2006). Note, *Spcdc25* expression can replace cytokinins to induce
276 vegetative shoot formation in *de novo* organogenesis (Suchomelova *et al.*, 2004b), it can
277 replace a cytokinin treatment that culminates in CDK dephosphorylation (Zhang *et al.*,
278 2005) and it can replace a cytokinin requirement for mitosis (Orchard *et al.*, 2005).
279 These data are all consistent with *Spcdc25* expression, at least partly replacing a critical
280 cytokinins (another component of multifactorial flowering model) requirement to
281 establish florally competent SAMs. The close link between increased rates of cell
282 division and *FLO* expression in *Antirrhinum* (Vincent *et al.*, 1995) also argue for earlier
283 expression of meristem identity genes in cdc25 plants.
284 In DN plants, time to flower is affected by a balance between floral stimulus
285 from leaves and possible inhibitors from the root and the time taken for SAMs to
286 become florally competent (Tran Thanh Van, 1973; Tran Thanh Van *et al.*, 1974;

McDaniel *et al.*, 1996). Thus premature flowering in cdc25 plants could be because of strengthened floral stimulus or earlier floral competence, or both. We reject the idea of root inhibition of flowering in the plants reported on here because cdc25 plants flowered early regardless of the presence of a root system.

If the floral stimulus is strong enough and transmitted regardless of developmental time, then flowering of plants soon after germination might be predicted providing the SAM was florally competent. Apart from *Pharbitis nil* and *Chenopodium amaranthe* (Machackova *et al.*, 1993) most plants pass a juvenile-to-mature phase before flowering can occur. Here, cdc25 plants have a shortened time-to-flower, which requires the SAM to acquire floral competence more rapidly than WT. In cdc25 plants, that were repeatedly sub cultured on 3% sucrose, time to flower was progressively shorter.

In photoperiod-sensitive plants, carbohydrates have a critical function in the floral transition (Corbesier *et al.*, 1998; Roldan *et al.*, 1999). However, reports dealing with influence of carbohydrates on flowering in DN plants are rather scarce, e.g. in tobacco (Konstantinova *et al.*, 1972; Konstantinova *et al.*, 1976) and in tomato (Dielen *et al.*, 2004). Tran Than Van (1973) studying tobacco showed that epidermal thin layers (ETLs) from floral plants could make floral buds in culture but ETLs from vegetative plants would only form vegetative buds. Our results are distinctly different because in cdc25 plants, nodal segments flowered regardless of the developmental state of plants. Again, this all points to cdc25 plants developing early floral competence.

The determination of endogenous carbohydrate levels in leaves revealed that cdc25 plants have higher concentrations of glucose and fructose compared to WT whilst sucrose was detected in cdc25 plants it was barely detectable in WT. Therefore, it is

311 also necessary to consider endogenous sugar amounts and their contribution to
312 flowering in cdc25 plants. Whether the role of sugars in DN plants is a morphogenetic
313 signal or just a nutritive one is an on-going debate. Several authors reported dramatic
314 increases in the fluxes of sucrose reaching the apex after induction in photoperiodic
315 plants. As this change long preceded any morphological events, they suggest a message-
316 like role of sucrose in flowering (Lejeune *et al.*, 1993; Corbesier *et al.*, 1998; Dielen *et*
317 *al.*, 2001). Essentially this was also a conclusion drawn from flowering responses of
318 *Pharbitis nil* in culture (Durdan *et al.*, 2000; Parfitt *et al.*, 2004).

319 Roldán *et al.* (1999) proposed that sucrose could promote flowering by regulating
320 the expression of the flowering repressor *FLC,* a key regulator of the autonomous
321 flowering regulatory pathway (Putterill *et al.*, 2004), and probably also of day-length
322 controlled ones (Noh *et al.*, 2004). Note that *Spcdc25* expression and exogenous sucrose
323 had an additive effect in shortening time-to-flower. Knowing the extent to which this
324 mitotic activator stimulated cell division in SAMs would be very worthwhile. In DN
325 tobacco, *Spcdc25* expression could replace a cytokinin signal that normally induced
326 vegetative buds in culture (Suchomelova *et al.*, 2004b). Hence parallel cytokinin-
327 induced signalling for increased sucrose supply to the SAM at one level, and cytokinin-
328 induced cell division at another would be central to acquisition of floral competence. In
329 support of this, cdc25 cultures (line C) exhibited lower cytokinin content compared to
330 WT (our unpublished data).

331 The cdc25 plants have less developed root systems when evaluated on a dry
332 weight basis, which would lessen levels of putative floral inhibitors from the root (Fig.
333 5). This might be why the acropetal flowering response present in WT was abolished in
334 cdc25 plants. But as discussed above, cdc25 plants flowered equally well with or

without a root system. In addition, the rate of leaf initiation was slower in cdc25 plants compared with WT under our given experimental conditions (Tab.1). Thus earlier flowering in cdc25 plants cannot be ascribed to faster growth rates of above ground regions.

Surprisingly, acropetal floral potential (Mcdaniel & Hartnett, 1993) observed when younger as opposed to older nodes were cultured, was not evident in cdc25 plants (Fig. 2 and 3). A consensus view is that the floral gradient results from integrated signals of numerous chemical components. Using a late flowering mutant *uniflora* (Dielen *et al.*, 2001) identified sucrose, cytokinins and nitrogenous nutrients that promoted the floral transition in day-neutral tomato. Moreover, the C:N ratio in phloem sap increased during inductive treatments and the inequality in C/N supply may be important at floral transition in *Sinapis alba* and *Arabidopsis* (Corbesier *et al.*, 2002). Much more sucrose was detected in the leaves of cdc25 plants but hexoses were the most abundant water-soluble carbohydrates.

We report for the first time that *Spcdc25* expression and increased sucrose supply act synergistically to cause early flowering. We suggest that expression of *Spcdc25* in the SAM renders it cytokinin autonomous, as it does in tobacco cells in culture (Orchard *et al.*, 2005) as well as in *de novo* shoot formation (Suchomelova *et al.*, 2004b) and that sucrose interacts with a florally competent SAM. *In planta*, we further hypothesise that in cdc25 plants, the SAM has an enhanced rate of cell division, which is very important aspect of the SAM acquiring competence to flower.

Acknowledgements

The work was supported by grants No. 133/2000 and 207/2005 of the Grant Agency of the Charles University, Czech Republic.

References:

Aksenova NP, Milyaeva EL, Romanov GA. 2006. Florigen goes molecular: Seventy years of the hormonal theory of flowering regulation. *Russian Journal of Plant Physiology* **53**(3): 401-406.

Bell MH, Halford NG, Ormrod JC, Francis D. 1993. Tobacco Plants Transformed with Cdc25, a Mitotic Inducer Gene from Fission Yeast. *Plant Molecular Biology* **23**(3): 445-451.

Bernier G. 1988. The Control of Floral Evocation and Morphogenesis. *Annual Review of Plant Physiology and Plant Molecular Biology* **39**: 175-219.

Bernier G, Havelange A, Houssa C, Petitjean A, Lejeune P. 1993. Physiological Signals That Induce Flowering. *Plant Cell* **5**(10): 1147-1155.

Bernier G, Kinet JM, Sachs RM 1981. The Physiology of Flowering. Vols. 1 and 2. Boca Raton, FLA., USA: CRC Press.

Blazquez MA, Ferrandiz C, Madueno F, Parcy F. 2006. How floral meristems are built. *Plant Molecular Biology* **60**(6): 855-870.

Bodson M, Outlaw WH. 1985. Elevation in the Sucrose Content of the Shoot Apical Meristem of Sinapis-Alba at Floral Evocation. *Plant Physiology* **79**(2): 420-424.

Boss PK, Bastow RM, Mylne JS, Dean C. 2004. Multiple Pathways in the Decision to Flower: Enabling, Promoting, and Resetting. *Plant Cell* **16**(suppl_1): S18-31.

Corbesier L, Bernier G, Perilleux C. 2002. C : N ratio increases in the phloem sap during floral transition of the long-day plants Sinapis alba and Arabidopsis thaliana. *Plant and Cell Physiology* **43**(6): 684-688.

Corbesier L, Kustermans G, Perilleux C, Melzer S, Moritz T, Havelange A, Bernier G. 2004. Gibberellins and the floral transition in Sinapis alba. *Physiologia Plantarum* **122**(1): 152-158.

Corbesier L, Lejeune P, Bernier G. 1998. The role of carbohydrates in the induction of flowering in Arabidopsis thaliana: comparison between the wild type and a starchless mutant. *Planta* **206**(1): 131-137.

Dennin KA, Mcdaniel CN. 1985. Floral Determination in Axillary Buds of Nicotiana-Silvestris. *Developmental Biology* **112**(2): 377-382.

Dielen V, Lecouvet V, Dupont S, Kinet JM. 2001. In vitro control of floral transition in tomato (Lycopersicon esculentum Mill.), the model for autonomously flowering plants, using the late flowering uniflora mutant. *J Exp Bot* **52**(357): 715-723.

Dielen V, Quinet M, Chao J, Batoko H, Havelange A, Kinet JM. 2004. UNIFLORA, a pivotal gene that regulates floral transition and meristem identity in tomato (Lycopersicon esculentum). *New Phytologist* **161**(2): 393-400.

Doonan JH 1998. Cell division during floralmorphogenesis in Antirrhinum majus. In: D. Francis, D. DuditsD. Inze eds. *Plant Cell Division*. London and Miamai: Portland Press, 207-221.

Durdan SF, Herbert RJ, Rogers HJ, Francis D. 2000. The determination time of the carpel whorl is differentially sensitive to carbohydrate supply in Pharbitis nil. *Plant Physiology* **123**(1): 189-200.

Gebhardt JS, Mcdaniel CN. 1991. Flowering Response of Day-Neutral and Short-Day Cultivars of Nicotiana-Tabacum-L Interactions among Roots, Genotype, Leaf Ontogenic Position and Growth-Conditions. *Planta* **185**(4): 513-517.

Gegas VC, Doonan JH. 2006. Expression of cell cycle genes in shoot apical meristems. *Plant Mol Biol* **60**(6): 947-961.

Hartig K, Beck E. 2006. Crosstalk between auxin, cytokinins, and sugars in the plant cell cycle. *Plant Biology* **8**(3): 389-396.

Houssa P, Bernier G, Kinet JM. 1991. Qualitative and Quantitative-Analysis of Carbohydrates in Leaf Exudate of the Short-Day Plant, Xanthium-Strumarium L during Floral Transition. *Journal of Plant Physiology* **138**(1): 24-28.

Huang T, Bohlenius H, Eriksson S, Parcy F, Nilsson O. 2005. The mRNA of the Arabidopsis gene FT moves from leaf to shoot apex and induces flowering. *Science* **309**(5741): 1694-1696.

Hughes AP. 1965. Plant Growth and Aerial Environment .9. A Synopsis of Autecology of Impatienns Parviflora. *New Phytologist* **64**(3): 399-&.

Chailakhyan MK, Khazakhyan CK. 1974a. Effect of Roots on Growth and Flowering of Plants of Photoperiodically Neutral Species. *Doklady Akademii Nauk Sssr* **217**(4): 975-978.

Chailakhyan MK, Khazakhyan CK. 1974b. Interaction between Leaves and Shoots during Flowering of Plants of Photoperiodically Neutral Species. *Doklady Akademii Nauk Sssr* **217**(5): 1214-1217.

Jack T. 2004. Molecular and genetic mechanisms of floral control. *Plant Cell* **16 Suppl**: S1-17.

Jacqmard A, Gadisseur I, Bernier G. 2003. Cell division and morphological changes in the shoot apex of Arabidopsis thaliana during floral transition. *Annals of Botany* **91**(5): 571-576.

Kelly AJ, Bonnlander MB, Meeks-Wagner DR. 1995. NFL, the tobacco homolog of FLORICAULA and LEAFY, is transcriptionally expressed in both vegetative and floral meristems. *Plant Cell* **7**(2): 225-234.

Konstantinova TN, Bavrina TV, Aksenova NP. 1976. Particularities of the regulation of flowering in photoperiod-responsive and day-neutral tobacco species under in vivo and in vitro. *Soviet Plant Physiology* **23**: 365-371.

Konstantinova TN, Bavrina TV, Aksenova NP, Golyanovskaya SA. 1972. The effect of glucose on morphogenesis in stem calli of day-neutral tobacco, cv. Trapezoid. *Soviet Plant Physiology* **19**: 89-97.

Lang A 1965. Physiology of flower initiation In: W. Ruhland ed. *Encyclopedia of Plant physiology, Vol. XV, Part 1*. Berlin: Springer-Verlag, 1380-1536.

Lang A 1989. Nicotiana. In: A. H. Halevy ed. *Handbook of flowering, Vol. 6*. Boca Raton, FLA., USA: CRC Press, 427-483.

Lejeune P, Bernier G, Kinet JM. 1991. Sucrose Levels in Leaf Exudate as a Function of Floral Induction in the Long Day Plant Sinapis-Alba. *Plant Physiology and Biochemistry* **29**(2): 153-157.

Lejeune P, Bernier G, Requier MC, Kinet JM. 1993. Sucrose Increase during Floral Induction in the Phloem Sap Collected at the Apical Part of the Shoot of the Long-Day Plant Sinapis-Alba L. *Planta* **190**(1): 71-74.

Lejeune P, Bernier G, Requier MC, Kinet JM. 1994. Cytokinins in Phloem and Xylem Saps of Sinapis-Alba during Floral Induction. *Physiologia Plantarum* **90**(3): 522-528.

Lipavska H, Svobodova H, Albrechtova J, Kumstyrova L, Vagner M, Vondrakova Z. 2000. Carbohydrate status during somatic embryo maturation in Norway spruce. *In Vitro Cellular & Developmental Biology-Plant* **36**(4): 260-267.

Machackova I, Krekule J, Eder J, Seidlova F, Strnad M. 1993. Cytokinins in Photoperiodic Induction of Flowering in Chenopodium Species. *Physiologia Plantarum* **87**(2): 160-166.

Masek T, Vopalensky V, Suchomelova P, Pospisek M. 2005. Denaturing RNA electrophoresis in TAE agarose gels. *Analytical Biochemistry* **336**(1): 46-50.

Mcdaniel CN 1992. Determination to flower in *Nicotiana*. In: R. A. Pederson ed. *Current Topics in Developmental Biology*. New York: Academic Press, 1-37.

Mcdaniel CN, Hartnett LK. 1993. Floral-Stimulus Activity in Tobacco Stem Pieces. *Planta* **189**(4): 577-583.

McDaniel CN, Hartnett LK, Sangrey KA. 1996. Regulation of node number in day-neutral Nicotiana tabacum: A factor in plant size. *Plant Journal* **9**(1): 55-61.

McKibbin RS, Halford NG, Francis D. 1998. Expression of fission yeast cdc25 alters the frequency of lateral root formation in transgenic tobacco. *Plant Molecular Biology* **36**(4): 601-612.

Miller MB, Lyndon RF. 1976. Rates of Growth and Cell-Division in Shoot Apex of Silene during Transition to Flowering. *Journal of Experimental Botany* **27**(101): 1142-1153.

Murashige T, Skoog F. 1962. A Revised Medium for Rapid Growth and Bio Assays with Tobacco Tissue Cultures. *Physiologia Plantarum* **15**(3): 473-&.

Noh YS, Bizzell CM, Noh B, Schomburg FM, Amasino RM. 2004. EARLY FLOWERING 5 acts as a floral repressor in Arabidopsis. *Plant J* **38**(4): 664-672.

Nougarède A, Francis D, Rondet P. 1991. Location of cell cycle changes in relation to morphological changes in the shoot apex ofSilene coeli-rosa immediately before sepal initiation. *Protoplasma* **V165**(1): 1-10.

Nougarède A, Rembur J, Saint-Côme R. 1987. Rates of cell division in the young prefloral shoot apex ofChrysanthemum segetum L. *Protoplasma* **V138**(2): 156-160.

Nurse P. 1990. Universal Control Mechanism Regulating Onset of M-Phase. *Nature* **344**(6266): 503-508.

Orchard CB, Siciliano I, Sorrell DA, Marchbank A, Rogers HJ, Francis D, Herbert RJ, Suchomelova P, Lipavska H, Azmi A, Van Onckelen H. 2005. Tobacco BY-2 cells expressing fission yeast cdc25 bypass a G2/M block on the cell cycle. *Plant Journal* **44**(2): 290-299.

Ormrod JC, Francis D. 1986. Mean Rate of DNA-Replication and Replicon Size in the Shoot Apex of Silene-Coelirosa L during the Initial 120 Minutes of the 1St Day of Floral Induction. *Protoplasma* **130**(2-3): 206-210.

Parfitt D, Herbert RJ, Rogers HJ, Francis D. 2004. Differential expression of putative floral genes in Pharbitis nil shoot apices cultured on glucose compared with sucrose. *Journal of Experimental Botany* **55**(406): 2169-2177.

Putterill J, Laurie R, Macknight R. 2004. It's time to flower: the genetic control of flowering time. *Bioessays* **26**(4): 363-373.

Robinson LW, Wareing PF. 1969. Experiments on Juvenile-Adult Phase Change in Some Woody Species. *New Phytologist* **68**(1): 67-&.

Roldan M, Gomez-Mena C, Ruiz-Garcia L, Salinas J, Martinez-Zapater JM. 1999. Sucrose availability on the aerial part of the plant promotes morphogenesis and flowering of Arabidopsis in the dark. *Plant J* **20**(5): 581-590.

Suchomelova P, Uchytilova L, Lipavska H. 2004a. Tobacco cells transformed with fission yeast cdc25 gene display characteristics evocable by cytokinin application. *Acta Physiologiae Plantarum* **26**(3 Suppl.): 161.

Suchomelova P, Velgova D, Masek T, Francis D, Rogers HJ, Marchbank AM, Lipavska H. 2004b. Expression of the fission yeast cell cycle regulator cdc25 induces de novo shoot formation in tobacco: evidence of a cytokinin-like effect by this mitotic activator. *Plant Physiology and Biochemistry* **42**(1): 49-55.

Tran Thanh Van M. 1973. Direct flower neoformation from superficial tissue of small explants of Nicotiana tabacum L. *Planta* **115**(1): 87-92.

Tran Thanh Van M, Nguyen Thi D, Averil C. 1974. Regulation of organogenesis in small explants of superficial tissue of Nicotiana tabacum L. *Planta* **V119**(2): 149-159.

Vincent CA, Carpenter R, Coen ES. 1995. Cell lineage patterns and homeotic gene activity during Antirrhinum flower development. *Curr Biol* **5**(12): 1449-1458.

Zeevaart JAD. 1962. The Juvenile Phase in Bryophyllum-Daigremontianum. *Planta* **58**(5): 543-548.

Zhang KR, Diederich L, John PCL. 2005. The cytokinin requirement for cell division in cultured Nicotiana plumbaginifolia cells can be satisfied by yeast cdc25 protein tyrosine phosphatase. Implications for mechanisms of cytokinin response and plant development. *Plant Physiology* **137**(1): 308-316.

Table 1: The rate of leaf initiation as affected by *Spcdc25* expression

Sucrose	cdc25						WT					
	No. of leaves at time of flowering		**No. of days to flowering**		**Rate of leaf initiation (per day)**		**No. of leaves at time of flowering**		**No. of days to flowering**		**Rate of leaf initiation (per day)**	
	apex	**base**	**apex**	**base**	**apex**	**base**	**apex**	**base**	**apex**	**base**	**apex**	**base**
3%	65	53	233	208	0,27	0.25	223	154	350	350	0,66	0.44
5%	33	26	182	175	0.18	0.15	60	90	231	303	0.26	0.3
7%	22	20	143	112	0.15	0.17	53	81	216	283	0.24	0.29

apex - respective base - apical resp. basal segment derived plants. Mind that control plants did not flower on the medium with 3% sucrose even when cultivation was prolonged till 350 days and only two thirds of WT on 5% sucrose that initiated flowering is involved in the quantification.

Figures:

Fig. 1

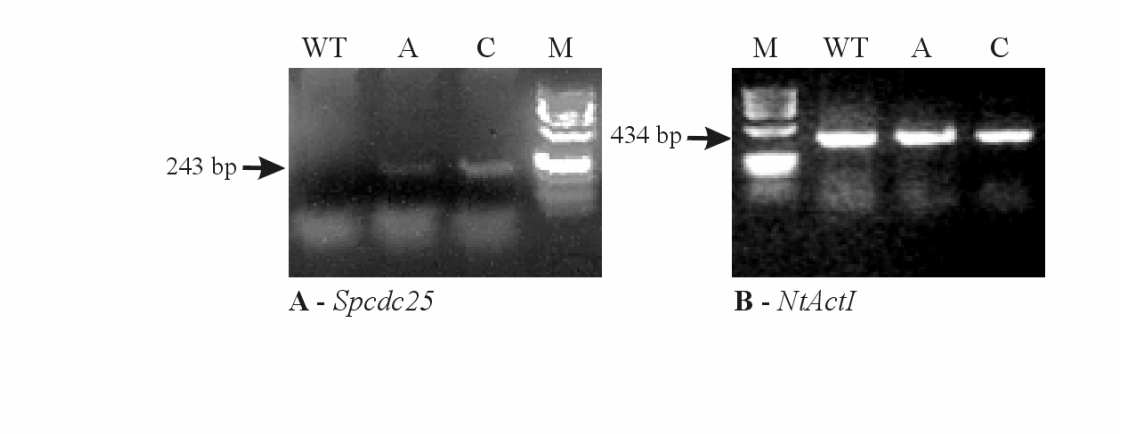

Detection of *Spcdc25* transcripts in transgenic tobacco plants. Semi-quantitative RT PCR analyses of *Spcdc25* transcripts (a) and constitutively expressed gene for actin *NtActI* (b). RNA was isolated from leaves of 1 month old seedlings, **WT** - non-transformed plant material, **A** - transformant A , **C** – transformant C, **M**= DNA molecular weight marker IX (Roche).

Fig. 2:

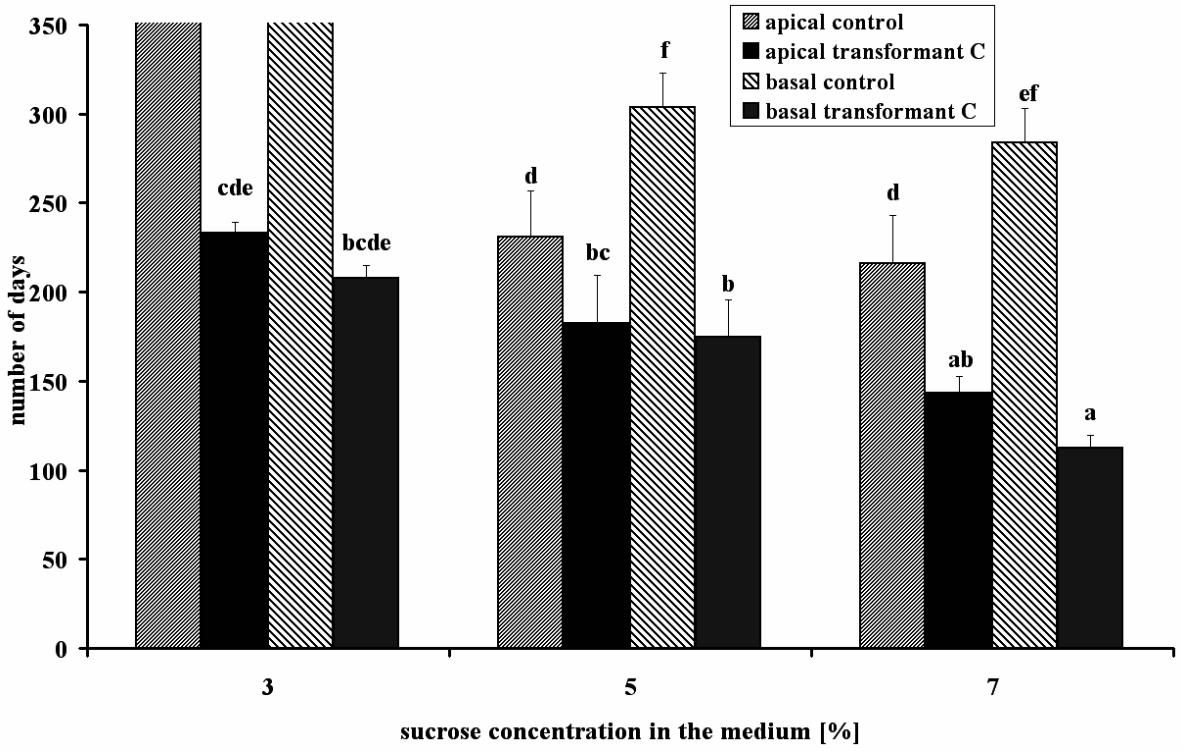

Effect of different sucrose supply on the number of days to flowering in **WT** (control) and cdc25 plants (transformant **C**). The plants were repeatedly cultivated either from apical or basal segments. (n=3-12). WT did not flower on 3% sucrose. Four out of the twelve **WT** controls cultivated on 5 % sucrose did not flower by the end of the experiment (330 days) (data not included in the figures). Statistically significant differences between variants are indicated by different letters upon columns.

Fig. 3:

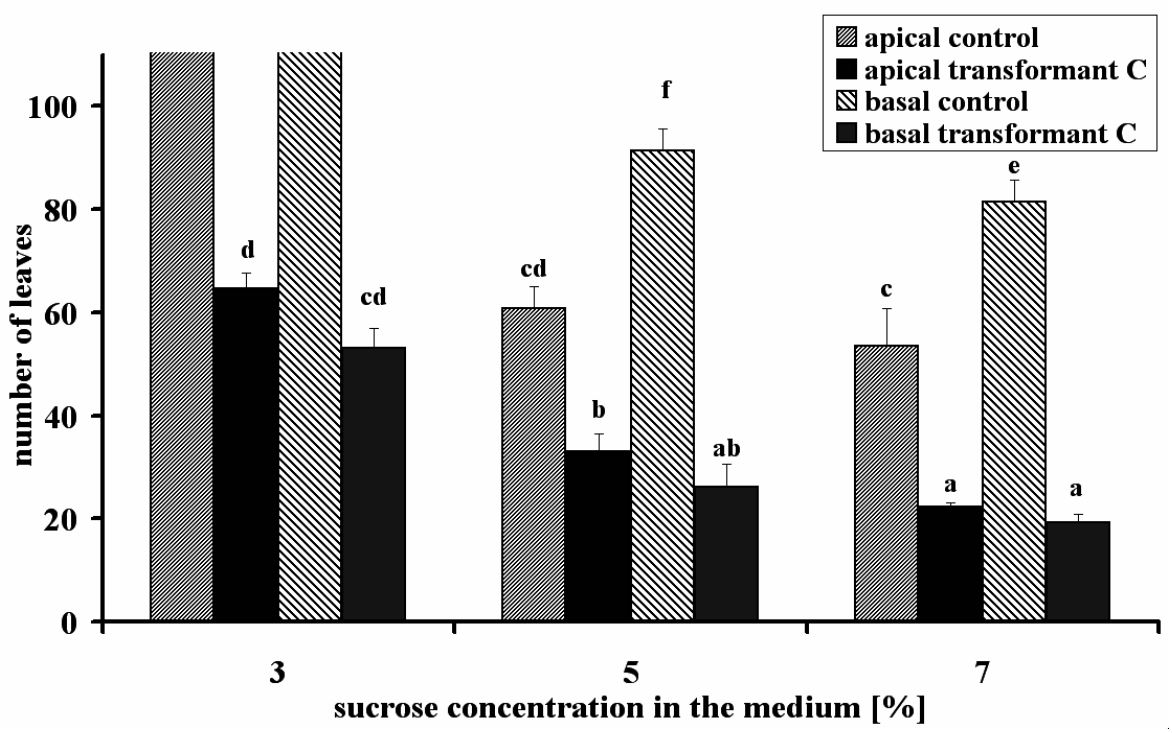

Effect of different sucrose supply on the total number of leaves produced until flowering in **WT** (control) and cdc25 plants (transformant **C)**. The plants were repeatedly cultivated either from apical or basal segments. (n=3-12). WT controls did not flower on 3% sucrose medium. Four out of the twelve controls cultivated on 5 % sucrose did not flower even at the end of the experiment (data not included in the figures). Statistically significant differences between variants are indicated by different letters upon columns.

Fig. 4:

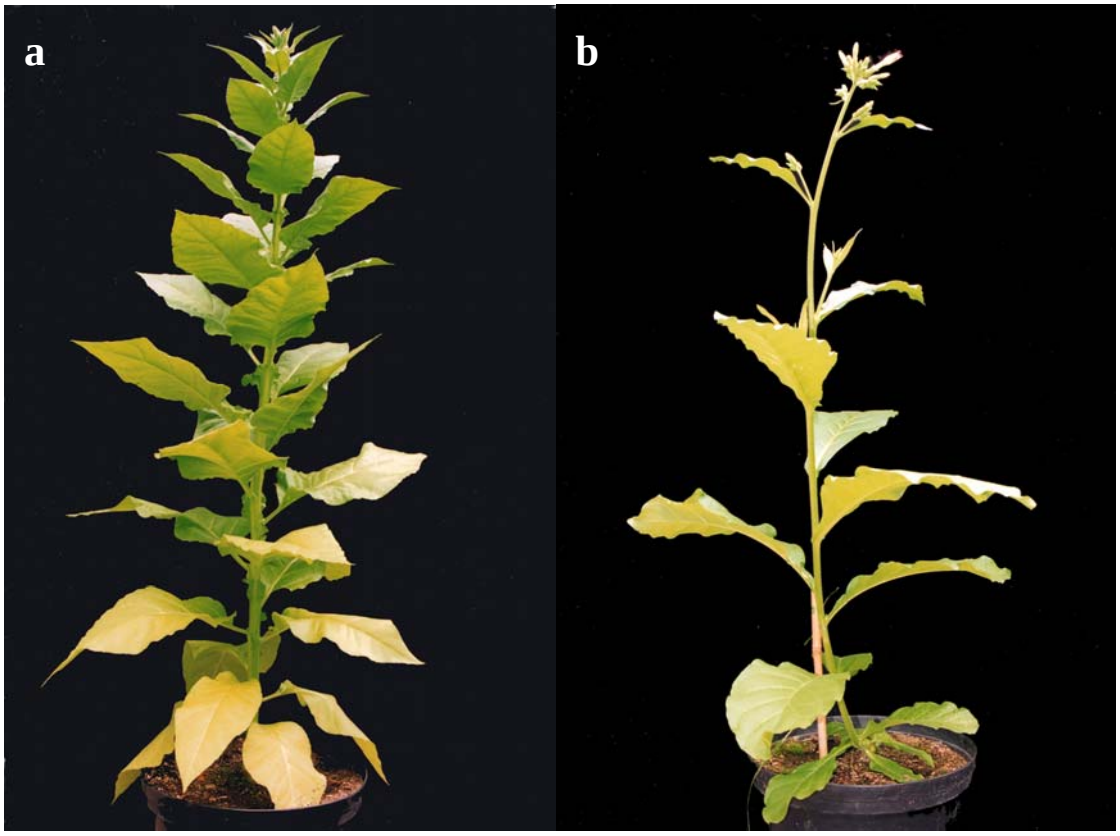

Habitus of the tobacco plants at the flowering onset: a) WT b) cdc25 plant line C.

Fig. 5:

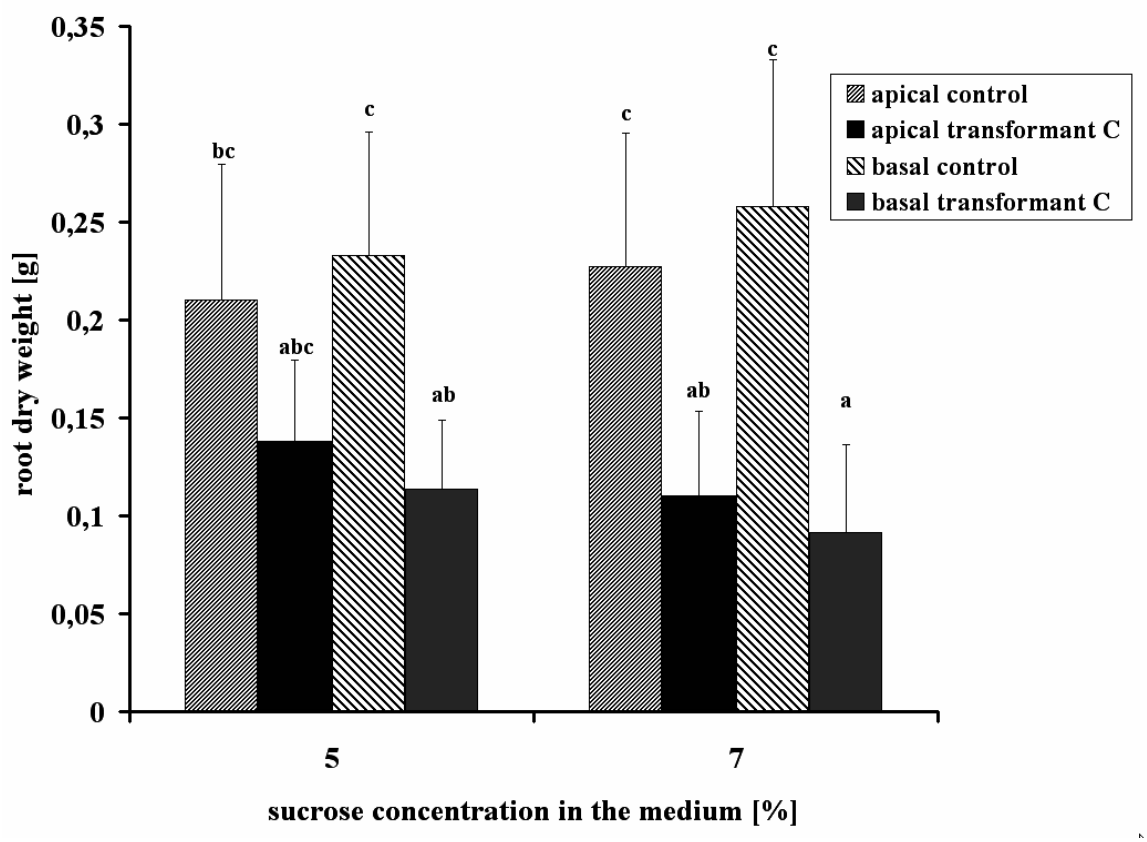

Dry weights of root system of **WT** and cdc25 plants (transformant **C**) in culture media supplemented with 5% and 7 % sucrose. The root system was sampled at the time of segment subculture. (n= 5-11). Statistically significant differences between variants are indicated by different letters upon columns.

632 **Fig. 6:**

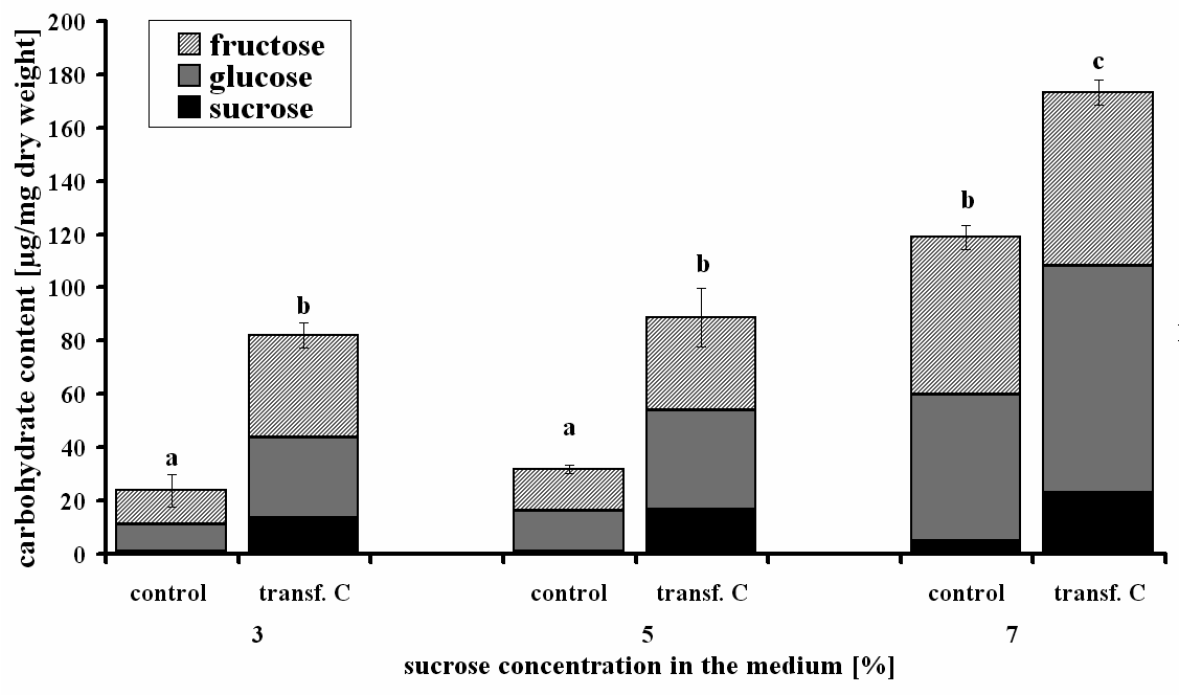

633

634 Contents of endogenous non-structural carbohydrates in the leaves of **WT** and
635 cdc25 transgenic tobacco (transformant **C**) after 77 days of cultivation. (n=3-5).
636 Statistically significant differences between variants are indicated by different letters
637 upon columns.

The Plant Journal (2005) **44**, 290–299 doi: 10.1111/j.1365-313X.2005.02524.x

Tobacco BY-2 cells expressing fission yeast *cdc25* bypass a G2/M block on the cell cycle

Craig B. Orchard[1,2], Ilario Siciliano[1,2], David A. Sorrell[1,3], Angela Marchbank[1], Hilary J. Rogers[1], Dennis Francis[1,*], Robert J. Herbert[2], Petra Suchomelova[4], Helena Lipavska[4], Abdelkrim Azmi[5] and Harry Van Onckelen[5]

[1]*School of Biosciences, Cardiff University, PO Box 915, Cardiff CF10 3TL, UK,*

[2]*Department of Applied Sciences, Geography and Archaeology, University College, Worcester, Henwick Grove, Worcester WR2 6AJ, UK,*

[3]*Polgen Division, Cyclacel Ltd, Babraham Institute, Babraham, Cambridge, CB2 4AT, UK,*

[4]*Department of Plant Physiology, Faculty of Science, Charles University, Vinicna 5, Prague 2, Czech Republic, and*

[5]*Department of Biology, Universiteit Antwerpen (UIA), Universiteitsplein 1, B-2610 Antwerp, Belgium*

Received 1 June 2005; revised 15 July 2005; accepted 25 July 2005.
[*]For correspondence (fax +44 29 2087 4305; e-mail francisd@cardiff.ac.uk).

Summary

The mitotic inducer gene from *Schizosaccharomyces pombe*, *Spcdc25*, was used as a tool to investigate regulation of G2/M in higher plants using the BY-2 (*Nicotiana tabacum*) cell line as a model. *Spcdc25*-expressing BY-2 cells exhibited a reduced mitotic cell size through a shortening of the G2 phase. The cells often formed isodiametric double files both in BY-2 cells and in cell suspensions derived from 35S::*Spcdc25* tobacco plants. In *Spcdc25*-expressing cells, the tobacco cyclin-dependent kinase, NtCDKB1, showed high activity in early S phase, S/G2 and early M phase, whereas in empty vector cells CDKB1 activity was transiently high in early S phase but thereafter remained lower. *Spcdc25*-expressing cells also bypassed a block on G2/M imposed by the cytokinin biosynthetic inhibitor lovastatin (LVS). Surprisingly, cytokinins were at remarkably low levels in *Spcdc25*-expressing cells compared with the empty vector, explaining why these cells retained mitotic competence despite the presence of LVS. In conclusion, synchronised *Spcdc25*-expressing BY-2 cells divided prematurely at a small cell size, and they exhibited premature, but sustained, CDKB1 activity even though endogenous cytokinins were virtually undetectable.

Keywords: *Nicotiana tabacum*, cell size, cytokinins, *BY-2 cell line CDKA/B*, plant cell cycle.

Introduction

The plant cell cycle is regulated by cyclin-dependent protein kinases (CDKs), which are themselves phosphoregulated (Joubes *et al.*, 2000). In fission yeast (*Schizosaccharomyces pombe*), *Spwee1* and *Spcdc25* are phosphoregulators of the G2/M transition. *Spwee1* encodes a protein kinase that in G2 phosphorylates the Y15 residue near to the NH_2-terminus of the Cdc2 protein; this suppresses the kinase activity of the CDK (Gould and Nurse, 1989; Russell and Nurse, 1987). *Spcdc25* encodes a tyrosine phosphatase that in late G2 dephosphorylates the Cdc2 kinase on the same tyrosine residue (Y15) (Russell and Nurse, 1986). Following binding of Cdc2 with a B-type cyclin, dephosphorylation of Cdc2 by Cdc25 is the final all-or-nothing signal that triggers Cdc2 kinase activity driving cells into division (see O'Farrell, 2001).

In *S. pombe*, overexpression of *cdc25* induced a short-cell phenotype. The cells divided prematurely through a shortening of the G2 phase, but surprisingly there was little change in the overall length of the cell cycle (Russell and Nurse, 1986). In this case, a lengthening of G1 compensated for the shortened G2. Overexpressing *wee1* had the converse effect, resulting in a long-cell phenotype (Russell and Nurse, 1987). This suggests strongly that by competing for the same substrate Wee1 and Cdc25 regulate cell size at division, although *wee1* is regarded as the main genetic element in this control (Sveiczer *et al.*, 1996); presumably, other size-related signals impinge on this complex that finally enable Cdc25 to out-compete Wee1.

In plants, a homologue to *wee1* has been identified in *Zea mays* (Sun *et al.*, 1999) and in *Arabidopsis thaliana* (Sorrell *et al.*, 2002). Most recently, a gene has been identified that encodes a small CDC25 protein (*Arath; CDC25*) that lacks a regulatory domain but can dephosphorylate plant CDKs (Landrieu *et al.*, 2004). *Spcdc25* also dephosphorylated tobacco CDC2 kinase *in vitro* (Zhang *et al.*, 1996). In wild-type (WT) cultures of *Nicotiana plumbaginafolia* that were depleted of exogenous cytokinin cells were arrested in G2 and CDC2 kinase was inactivated. However, the addition of cytokinin (kinetin) led to dephosphorylation of CDC2 and entry of cells into mitosis (Zhang *et al.*, 1996). Moreover, induction of *Spcdc25* expression in the same culture system could induce cell division in cultures depleted of auxin and cytokinin (Zhang *et al.*, 2005). These data suggest strongly that there is a cytokinin-mediated signal transduction chain that regulates the G2/M transition through activation of a Cdc25-like phosphatase (Zhang *et al.*, 2005). However, the levels of endogenous cytokinins were not reported on. Interestingly, WT BY-2, cells are dependent on zeatin and zeatin riboside synthesis at the G2/M transition because suppression of their synthesis by lovastatin (LVS) blocked the G2/M transition (Laureys *et al.*, 1998; Redig *et al.*, 1996). Lovastatin inhibits the isoprenoid pathway of cytokinin biosynthesis (Crowell and Salaz, 1992).

In *Nicotiana tabacum*, constitutive *Spcdc25* expression resulted in a small mitotic cell size (Bell *et al.*, 1993) and induction of *Spcdc25* in cultured roots also resulted in a small mitotic cell size (McKibbin *et al.*, 1998). Induction of *Spcdc25* expression in tobacco leaves resulted in variable cell size and cell proliferation in the lamina margins followed by alterations in leaf shape (Wyrzykowska *et al.*, 2002).

The aim of the work reported here was to use *Spcdc25* as a tool to investigate regulation of the G2/M transition in the plant cell cycle using the tobacco BY-2 cell line as a model (Nagata *et al.*, 1992). We tested whether the *Spcdc25*-induced reduction in cell size reported by McKibbin *et al.* (1998), was because of a shortening of the S phase or G2, or both. We also assayed CDKA and CDKB1 to examine whether either enzyme was precociously active in the cell cycle of synchronised *Spcdc25*-expressing cells. Another important aim was to measure endogenous cytokinins in *Spcdc25*-expressing cells compared with an empty vector $\pm$ LVS. This provided an independent test of Zhang *et al.*'s (2005) cytokinin-regulated model of the G2/M transition in the plant cell cycle.

Spcd25-expressing cells not only divide prematurely but show early and persistently high CDKB1 activity and altered planes of cell division. Moreover, synchronised entry of *Spcdc25*-expressing cells from G2 to mitosis was unaffected by LVS, and, most surprisingly, *Spcd25*-expressing cells have an extremely low endogenous cytokinin content.

Results

Spcdc25 *is expressed but the lines are less stable than empty vector controls*

The BY-2 cell line was transformed through a modified CaMV 35S promoter (BIN-HYG-TX) that has an attenuated level of expression compared with the conventional CaMV 35S promoter (Gatz *et al.*, 1992). Periodically, it became necessary to generate new transgenic lines because after about 12–15 months in culture *Spcdc25*-expressing cells unexpectedly stop growing. The mortality of *Spcdc25*-expressing lines, which was not incurred with comparable empty vector (EV) lines, suggests strongly that *Spcdc25* expression eventually becomes lethal in BY-2 cells (see Discussion).

RT-PCR confirmed the expression of *Spcdc25* RNA (Figure 1) and Western blots confirmed the expression of *Spcdc25* at the protein level (Figure 1). The Spcdc25 antiserum also revealed a weaker signal in EV cells (Figure 1). Notably, Zhang *et al.* (2005) observed CDC25-like phosphatase activity in their WT tobacco cultures. The weak signal (Figure 1), which was also detected in WT (data not shown), may be due to the expression of endogenous tobacco *CDC25.* However, if this is the case, the tobacco CDC25 protein is substantially larger than the predicted size of the Arabidopsis CDC25 protein (Landrieu *et al.*, 2004; Sorrell *et al.*, 2005).

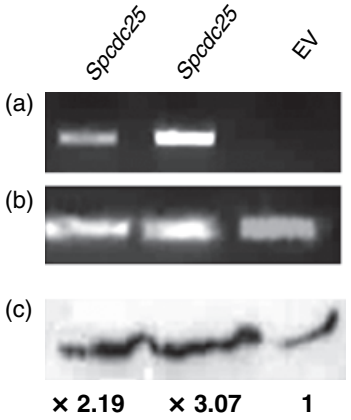

Figure 1. Spcdc25 cells express *Spcdc25* at the mRNA and protein levels.
RT-PCR and Western analysis of *Spcdc25* expression in the BY-2 cell lines used in this study.
Top panel (a): expression of *Spcdc25* (product size 718 bp), in two independent lines carrying the *Spcdc25* construct; EV is the empty vector.
Middle panel (b): 18S RNA control (product size 459 bp).
Bottom panel (c): Western blots of protein from the same *Spcdc25*EC compared with EV, probed with an antibody to *S. pombe* Cdc25. The Western signals were quantified in relation to the EV signal.

Spcdc25 *induces premature cell division through a shortening of the G2 phase but not the S phase*

Spcdc25-expressing cells (referred to hereafter as *Spcdc25*EC) synchronised with aphidicolin exhibited a first peak in the mitotic index (the sum of prophase, metaphase, anaphase and telophase as a percentage of all cells) at 6 h, compared with a first peak at 10 h in corresponding EV cells (Figure 2). The initial rise in the mitotic index is the time taken for cells previously blocked in late S phase to reach mitosis. Hence the G2 phase in *Spcdc25*EC was 2 h and in EV 6 h (Figure 2). Patterns of alteration in amounts of DNA, obtained by microdensitometry, are consistent with a shorter G2 in *Spcdc25*EC compared with EV (upper- and lowermost panels in Figure 2).

Expression of histone H4 is a marker of the S phase, and in both *Spcdc25*EC and EV a strong H4 profile was evident from 0–4 h followed by a drop to less than 20% of the maximum (Figure 2). Hence, the S phase lasts for 4 h in both *Spcdc25*EC and in EV cells. The interval between peaks in the mitotic index is the cell cycle time: 11 and 12 h for *Spcdc25*EC and EV, respectively. Note that in the *Spcdc25*EC the distinctive and highly repeatable change to the cell cycle was a reduction in the duration of G2.

CDKB1 activity is consistently high in S-phase S/G2 and G2/M in Spcdc25-*expressing cells*

If *Spcdc25* cells have a short G2 phase as a direct result of increased Cdc25 phosphatase activity, then CDKs that propel cells into division ought to be highly active at earlier sample times compared with EV cells. This hypothesis was tested by assaying CDKA and CDKB1. Note that samples were taken from 1–9 h (*Spcdc25*EC) or 1–14 h (EV), i.e. before, during and after the first mitotic peak (the mitotic index amplitude) (Figure 3).

In the *Spcdc25*EC lines, CDKB1 activity was consistently high at 1 h (early S phase) and at 3–4 h (90% of maximum

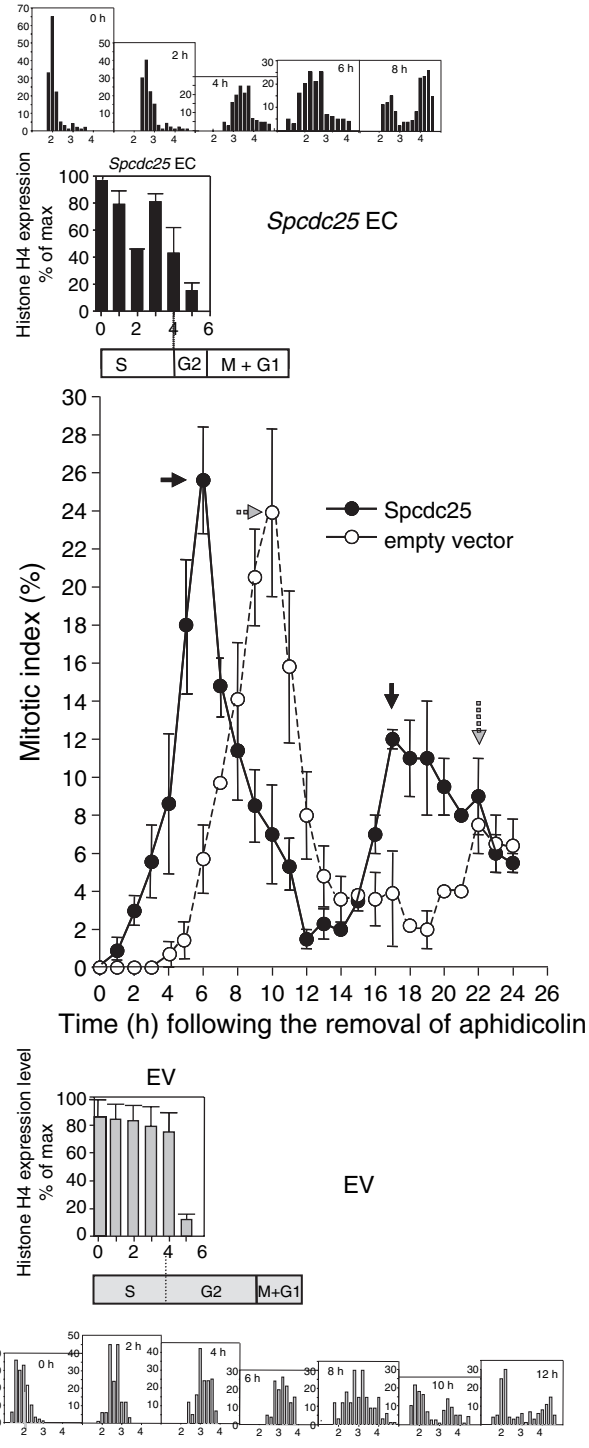

Figure 2. Synchronised *Spcdc25*-expressing BY-2 lines exhibit a premature rise in the mitotic index and a short G2 phase.
The mitotic index (means ± SE) from independent *SpCDC25* lines and corresponding means from EV, following release from aphidicolin ($n = 3$). The earlier rise in the mitotic index in *Spcdc25*EC is consistent with a shorter G2 (2 h) compared with EV (G2 = 6 h = the first significant rise in the mitotic index). Arrows indicate the peaks of mitotic index which is a measure of the duration of the cell cycle: *Spcdc25*EC = 11 h (6–17 h on the *x*-axis) and in EV = 12 h (10–22 h). Immediately above and below the mitotic index data are mean (±SE) histone H4 expression levels from replicates ($n = 2$). The S phase is measured from zero to the sample time immediately before a signal that was <20% of the maximum (S phase = 4 h in both). The durations of G2 and G1 + M are added to the horizontal bar charts. In summary G1 + M was obtained by difference (i.e. *C* – (G2 + S):

	*SpCDC25*EC	EV
S phase	4	4
G2	2	6
G1 + M	5	2
C	11	12

The uppermost and lowermost bar charts, indicate temporal changes in nuclear DNA amounts (*C* values) in interphase cells following the release from aphidicolin: ordinate = frequency, abscissa = amounts of nuclear DNA (*C* values). Each density value was normalised against prophase (4*C*) and half-telophase (2*C*) mitotic figures. Note that in histograms lacking 4*C* values, those samples and 'mitotic' samples were stained simultaneously ($n = 150$).

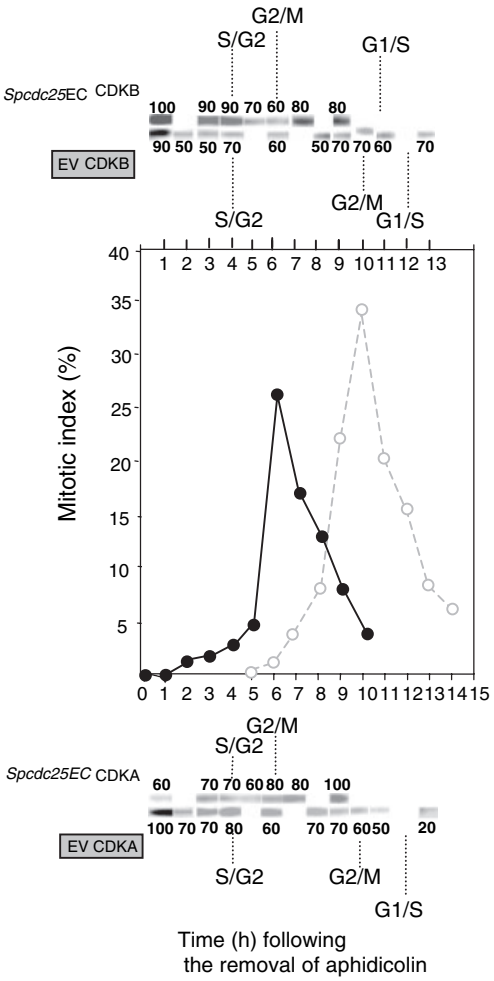

Figure 3. Premature CDKB1 activity in S phase, G2/M and M in *Spcdc25*EC.
*Spcdc25*EC and EV cells were synchronised as explained earlier, and mitotic indices recorded for between 12 and 14 h following the release from aphidicolin. (Note that the timings of the increases and peaks in these new mitotic index data are identical to those shown in Figure 2.)
The mean histone H1 kinase activities of the CDKA and CDKB1 immunoprecipitates are quantified as a percentage of maximum activity for each assay ($n = 2$).
The quantitative data, either rounded up or down to the nearest 10, are presented for each gel image. Cell cycle phase transitions are added to each row of gel images. Note that the gel images are *representative* of images the two replicate experiments and that key phase transitions are inserted as shown by vertical dotted lines.

(S/G2)). It dipped to 60–70% of maximum at 5 and 6 h before rising again at 7 h (80% of maximum at early M phase) and 9 h (80% of maximum). In EV, CDKB activity was transiently high at 1 h (early S phase), but from there on it was between 50 and 70% of maximum. Note that M phase in WT BY-2 cells is between 1 and 2 h (Francis *et al.*, 1995; Herbert *et al.*, 2001; Porceddu *et al.*, 2001; Sorrell *et al.*, 2001), which would place the 9 h signal for *Spcdc*25EC (80% maximum) at M/G1 and the 13 h signal for EV in the S phase of the *next* cell cycle.

In the *Spcdc25*EC, CDKA activity was relatively constant between 1 and 5 h (60–70% maximum, S phase and early G2), but increased to 80% at 6 h (G2/M) and was 100% of the maximum at 9 h ('M/G1'). In the EV, CDKA activity was maximal at 1 h (early S phase) and was also high at 4 h (80% maximum, S/G2). Between 6 and 11 h it was between 60 and 70% of maximum, before dropping to 20% of maximum at 13 h (S phase of the next cell cycle).

To summarise, a clear and repeatable feature of these assays was premature and persistent CDKB1 activity in *Spcdc25*EC compared with EV.

Mitotic cell size is smaller in Spcdc25*-expressing lines*

Overexpression of *Spcdc25* in fission yeast and in tobacco plants resulted in a decrease in mitotic cell size (McKibbin *et al.*, 1998; Russell and Nurse, 1987). Indeed, in the latter it was the most characteristic feature of the transgenic plants (see Introduction). The shortened G2 phase in the BY-2 cells expressing *Spcdc25* would suggest premature cell division at a reduced cell size. In *Spcdc25*EC, the mitotic cell area was indeed significantly smaller compared with EV and compared with hitherto unpublished data for WT (Figure 4, $P < 0.001$). However, the mean mitotic cell area for EV cells was not significantly different from WT ($P > 0.05$). In other words, neither the transformation process *per se* nor expression of the antibiotic resistance gene affected mitotic cell size.

Cells expressing Spcdc25 *form doublets of small cells*

Not only did we observe a reduced cell size at division, but the cells also exhibited a tendency to form in doublets as

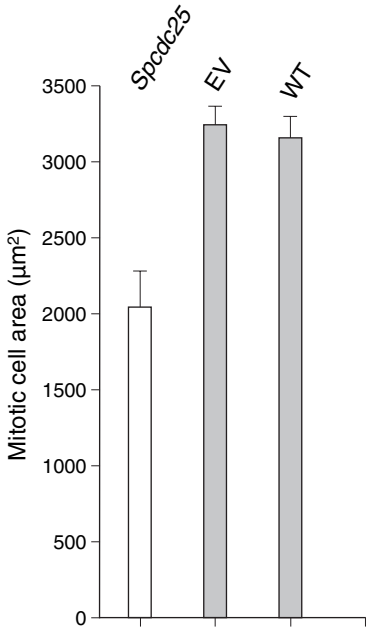

Figure 4. The mean (±SE) mitotic cell area (μm^2) is smaller in *Spcdc25*EC than in EV and WT ($n \geq 50$).

opposed to the single-cell filaments characteristic of WT and EV lines (Figure 5). We quantified this observation by scoring the frequency of doublets in *Spcdc25*EC during normal log-stationary phase growth. On each day of the 7-day culture period, filaments of six cells or more in length were scored as either single or double. Notably, between 19 and 34% of filaments were present as doublets in *Spcdc25*EC on day 4 compared with singlets in EV (Table 1). Although the frequency of doublets in *Spcdc25*EC varied, such doublets were either observed rarely or not at all in EV (Figure 5, Table 1).

A cell suspension established from internodal tissue from 35S::*Spcdc25* tobacco also exhibited small isodiametric doublets of cells (Figure 5d), confirming our observations in BY-2 cells.

Spcdc25*EC* overcome a block imposed by lovastatin

Zhang *et al.* (1996) reported that both *Spcdc25* and cytokinin treatment could dephosphorylate plant Cdc2 in late G2 of the cell cycle (see Introduction). We therefore tested whether *Spcdc25* expression is dependent on a cytokinin signal by treating BY-2 cells with LVS, a known inhibitor of cytokinin biosynthesis in late G2. Cells were synchronised, LVS was added 1 h following the removal of aphidicolin and samples were taken during mitotic index

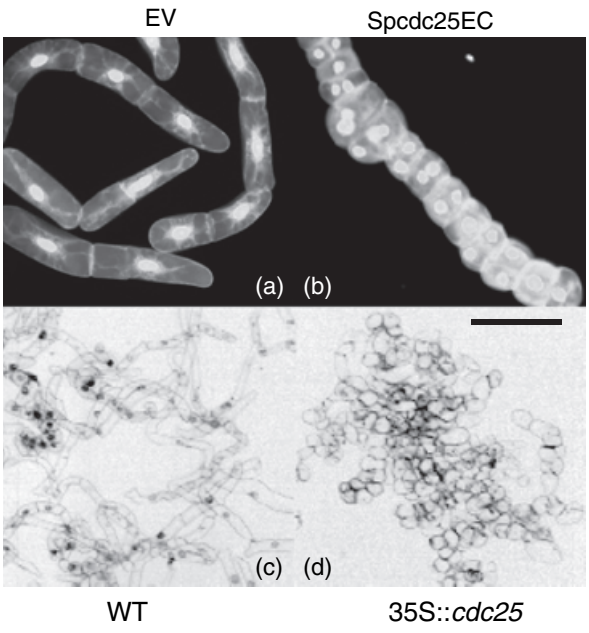

Figure 5. *Spcdc25*-expressing BY-2 cells form in isodiametric double filaments.
Interphase BY-2 cells stained with Hoechst viewed by fluorescence (a,b) or bright field optics (c,d): (a) EV, (b) *Spcdc25*EC, (c) cell suspension established from tobacco internodal tissue and (d) a cell suspension established from internodal tissue of 35S::Sp*cdc25* tobacco. The bar scale = 100 μm in all cases.

Table 1 The range of percentage frequency of doublets of BY-2 cells (double filaments six cells or more in length) in the *Spcdc25*EC compared with EV, during the normal 7 days of BY-2 batch culture at 27°C ($n = 300$)

	Range % frequency of doublets in:	
Day of culture	*Spcdc25*EC	EV
1	2–6	0
2	7–10	1
3	18–24	0
4	19–34	0
5	9–26	0
6	3–17	0
7	2–4	0

amplitudes so as to compare the G2/M transition in both *Spcdc25*EC and EV. In *Spcdc25*EC, the addition of LVS did not affect the mitotic index compared with the control (Figure 6). However, in the EV, LVS inhibited the mitotic index so that an expected curve was suppressed. Hence, the data are consistent in showing that in progressing from G2 to mitosis cells in the *Spcdc25*EC can escape a cell cycle block imposed by LVS.

Endogenous cytokinins are extremely low in Spcdc25 *cells.*

In *Spcdc25* cells, the flow of cells into mitosis was unaffected by LVS, suggesting that *Spcdc25* lines might exhibit an increased level of cytokinin to compensate for LVS inhibition. To test this hypothesis, samples were taken from the *Spcdc25*EC and EV at the same time as those taken to generate the mitotic indices shown in Figure 6. Cytokinins were measured in samples that included the G2/M transition: 2–5 h for *Spcdc25*EC and 0–10 h for EV. Levels of representative cytokinins are presented in Figure 7. Surprisingly, in *Spcdc25*EC the endogenous concentrations of cytokinins were extremely low or below detectable limits regardless of LVS treatment, thereby negating our hypothesis. However, LVS added to EV resulted in a predictable reduction in levels of endogenous cytokinins (Figure 7).

Discussion

Spcdc25 *shortens G2*

In the BY-2 cell line, *Spcdc25* induces a small cell size at mitosis because of a 50% reduction in the G2 phase (Figure 8) This mechanism was only hypothesised in previous work (McKibbin *et al.*, 1998).

In fission yeast, overexpression of *Spcdc25* induces a reduction in mitotic cell length. However, the cell cycle duration was very similar to that in WT with a lengthening of G1 compensating for the shortening of G2 (Russell and Nurse, 1986). This is slightly different from the *Spcdc25*EC

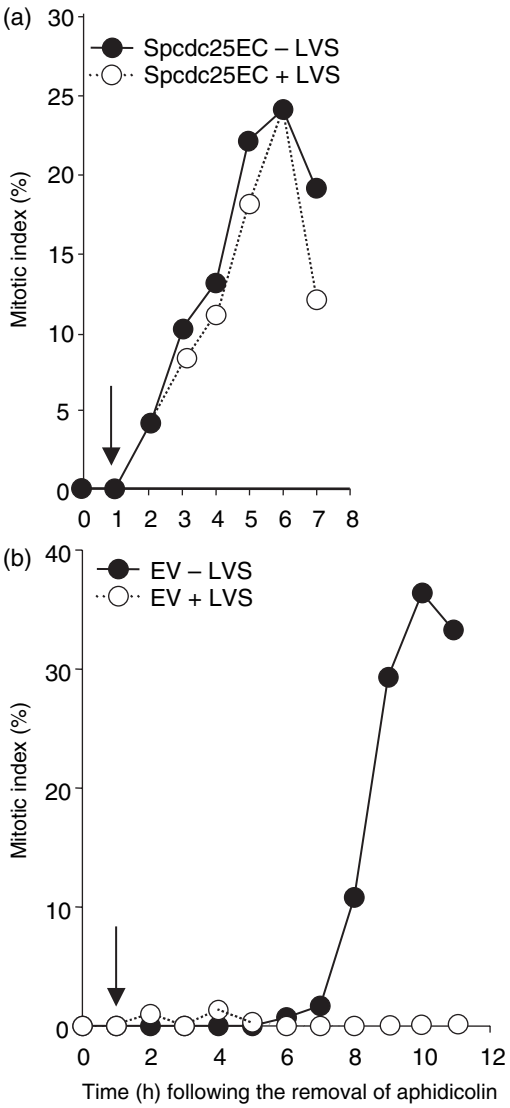

Figure 6. *Spcdc25*EC escape a LVS-induced block.
Changes to the mitotic index ±10 μM LVS given at 1 h following aphidicolin release (↓) in (a) *Spcdc25*EC and (b) EV. (Note that the timings of the increases and peaks of these new data are identical to those shown in Figures 2 and 3.)

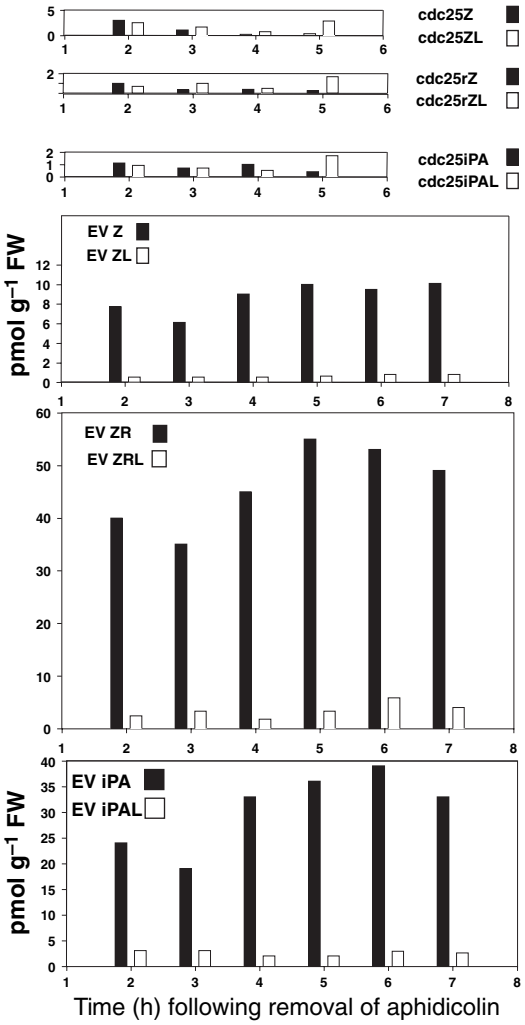

Figure 7. Cytokinins are virtually undetectable in *Spcdc25*EC.
Levels of zeatin (Z), zeatin riboside (ZR) and N^6-(Δ^2isopentenyl)-adenine (iPA) in *Spcdc25*EC and EV ± LVS. Samples were taken hourly from the same experiment used to generate mitotic indices in Figure 6.
Top three panels: *Spcdc25*EC ± LVS. Black bars, cytokinin level; white bars, cytokinin level + LVS.
Bottom three panels: EV ± LVS. Black bars, cytokinin level; white bars, cytokinin level + LVS.

where the duration of the cell cycle was reduced by 1 h compared with EV, although there was a compensatory lengthening in M + G1 (Figure 8).

Premature cell division is preceded by earlier CDK activities in Spcdc25 *cells compared with EV*

In *Spcdc25*EC, we detected persistently high CDKB1 kinase activity in early S phase, S/G2 and early M (Figure 3). However, CDKA activity was relatively constant before peaking in M + G1 (Figure 3a). In EV, CDKA activity was very similar to WT (Porceddu *et al.*, 2001; Sorrell *et al.*, 2001).

In the EV cells, CDKB1 activity data gave an isolated peak in early S phase, whereas in WT CDKB activity peaks in G2/M (Porceddu *et al.*, 2001; Sorrell at al., 2001). Zhang *et al.* (2005) showed that activation of CDK activity is dependent

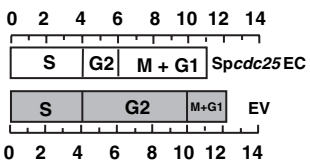

Figure 8. Cell cycle and component phases (h) for *Spcdc25*EC and EV.

on native CDC25-like activity. Also, in early S phase of WT a strong signal can be seen for CDKB1 at the RNA level (Figure 2b of Sorrell *et al.*, 2001). Therefore isolated CDKB1 activity in early S phase in the EV cells may not be completely surprising given that CDC25 activity can be high at G1/S (e.g. mammalian *CDC25B* in Jinno *et al.*, 1994). Also, note that the EV cell cycle has a very short M + G1 of 2 h compared with 5 h in *Spcdc25*EC and WT (Herbert *et al.*, 2001) and that the transient CDKB1 activity coincides with this perturbation.

We have shown that premature and sustained CDKB1 activity can result in premature cell division at a small mitotic size. Intriguingly, *Spcdc25* expression has its greatest influence on tobacco CDKB1. Note that unlike CDKA, CDKB1 activity is highest solely at the G2/M transition in WT BY-2 cells (Porceddu *et al.*, 2001; Sorrell *et al.*, 2001). Also, in Arabidopsis, the B type that has the PPTLRE signature only functions during G2 and M phase and is unique to plants. However, in both tobacco and Arabidopsis, CDKA activity is high during S, G2 and M, and in Arabidopsis CDKA has the strongly conserved PSTAIRE motif also found in yeast and animal CDKAs (Joubes *et al.*, 2000).

Spcdc25 *induces sister filaments of cells*

A strikingly visual result in these transformed lines was the appearance of double filaments of near-isodiametric cells in the *Spcdc25*-expressing lines and in a cell suspension derived from transgenic tobacco plants expressing *Spcdc25* constitutively. This is an unusual occurrence in WT BY-2 cells that typically grow in long single filaments, and cell length ratios are typically between 2:1 and 6:1 (unpublished data). Such filaments of long cells arise by transverse divisions. In *Spcdc25*EC the cells are considerably smaller in area, mainly due to a reduction in cell length resulting in isodiametric cells (Figure 5). Indeed, in some cases the width of the cell exceeds what should be its length as viewed along a filament of cells. Thus, we conclude that *Spcdc25*-induced reduction in cell length permits cells to divide either transversely *or* longitudinally.

When *Spcdc25* transcripts were induced in cultured tobacco roots, there was an increase in the frequency of lateral roots per primary root length (McKibbin *et al.*, 1998). Lateral root primordia are initiated from the pericycle close to the primary apical meristem and immediately adjacent to protoxylem poles (Dubrovsky *et al.*, 2001). Formative divisions are transverse as large 'mother' cells partition into smaller descendants. This is followed by a change in the plane of cell division from transverse to longitudinal so that these youngest primordia appear as a double filament of near-isodiametric cells (Dubrovsky *et al.*, 2001); they are not dissimilar in appearance to the double filaments observed in the *Spcdc25*-expressing BY-2 lines reported here.

Spcdc25-*expressing cells overcome a cytokinin requirement at G2/M*

As mentioned in the Introduction, there is accumulating evidence for a cytokinin-regulated G2/M transition in the plant cell cycle: LVS blocks cytokinin biosynthesis and prevents cells from traversing G2/M (Laureys *et al.*, 1998; Redig *et al.*, 1996). Cytokinin treatment activates the G2/M transition (Zhang *et al.*, 1996) and either *Spcdc25* or a cytokinin treatment can dephosphorylate plant CDC2 (Zhang *et al.*, 1996, 2005). Our data show that *Spcdc25*EC can traverse from G2 to M regardless of a LVS block on the cell cycle, whereas just like in WT (Redig *et al.*, 1996) this transition was blocked in EV cells.

We have shown BY-2 proliferative cells that do not rely on endogenous cytokinins. *SpCdc25*EC have remarkably low amounts of cytokinins compared with EV and with WT (Laureys *et al.*, 1998). Indeed, the levels of various cytokinins were virtually below detectable limits. Thus, the reason why *Spcdc25*EC can overcome a block imposed by LVS is because there is nothing for LVS to block. Clearly, EV cells require cytokinins for G2/M progression but *Spcdc25*EC do not. In fact the cytokinin data are consistent with *Spcdc25* expression leading to an inhibition of cytokinin biosynthesis.

In the *Spcdc25*EC cell size is stabilised to be about two-thirds that of the EV, a similar result to that obtained when *Spcdc25* was overexpressed in fission yeast (Russell and Nurse, 1986). However, for about 12–15 months constitutively expressing cells do not divide at a reduced cell size at each division (which would eventually result in mitotic catastrophe). In fission yeast, when the normal mitotic size control is abolished, such as by the overexpression of *Spcdc25*, a G1/S minimum size controller stabilises cell size thereby preventing the continual drift towards smaller cell sizes (Sveiczer *et al.*, 1996). The eventual demise of *Spcdc25*-expressing cultures after about 12 months might be because a cell size checkpoint is eventually over-ridden by *Spcdc25* expression.

In conclusion, in *Spcdc25*EC a shortened G2 phase and a small mitotic cell size are entirely consistent with premature CDKB1 kinase activity. In BY-2 cells small cell size is coincident with either transverse or longitudinal division. Finally, the data from the LVS treatments and cytokinin measurements show that *Spcdc25*EC are not dependent on endogenous cytokinins to progress from G2 to mitosis. The very recent cloning of *Arath;CDC25* (Landrieu *et al.*, 2004), which when overexpressed in fission yeast induces a short cell length (Sorrell *et al.*, 2005), means that a model: cytokinin → native CDC25 → CDKB1 → G2/M, can now be tested *in planta*.

Experimental procedures

The tobacco BY-2 cell line

The tobacco BY-2 cell line was cultured at 27°C in darkness in modified Linsmaier and Skoog (1965) medium and was subcultured in exactly the same way as detailed previously (Herbert *et al.*, 2001).

Transformation of the BY-2 cell line with Spcdc25

Stable transformation of BY-2 cells was achieved using a modified version of the method described by An (1985). Isolated colonies of *Agrobacterium tumefaciens* strain LBA4404 harbouring either the binary vector pBTX (empty vector) or pBTX-CDC25 (McKibbin *et al.*, 1998) were picked from fresh 2YT-kanamycin (50 μg ml^{-1}) plates and cultured overnight in 7 ml 2YT (without antibiotic) in 50 ml conical flasks at 30°C with shaking. Four millilitre aliquots of 6-day-old stationary phase BY-2 cells containing 20 μM of freshly added Acetosyringon (Sigma-Aldrich, Gillingham, UK) were co-cultivated with 100 μl of *Agrobacterium* culture in 90 mm Petri dishes sealed with Nescofilm for 2 days at 27°C in the dark without shaking. Cells were washed with 1 l of BY-2 medium using a cell dissociation sieve fitted with a 100 μm mesh (Sigma-Aldrich) and resuspended in 5 ml BY-2 medium containing 250 μg ml^{-1} Timentin (Melford Laboratories, UK), and 2.5 ml aliquots plated onto solidified BY-2 medium (0.8% agar) supplemented with 250 μg ml^{-1} Timentin and 80 μg ml^{-1} hygromycin. Plates were sealed with Micropore tape and incubated at 27°C in the dark. Isolated hygromycin-resistant calli (each individual callus was considered as an independent clone) appeared after 2–4 weeks, and were harvested and grown for a further 2 weeks on fresh plates. Calli were then transferred to 50 ml BY-2 medium supplemented with 250 μg ml^{-1} Timentin and 80 μg ml^{-1} hygromycin and incubated at 27°C and 75 ***g*** in the dark until the cultures reached stationary phase (1–3 weeks). Cultures were subsequently maintained as described for WT BY-2 cells using medium containing both 250 μg ml^{-1} Timentin and 80 μg ml^{-1} hygromycin, with the Timentin being omitted after the first subculture. Cultures were subjected to at least four rounds of subculturing before being used in synchrony experiments.

Synchronisation, mitotic index, cell size and microdensitometry

Each of the transformed cell lines was synchronised with aphidicolin using the exact protocol of Nagata *et al.* (1992). A 24 h exposure to, and subsequent removal of, this inhibitor of DNA replication will cause the vast majority of cycling cells to accumulate in late G1 at the boundary with the S phase. However, a minority of cells, trapped at the end of S phase will be the first to arrive at mitosis ahead of the bulk of cells previously held at G1/S. Hence, we measured the duration of G2 from zero to the initial rise of the mitotic index.

Following release from aphidicolin, and using Hoechst staining (Sigma-Aldrich) (Herbert *et al.*, 2001), the mitotic index was measured at hourly intervals for 24–26 h. In a separate experiment, LVS (Sigma-Aldrich) was added at a final concentration of 10 μm immediately following the removal of aphidicolin. Cells were sampled at hourly intervals for 10–12 h.

For each experiment a minimum of 200 cells per slide were scored on random transects across the width of the coverslip encompassing three replicate slides per sampling time per experiment. Images of cells in mitosis (prophase, metaphase or anaphase but not half-telophases) initially observed with an Olympus BH2 (UV, λ = 420 nm) were downloaded into a PC and the mitotic cell areas measured by image analysis using Sigmascan® (Jandel Scientific, San Rafel, CA, USA).

Following the removal of aphidicolin, samples were also taken every 2 h and fixed in 3:1 absolute ethanol:glacial acetic acid and stained by the Feulgen reaction (Powell *et al.*, 1988). The major modification was that in between each of the steps of the procedure – fixation, hydrolysis (5 M HCl for 25 min at 25°C), 2× rinse in ice-cold distilled water (5°C) and 2 h in Feulgen's reagent (25°C) – the cells were spun down gently (2000 ***g*** for 3 min), supernatant was removed and the next reagent added. Cells were then maintained in 45% (v/v) acetic acid. About 20 μl of cells were added to microscope slides and nuclear densities were determined using an M85A Scanning Microdensitometer (Vickers, York, UK) at 560 nm.

RNA extraction, cDNA synthesis and RT-PCR

Total RNA was extracted from tobacco BY-2 cells using TRI reagent (Sigma-Aldrich) and residual genomic DNA was removed by DNase treatment (Ambion Inc., Austin, TX, USA). Ribonucleic acid (5 μg) was treated with Superscript II reverse transcriptase (GibcoBRL, Paisley, UK). Complementary DNA was subjected to PCR with specific primers to *Spcdc25:* P2, 5′-GCGCGTCGACCATT-AACGTCTGGGGAAGC-3′ and P7, 5′-TTAGGTCCCCTTCTCCGATG-3′ amplifying a fragment of 718 bp, and to 18S rRNA: PUV, 5′-TTCCATGCTAATGTATTCAGAG-3′ and PUV4, 5′-ATGGTGGTG-ACGGGTGAC-3′ amplifying a fragment of 459 bp. Thermocycle conditions were: 35 cycles at 94°C (30 sec), 55°C (45 sec) and 72°C (1 min 20 sec). Separate cDNA reactions omitting reverse transcriptase were PCR amplified to confirm the absence of contaminating genomic DNA.

Expression of histone H4 was determined by semiquantitative RT-PCR using limited PCR cycles (30 cycles), essentially as described in Sorrell *et al.* (2002, 2005). Histone H4-specific primers H4F, 5′-GGCACAGGAAGGTTCTGAGGGATAACA-3′, and H4R, 5′-TAACCGCCGAAACCGTAGAGAGTCC-3′, amplifying a fragment of 320 bp were used. The optimal PCR cycle was determined by quantifying the PCR product for alternate cycles from cycle 24 to 38 of the PCR reaction, and choosing a cycle within the linear response of the curve (data not shown). Internal standards of cDNA dilutions were included with the samples to ensure linear amplification of the target at the cycle number used. Three replicates of the PCR reactions were performed to ensure consistent data and PCR products were quantified from ethidium bromide-stained agarose gels using GeneGenius (Syngene, Cambridge, UK) software.

*Tobacco cells transformed with 35SCaMV::*Spcdc25

Plants of *N. tabacum* cv. *Samsun* were grown in plastic boxes and leaf discs were transformed with a 35S CaMV::*Spcdc25* construct using *Agrobacterium*-mediated transformation as described in Bell *et al.* (1993). Primary transgenics known to be expressing *Spcdc25* by RT-PCR were selfed and seed was collected. One batch of this transgenic seed was sent from Cardiff University to the laboratory at the Department of Plant Physiology, Charles University, Prague. Seeds were germinated under standard *in vitro* conditions and internodes from 6-week-old plants were transferred to modified Murashige and Skoog (1962) liquid medium supplemented with 1 mg l^{-1} NAA and 1 mg l^{-1} 2,4-D (2,4-dichlorophenoxyacetic acid), and were cultivated on a rotary shaker in a 16 h photoperiod at 25°C.

Protein assays

Proteins were extracted from 5 ml of synchronised cultures essentially as described in Cockcroft *et al.* (2000). Equal amounts of protein were loaded onto gels, and loading was verified by Coomassie staining of replicate gels. Transfer to membranes was checked by Ponceau staining. For CDK assays immunoprecipitations were carried out using antisera raised to CDKA and CDKB1 (kindly provided by Drs Jim Murray and Marget Menges, Institute of Biology, Cambridge University) as described in Sorrell *et al.* (2001). Histone H1 protein kinase assays were as described in Cockcroft *et al.* (2000) using 2 μl of antiserum. Incorporation was assayed by quantification of autoradiographs using GeneGenius (Syngene, Cambridge, UK). For Western blots, an affinity-purified Spcdc25 antiserum was kindly provided by Dr Sergio Moreno, Centro de Investigación del cancer, Salamanca, Spain.

Cytokinin measurements

Frozen cell samples were ground in liquid nitrogen and transferred in Bieleski buffer (Bieleski, 1964). The deuterated standards were added to the extracts and incubated overnight at −20°C. Afterwards the cytokinins were purified on a combination of DEAE-Sephadex and RP-C18 cartridges. The purified extracts were loaded onto immunoaffinity columns containing monoclonal antibodies against cytokinins. After the immunoaffinity purification procedure, the cytokinins were analysed by HPLC linked to a Quattro II mass spectrometer equipped with an electrospray interface (Prinsen *et al.*, 1995). Analysis of the chromatograms obtained was done using MASSLYNX software (Micromass) and the cytokinin concentrations were calculated according to the principle of isotope dilution.

Acknowledgements

We thank Dr Luc Roef of Professor H. Van Onckelin's group (University of Antwerp) and Dr Margit Menges of Professor J. A. H. Murray's group (Cambridge University) for invaluable advice about BY-2 transformations and CDK assays and to M.M. for supplying CDKA and CDKB1 antibodies, and Dr Sergio Moreno (Centro de Investigación del Cancér, Salamanca, Spain) for the gift of the Spcdc25 antibody. We also thank BBSRC (P10942) and the Czech Republic's Ministry of Education, Youth and Sports (00A081) for research grants. C.B.O. and I.S. thank UC Worcester and Cardiff University for research studentships.

References

An, G.H. (1985) High-efficiency transformation of cultured tobacco cells. *Plant Physiol.* **79**, 568–570.

Bell, M.H., Halford, N.G., Ormrod, J.C. and Francis, D. (1993) Tobacco plants transformed with *cdc25*, a mitotic inducer gene from fission yeast. *Plant Mol. Biol.* **23**, 445–451.

Bieleski, R.L. (1964) The problem of halting enzyme action when extracting plant tissues. *Anal. Biochem.* **121**, 431–442.

Cockcroft, C.E., den Boer, B.G., Healy, J.M.S. and Murray, J.A.H. (2000) Cyclin D control of growth rate in plants. *Nature*, **405**, 575–579.

Crowell, D.N. and Salaz, M.S. (1992) Inhibition of growth of cultured tobacco cells at low concentrations of lovastatin is reversed by cytokinin. *Plant Physiol.* **100**, 2090–2095.

Dubrovsky, J.G., Rost, T.L., Colon-Carmona, A. and Doerner, P. (2001) Early primordium morphogenesis during lateral root initiation in *Arabidopsis thaliana*. *Planta*, **214**, 30–36.

Francis, D., Davies, M.S., Braybrook, C., James, N.C. and Herbert, R.J. (1995) An effect of zinc on M-phase and G1 of the plant cell cycle in the synchronous TBY-2 tobacco cell suspension. *J. Exp. Bot.* **46**, 1887–1894.

Gatz, C., Frohberg, C. and Wendenberg, R. (1992) Stringent repression and homogenous derepression by tetracycline of a modified CaMV 35S promoter in intact transgenic tobacco plants. *Plant J.* **2**, 397–404.

Gould, K.L. and Nurse, P. (1989) Tyrosine phosphorylation of the fission yeast cdc2 protein kinase regulates entry into mitosis. *Nature*, **342**, 39–45.

Herbert, R.J., Vilhar, B., Evett, C., Orchard, C.B., Rogers, H.J., Davies, M.S. and Francis, D. (2001) Ethylene induces cell death at particular phases of the cell cycle in the tobacco BY-2 cell line. *J. Exp. Bot.* **52**, 1615–1623.

Jinno, S., Suto, K., Nagata, A., Igarashi, M., Kanaoka, Y., Nojima, H. and Okayama, H. (1994) Cdc25 is a novel phosphatase functioning early in the cell cycle. *EMBO J.* **13**, 1549–1556.

Joubes, J., Chevalier, C., Dudits, D., Heberle-Bors, E., Inze, D., Umdea, M. and Renaudin, J.P. (2000) CDK-related protein kinases in the plant cell cycle. *Plant Mol. Biol.* **43**, 607–620.

Landrieu, I., da Costa, M., De Veylder, L. *et al.* (2004) A small CDC25 dual-specificity tyrosine-phosphatase isoform in *Arabidopsis thaliana*. *Proc. Natl Acad. Sci. USA*, **101**, 13380–13385.

Laureys, F., Dewitte, W., Witters, E., Van Montague, M., Inze, D. and Van Onckelen, H. (1998) Zeatin is indispensable for the G2-M transition in tobacco BY-2 cells. *FEBS Lett.* **426**, 29–32.

Linsmaier, E.M. and Skoog, F. (1965) Organic growth factor requirement of tobacco tissue. *Physiol. Plant.* **18**, 100–127.

McKibbin, R., Halford, N.G. and Francis, D (1998) Expression of fission yeast *cdc25* alters the frequency of lateral root formation in transgenic tobacco. *Plant Mol. Biol.* **36**, 601–612.

Murashige, T. and Skoog, F. (1962) A revised medium for rapid growth and bioassay with tobacco tissue cultures. *Physiol. Plant.* **15**, 473–479.

Nagata, T., Nemoto, Y. and Hasezewa, S. (1992) Tobacco BY-2 cell line as the 'HeLa' cell line in the cell biology of higher plants. *Int. Rev. Cytol.* **132**, 1–30.

O'Farrell, P.H. (2001) Triggering the all-or-nothing switch into mitosis. *Trends Cell Biol.* **11**, 512–519.

Porceddu, A., Stals, H., Reichheld, J.P., Segers, G., De Veylder, L., Pinho Barroco de, R., Casteels, P., Van Montagu, M., Inze, D. and Mironov, V. (2001) A plant-specific cyclin-dependent kinase is involved in the control of the G2M transition in plants. *J. Biol. Chem.* **276**, 36364–36360.

Powell, M.J., Davies, M.S. and Francis, D. (1988) Effects of zinc on meristem size and proximity of root hairs and xylem elements to the root tip in a zinc-tolerant and non-tolerant cultivar of *Festuca rubra* L. *Ann. Bot.* **61**, 723–726.

Prinsen, E., Redig, P., Van Dongen, W., Esmans, E. and Van Onckelen, H.A. (1995) Quantitative analysis of cytokinins by electrospray tandem mass spectrometry. *Rapid Commun. Mass Spectrom.* **9**, 948–953.

Redig, P., Shaul, O., Inze, D.H., Van Montague, M. and Van Onckelen, H. (1996) Levels of endogenous cytokinins, indole-3-acetic acid and abscisic acid during the cell cycle of synchronised tobacco BY-2 cells. *FEBS Lett.* **391**, 175–180.

Russell, P. and Nurse, P. (1986) *cdc25*+ functions as an inducer of mitotic control of fission yeast. *Cell*, **45**, 145–153.

Russell, P. and Nurse, P. (1987) Negative regulation of mitosis by *wee1*$^{+}$, a gene encoding a protein kinase homologue. *Cell*, **49**, 559–567.

Sorrell, D.A., Menges, M., Healy, J.M.S., Deveaux, Y., Amano, C., Kagami, H., Shinmo, A., Doonan, J.H., Sekine, M. and Murray,

J.A.H. (2001) Cell cycle regulation of cyclin-dependent kinases in tobacco cultivar Bright Yellow-2 cells. *Plant Physiol.* **126**, 1214–1223.

Sorrell, D.A., Marchbank, A., McMahon, K., Dickinson, J.R., Rogers, H.J. and Francis, D. (2002) A WEE1 homologue from *Arabidopsis thaliana*. *Planta*, **215**, 518–522.

Sorrell, D.A., Chrimes, J.R., Rogers, H.J. and Francis, D. (2005) The Arabidopsis CDC25 induces a short cell length when overexpressed in fission yeast: evidence for cell cycle function. *New Phytol.* **165**, 425–428.

Sun, Y., Dilkes, B.P., Zhang, C., Dante, R.A., Carneiro, N.P., Lowe, K.S., Jug, R., Gordon-Kamm, W.J. and Larkins, B.A. (1999) Characterization of maize (*Zea mays* L.) Wee1 and its activity in developing endosperm. *Proc. Natl Acad. Sci. USA*, **96**, 4180–4185.

Sveiczer, A., Novak, B. and Mitchison, J.M. (1996) The size control of fission yeast revisited. *J. Cell Sci.* **109**, 2947–2957.

Wyrzykowska, J., Pien, S., Shen, W.H. and Fleming, A.J. (2002) Manipulation of leaf shape by modulation of cell division. *Development*, **129**, 957–964.

Zhang, K., Letham, D.S. and John, P.C.L. (1996) Cytokinin controls the cell cycle at mitosis by stimulating the tyrosine dephosphorylation and activation of $p34^{cdc2}$-like histone kinase. *Planta*, **200**, 2–12.

Zhang, K., Diderich, L. and John, P.C.L. (2005) The cytokinin requirement for cell division in cultured *Nicotiana plumbaginofolia* cells can be satisfied by yeast Cdc25 tyrosine phosphatase. Implications for mechanisms of cytokinin response and plant development. *Plant Physiol.* **137**, 308–316.

Manuscript Draft

Manuscript Number:

Title: Tobacco cells transformed with fission yeast Spcdc25 mitotic inducer display growth and morphological characteristics as well as starch and sugar status evocable by cytokinin application.

Article Type: Research Paper

Keywords: carbohydrate status; cdc25; cell cycle; cell morphology; cytokinin; Nicotiana tabacum; Schizosaccharomyces pombe

Corresponding Author: Mrs. Helena Lipavska, RNDr., PhD.

Corresponding Author's Institution: Charles University in Prague

First Author: Petra Suchomelová-Mašková, M.Sc.

Order of Authors: Petra Suchomelová-Mašková, M.Sc.; Ondřej Novák, PhD; Helena Lipavska, RNDr., PhD.

Abstract: In plants, the G2/M control of cell cycle remains an elusive issue as doubts persist about activatory dephosphorylation - in other eucaryots provided by CDC25 phosphatase and serving as a final all-or-nothing mitosis regulator. We report on the effects of tobacco (Nicotiana tabacum L., cv. Samsun) transformation with yeast (Schizosaccharomyces pombe) cdc25 (Spcdc25) on cell characteristics. Transformed cell suspension cultures showed higher dry mass accumulation during exponential phase and clustered more circular cell phenotype compared to chains of elongated WT cells. Similar cell parameters, as in the transformants, can be induced in WT by cytokinins. Spcdc25 cells after cytokinin treatment showed giant cell clusters and growth inhibition. In addition, Spcdc25 expression led to altered carbohydrate status: increased starch and soluble sugars with higher sucrose: hexoses ratio, inducible in WT by cytokinin treatment. Taken together, the Spcdc25 transformation had cytokinin-like effect on studied characteristics. However, endogenous cytokinin determination revealed markedly lower cytokinin levels in Spcdc25 transformants. It indicates that the cells sense Spcdc25 expression as an increased cytokinin availability, manifested by changed cell morphology, and in consequence decrease endogenous cytokinin levels.

Clearly, the results on cell growth and morphology are consistent with the model of G2/M control including cytokinin-regulated activatory dephosphorylation. Nevertheless, no clear link is obvious between Spcdc25 transformation and carbohydrate status and thus the observed cytokinin-like effect on carbohydrate levels pose a problem. Hence, we propose that Spcdc25-induced higher CDK(s) activity at G2/M generates a signal modifying carbohydrate metabolism to meet high energy and C demands of forthcoming cell division.

Running title: Cytokinin-like characteristics of *Spcdc25* tobacco cells

Title: Tobacco cells transformed with fission yeast *Spcdc25* mitotic inducer display growth and morphological characteristics as well as starch and sugar status evocable by cytokinin application.

Author´s names: Petra Suchomelová-Mašková[a], Ondřej Novák[b], Helena Lipavská[a,*]

Institution:

[a] Department of Plant Physiology, Faculty of Science, Charles University in Prague, Viničná 5, 128 44, Prague 2, Czech Republic

[b] Laboratory of Growth Regulators, Palacký University & Institute of Experimental Botany, Academy of Sciences of the Czech Republic, Šlechtitelů 11, Olomouc, Czech Republic

Correspondence author: * Helena Lipavská, Department of Plant Physiology, Faculty of Science, Charles University in Prague, Viničná 5, 128 44, Prague 2, Czech Republic, fax number: +420221951704, e-mail address: lipavska@natur.cuni.cz

Abstract:

In plants, the G2/M control of cell cycle remains an elusive issue as doubts persist about activatory dephosphorylation - in other eucaryots provided by CDC25 phosphatase and serving as a final all-or-nothing mitosis regulator. We report on the effects of tobacco (*Nicotiana tabacum* L., cv. Samsun) transformation with yeast (*Schizosaccharomyces pombe*) *cdc25* (*Spcdc25*) on cell characteristics. Transformed cell suspension cultures showed higher dry mass accumulation during exponential phase and clustered more circular cell phenotype compared to chains of elongated WT cells. Similar cell parameters, as in the transformants, can be induced in WT by cytokinins. *Spcdc25* cells after cytokinin treatment showed giant cell clusters and growth inhibition. In addition, *Spcdc25* expression led to altered carbohydrate status: increased starch and soluble sugars with higher sucrose: hexoses ratio, inducible in WT by cytokinin treatment. Taken together, the *Spcdc25* transformation had cytokinin-like effect on studied characteristics. However, endogenous cytokinin determination revealed markedly lower cytokinin levels in *Spcdc25* transformants. It indicates that the cells sense *Spcdc25* expression as an increased cytokinin availability, manifested by changed cell morphology, and in consequence decrease endogenous cytokinin levels. Clearly, the results on cell growth and morphology are consistent with the model of G2/M control including cytokinin-regulated activatory dephosphorylation. Nevertheless, no clear link is obvious between *Spcdc25* transformation and carbohydrate status and thus the observed cytokinin-like effect on carbohydrate levels pose a problem. Hence, we propose that *Spcdc25*-induced higher CDK(s) activity at G2/M generates a signal modifying carbohydrate metabolism to meet high energy and C demands of forthcoming cell division.

Keywords:

carbohydrate status; *cdc25*; cell cycle; cell morphology; cytokinin; *Nicotiana tabacum*; *Schizosaccharomyces pombe*;

Abbreviations:

BAP – 6-benzylaminopurine

CDK – cyclin-dependent kinase

NSS – non-structural soluble saccharide

PPB – preprophase band

1. Introduction:

Temporal and spatial control of cell cycle is essential for initiation and maintenance of meristems and for regulation of organogenesis, therefore it represents one of the most intensively studied processes in contemporary plant biology. The basic mechanisms of cell cycle are conserved among all eucaryots and a lot of knowledge has been achieved with yeast and animal model organisms. The study of plant cell cycle, however, lacks behind, partly also because of the existence of unique regulatory pathways not described for other eukaryotes.

As in all eucaryotic organisms plant cell cycle progression is governed by cyclin-dependent kinase (CDK) activities. In yeasts, a single CDK associated with different cyclins regulates the progression through the cell cycle, while, in mammals, several distinct CDKs function at different stages of the cell cycle. In plants, the transition through G_1/S and G_2/M control points is regulated by CDKA and CDKA/B kinase activities, respectively. For activation of CDK, the presence of regulatory cyclin subunit is necessary; D-type cyclins at G_1/S and A and B-type cyclins, event. D-type cyclins as CDKB partners, at G_2/M (for review see e.g. [5, 13]). Beside these, the modulation of CDK/cyclin complex activity is provided by CDK inhibitors (predominantly active at G_1/S) and reversible (de)phosphorylation on conserved CDK amino acid residues (Thr 160-167, Thr 14 and Tyr 15). For fully active CDK/cyclin entering mitosis, it is necessary to be phosphorylated at Thr160-167 (accomplished by CDK-activating kinase) and desphosphorylated at Thr14 and Tyr15. In yeast this dephosphorylation, provided by Cdc25 phosphatase, is the most important regulation mechanism representing final positive regulator of mitosis [23]. A time ago inhibitory kinase Wee1 was characterised, exhibiting a large cell phenotype in plants with dominant – negative allele of this gene [35, 38]. During last decade, the effort to find plant activatory G_2/M phosphatase was not fully successful, the only *cdc25* orthologue has been identified in unicellular alga *Ostreococcus tauri* [14]. Although a Cdc25-like catalytic protein subunit with

in vitro CDK- binding and activatory capability has recently been identified in higher plants (*Arabidopsis* and rice), the gene is not able, unlike the algal one, to complement yeast *cdc25* mutant strains and its mutation exhibit no obvious phenotype in plants [15, 34]. All these pieces of knowledge are strongly arguing for further study of transgenic plants expressing foreign *cdc25* gene.

The cell division process is very sensitive to extra- and intracellular signals influencing mainly transition through control points. At G_1/S the rate-limiting factor is actual level of D cyclin, whose expression is under control of phytohormones, especially cytokinins, and sucrose [27, 28]. Cytokinin together with auxin induced the expression and probably activity of CDK throughout the cell cycle and cytokinins also repressed the expression of some CDK inhibitors [26]. The stimulatory cytokinin and auxin effects at G_2/M have been documented for mitotic cyclins expressions as well [26]. Cytokinins, however, seemed to be indispensable for entry into mitosis [16, 47]. One of the reasons could be that cytokinin stimulates dephosphorylation of CDK supposedly through activation of plant CDK phosphatase [47]. The authors demonstrated that fission yeast Cdc25 was able to dephosphorylate plant CDK and that the primary signal for plant CDK activatory dephosphorylation at mitosis entry came from cytokinin [47].

Many studies have been devoted to investigation of the effect of fission yeast *Spcdc25* expression on plant growth and development. Bell et al. [2] in glasshouse experiments with day-neutral tobacco constitutively expressing fission yeast *Spcdc25* gene showed, besides others, an earlier onset and enhanced intensity of flowering. Our study (Teichmanova et al., submitted) reported a marked positive effect of sucrose on flowering induction in day-neutral tobacco plants under in vitro and the remarkable impact of fission yeast *Spcdc25* expression on the flowering gradient, status of apical meristem and overall floral capacity. McKibbin et al. [17] demonstrated in *Spcdc25* plants higher amount of lateral root primordia composed of

smaller cells. We found out that the fission yeast *Spcdc25* expression exhibit a cytokinin-like effect on de novo organ formation on tobacco stem segments of transformed plants manifested by earlier and more abundant shoot formation and restricted root induction as well as cytokinin-independent shoot regeneration in transgenic material [37]. Moreover, Orchard et al. [24] in *Spcdc25*-expressing BY-2 cells observed earlier onset of mitosis in transgenic lines together with smaller cell size phenotype accompanied by extremely low cytokinin levels in transgenic cells. However, such long-living cultures could exhibit very specific phenotype caused at least partially by epigenetic changes with the potential risk of changes in cell cycle duration (see e.g. [33, 47]). We established newly derived tobacco (*Nicotiana tabacum*, cv. Samsun) cell cultures expressing fission yeast *Spcdc25* to determine the effect of mitotic activator on cellular morphogenesis and growth characteristics as opposed to wild type cell cultures. Another aim of this study was to examine to what extent it is possible to mimic the effect of transformation in wild type cultures by exogenous cytokinin application.

2. Results:

2.1. Growth and morphological characteristics

The cell suspension cultures, derived from stem segments of tobacco lines (A, C and F) independently transformed with fission yeast *Spcdc25* gene, were used for determination of the changes in cell characteristics. For evaluation of relative growth rates (dry weight at sampling time related to inoculum dry weight) the cultures on 14th day after subcultivation (the exponential growth phase) were selected. At this stage all tested *Spcdc25* transgenic cell suspension cultures reached significantly higher growth rates compared to the wild-type (WT) cell cultures (*figure 1A*). Nevertheless, time curves of relative growth rates showed that the exponential phase of WT cultures tends to be longer and the maximum relative biomass accumulation of WT cultures finally comparable to transgenic ones (data not shown).

The cell morphology and cell size were evaluated on 14th day after subcultivation and only mitotic cells were measured to compare cell parameters. For quantitative measurements two-dimensional image analysis was employed. Surprisingly, cells of tobacco lines A, C and F exhibited variable mitotic cell size. When compared with wild type, the average cell area of *Spcdc25* lines mitotic cells was similar or even increased (*figure 2*).

In contrast, the transformation with *Spcdc25* resulted in marked changes in cell shape. The evaluation of the parameter of circularity and elongation proved more circular (isodiametric) cell phenotype of transformed cells (*figure 3A,B*). In all *Spcdc25* transgenic lines the value of circularity was definitely significantly higher and the parameter of elongation lower than it was established for the WT cells. Even more pronounced effect of tobacco transformation with fission yeast *Spcdc25* gene was found as regards cell arrangement. WT cells commonly formed chains (*figure 4A*) as it was documented for other plant cell cultures e.g. model tobacco BY-2 cell culture. On the contrary, transformed cells were mostly arranged in clusters of different size (*figure 4B,D*) as we also documented earlier

for BY-2 [24]; and in some cases cell chains of doublets were observed in the cultures (*figure 4B*, in a slit). To strengthen the reliability of observed phenomena we evaluated also *Spcdc25* tobacco internode segment-derived calli cultivated on solid media as well as cell suspension cultures cultivated on roller enabling reduction of mechanical strains caused by mixing necessary for aeration of cultures and detected that similar cell characteristics prevailed (data not shown).

2.2. Starch and sugar content

When evaluating morphological cell characteristics we observed plenty of colourless bodies in the cytosol of *Spcdc25* transgenic cells. None or only few such bodies of small size were found in WT cells. Histochemical tests with Lugol solution proved them to be starch granules. The representative photographs of stained cells are documented in the *figure 5A, B and D*. All detected bodies in transgenic cells are stainable by kalium iodide while in the WT cells low number of small light brown coloured starch grains were found. Although the results of histochemical detection are rather persuasive we supplemented the observations with more precise biochemical determination of starch levels quantified by high performance liquid chromatography (HPLC). The amount of glucose obtained after enzymatic hydrolysis with α-amylase and amyloglucosidase is presented in the *figure 6*. As clearly visible, there were significantly higher or even manifold higher glucose levels in transgenic lines samples compared to WT ones.

To understand the carbohydrate context of changed starch levels we also compared the soluble carbohydrate levels, both in WT as well as transgenic cells. The same trend as for starch was observed as regards sugar levels. The total soluble carbohydrate amounts were slightly or significantly higher in studied transgenic lines in contrast to WT cells (*figure 7A*). Most remarkable difference was found in sucrose: hexoses ratio. In the transgenic cells the sucrose prevailed while WT cells contained mainly hexoses.

2.3. The effect of cytokinin treatment

Some of the above-described changes in transgenic cultures (morphological shifts as well as changes in saccharide levels) are referred to be achieved by exogenous cytokinin treatment. Besides these, we published earlier [37] that, in the system of de novo regeneration on internode stem segments, *Spcdc25* expression induces cytokinin-like shift in the organogenic response. Hence, we wondered whether the application of commonly used stable cytokinin (6-benzylaminopurine (BAP)) could simulate the effect of *Spcdc25* transformation in the WT cell cultures and what would be the effects of the cytokinin treatment in transgenic cell lines. As the tobacco cell cultures used in this study were independent of exogenous cytokinin, the possible effect of cytokinin treatment seemed to be quite simply interpretable.

2.3.1. Growth rates and cell characteristics

The treatment of cultures with exogenous cytokinin led to different response in WT and transgenics. While WT cells on medium with 1 $mg.l^{-1}$ BAP showed similar growth as transformed cells cultivated on cytokinin-free medium (*figure 1B*), in transformants more or less dramatic drop of growth was registered. Cytokinin supply to transformed cells even at very low concentrations (0.1 $mg.l^{-1}$) caused mostly a rapid decrease of biomass accumulation (*figure 1B*) and exposure of *Spcdc25* transgenic cultures to higher cytokinin concentration (1 $mg.l^{-1}$) led to even more pronounced drop in the growth. In wild type cell cultures twofold increase in cytokinin concentration (2 $mg.l^{-1}$) led to only moderate changes in growth rates (*figure 1B*) but a further increase in cytokinin application into the medium to 5 and 10 $mg.l^{-1}$ did not promote growth, even inhibited it (data not shown).

It is often stressed that cytokinin levels are in tight relationship with auxin ones. For BY-2 cells it was published that the cultures in medium where auxin was omitted showed similar characteristics as after cytokinin application [19].

Therefore, to change the endogenous auxin:cytokinin balance we transferred the cultures on growth regulator-free medium (omitting both, cytokinin and auxin). The difference between the responses was dramatic. Compared to the WT cultures (reaching 47% of auxin supported culture, *figure 1A*) the drop in growth rates in transgenic line was much more pronounced (5%). Cell characteristics were also at the centre of our interest. By exposure of cells to 1 $mg.l^{-1}$ BAP for 14 days WT cells failed to form regular chains, divided chaotically and instead, they formed clumps of variable size composed of more circular cells (*figure 4C*) similar to those of *Spcdc25* transformed cells cultivated without BAP. Sometimes cell chains of doublets were observed similar to transgenic line A. Transformed cells in BAP-containing medium, on the contrary, established giant clusters of hardly viable cells.

2.3.2. Starch and sugar contents

Similarly, to complete the characterisation of cultures under cytokinin treatment we measured the starch a soluble sugars contents. The BAP application to wild type cells caused again similar changes to those induced by the *Spcdc25* transformation. In BAP treated WT cells the amount and size of starch grains increased (*figure 5C*), and the rise in starch levels was also confirmed by biochemical determination of starch-originating glucose levels (*figure 6*).

Simultaneously we proved higher total soluble carbohydrate levels in exogenous cytokinin influenced WT cells together with sucrose:hexoses ratio shifted to sucrose, regardless of the BAP concentrations (1 $mg.l^{-1}$ or 2 $mg.l^{-1}$ BAP) (*figure 7B*).

2.4. Endogenous cytokinin levels

The results of cytokinin-like effect of *Spcdc25* transformation led us to check the endogenous cytokinin contents in transgenics to clarify whether actual changes in cytokinin levels or other regulatory mechanisms are responsible for observed phenomena. For cytokinin determination, the cell cultures of WT and transformant C on the 12^{th} day of subcultivation were used, similarly as for cell characteristics and growth measurements. Although the total cytokinin

levels are relatively low in both variants (*figure 8A*), it is clearly apparent that the levels are significantly lower in transgenics, reaching only one third of the WT cell levels. The graph presenting levels of individual cytokinins shows that the vast majority of cytokinins (over 90%) are *cis*-zeatin derivatives. In the samples there were comparable levels of *trans*-zeatin, slightly elevated levels of dihydrozeatin-type cytokinins in transformant C and slightly elevated levels of isopentenyladenine-type cytokinins in WT. Moreover, the levels of phosphates of all three types of cytokinins are also higher in WT (*figure 8B*).

3. Discussion

3.1. The cell cultures of all fission yeast Spcdc25 transformed tobacco lines under study exhibited higher dry mass accumulation during exponential phase in comparison to wild type (WT). There is a number of evidence that any change in cell cycle gene expression can cause a shift in cell cycle progression (see Introduction) consequently altering the rate of cell division. In yeast, the *cdc25* mitotic activator overexpression accelerates the entry of cells into mitosis [29]. Thus, transformation of plants with *Spcdc25* under strong promoter might be in cell cultures manifested as the acceleration of the cell cycle conducive smaller cell size phenotype and/or the shortening of G_2 phase with compensatory prolongation of G_1 phase. In fission yeast, *cdc25* overexpression led to a decrease in mitotic cell length through G_2 shortening, nevertheless the overall cell cycle duration was similar to WT [29]. Orchard et al. [24], however, found out in BY-2 cells expressing *Spcdc25* that G_2 phase was shortened, the mitotic cell size reduced and although there was a compensatory prolongation of G_1 phase, the cell cycle duration was still reduced. The observed enhanced dry mass accumulation in the *Spcdc25* cultures under study (*figure 1A*) is then in accordance with assumed cell division acceleration.

3.2. Transformed cells exhibited clustered, more circular cell phenotype compared to elongated in chains arranged WT cells. Further, we focused on cell size and shape determination to confirm the hypothesis that these characteristics are altered in consequence of *Spcdc25* expression. Given that *Spcdc25* expression leads to G_2 phase shortening, the premature entry into mitosis could cause a chaotic organisation of cell division. This assumption was proved by observed cell culture phenotype exhibiting low organisation (event. appearance of cell chains of doublets) (*figure 4A, B and D*). The finding is fully in accordance with the results obtained by Orchard et al. [24] in *Spcdc25* transformed BY-2 cells where sister filaments were documented. In addition we observed a significant alteration in

cell shape that was quantified by measurements of circularity and elongation parameters also arguing for acceleration of the entry into mitosis and differently organised cell plane building (*figure 3A,B*). It corresponds well with the data on fission yeast *wee1*$^-$ mutants that formed very short, almost round cells [32].

On the contrary, we repeatedly did not detect smaller cells in transgenic cell cultures (*figure 2*) as Orchard et al. [24] described for BY-2 *Spcdc25* cultures. One possible explanation of this discrepancy could be that G1 phase compensatory prolongation is deepened so that the overall cell cycle duration is similar to WT as in the case of fission yeast *cdc25* overexpression [29] or other mechanism regulating cell size at mitosis function in our plant material. Interestingly, Sorrell et al. [33] indicated that different results for D-cyclin expression profile in BY-2 cells compared to other plant species could be caused by specific properties of this culture, set by its longevity and "immortality" related to changed phenotype/genotype. This suggestion led us to speculate that the results achieved with the model system, as BY-2 is, could in some cases differ from those obtained with other tobacco cell cultures/lines.

3.3. Cytokinin application to WT cells induced similar changes in growth and morphological parameters to those induced by the Spcdc25 transformation. Changes in cell morphology resembling those found in *Spcdc25* transformants have been shown to be inducible with cytokinin application. Petrasek [25] found out that application of 4,5 μM 6-benzylaminopurine (BAP) to cytokinin-independent tobacco culture VBI-0 changed the filamentous phenotype to spherical one. This phenomenon strengthened with proceeding subcultures. The effect has been ascribed to indirect impact of BAP on cytoskeleton, especially microtubules [30]. Based on our results in context of contemporary models of cytokinin-induced regulation of G_2/M transition, other explanation of observed phenomena in VBI-0 cells is at disposal. BAP application to tobacco cultures could drive the cells faster into

mitosis, which results in disorganised building of cell division plane. Numerous data show tight relationship of cell cycle machinery with cytoskeleton. It has been shown, that cyclin-dependent kinase A (CDKA) co-localises with mitotic structures, e.g. preprophase band (PPB), anaphase spindle and phragmoplast [42]. Microinjection of purified active CDK/cyclin B complexes to stamen hair of *Tradescantia* accelerated prophase progression and induced rapid destabilisation of the PPB [12]. Moreover, the presence of nondegradable mitotic cyclin B1 in tobacco led to reorganisation of microtubules in phragmoplast as well as failure in organising cortical microtubules resulting in isodiametric shape of epidermal cells [44]. Ectopic expression of cyclin B2 in alfalfa besides acceleration of the entry into mitosis shortened the time-window of the appearance of the PPB, an important factor for the orientation of cell division [43].

Hence, the application of exogenous cytokinin (commonly used 6-benzylaminopurine (BAP)) was tested. The aim was to verify the idea that the *Spcdc25*-transformation-caused changes were of cytokinin-inducible nature in WT cells under study. The results validated the assumption as the WT cells after cytokinin treatments failed to form chains and were instead arranged in clusters or chains of cell doublets (*figure 4C*).

3.4. After BAP application, Spcdc25 transformed cells showed inhibition of growth and establishment of giant clusters of cells with markedly reduced viability. Providing that the influence of *Spcdc25* transformation and cytokinin application have additive nature we could expect that cytokinin treatment would further deepen Spcdc25-induced morphology characteristics. To summarise the results from experiments with cytokinin application, we state that any cytokinin supply that is stimulatory for WT cultures, the transgenic cells sense as inhibitory (presumably like “cytokinin overdose”) (*figure 1B*). The effect of auxin depletion from the medium can be interpreted similarly.

3.5. Are the results discussed above in harmony with contemporary model of the regulation at G_2/M transition in plants? The question is difficult to answer as 1) the introduced gene is not of plant origin, and in particular 2) a consensus has not been reached as regards the phosphorylation/dephosphorylation regulation of plant CDK activity and especially phosphatase responsible for CDK activation at G_2/M. CDKs in higher plants are probably, similarly as in other eucaryots, negatively controlled by phosphorylation at G_2 because tyrosine phosphorylation has been detected unambiguously under cytokinin deprivation, osmotic stress or DNA damage [31, 47] and orthologues of the Wee1 kinase have been described [9, 35, 41]. Recently, the first plant *cdc25* orthologue has been identified in unicellular alga *Ostreococcus tauri* [14]. It encodes a protein, which can complement fission yeast *cdc25* mutant. Soon after, in higher plant (*Arabidopsis*) a small isoform of tyrosine phosphatase has been identified [15, 34]. The sequence includes a catalytic domain of cdc25-like protein; nevertheless, it seems to function as a heterodimer whose regulatory subunit has not been revealed so far. However, *cdc25* expression was not enhanced in rapidly dividing compared with non-proliferative *Arabidopsis* tissues [34]. The failure to fully identify plant homologue of *cdc25* led recently [3] to suggestion that tyrosine dephosphorylation in plants might be achieved by a phosphatase unrelated to cdc25 or even that the CDC25-controlled onset of mitosis might have been evolutionarily replaced by a B-type CDK-dominated pathway, eventually resulting in the loss of the *cdc25* gene. However, the local expression of the *Spcdc25* gene in tobacco leaves resulted in modulation of cell division patterns [46]. Further, *Spcdc25* expression induces a small cell size in the root meristems of tobacco plants [17] and in tobacco BY-2 cells [24], and shortens G_2 phase of the BY-2 cell cycle through a premature peak of CDKB-kinase activity and bypasses a cytokinin requirement at G_2/M [24]. Hence, the results indicate that *Spcdc25* functions as a mitotic inducer in the plant cell cycle

and recognises G_2/M CDK(s) as substrates. Moreover, Sorrell et al. [34] reported on *Arabidopsis cdc25* inducing a short cell length when expressed in fission yeast.

Cdc25 plant homologue or protein fulfilling in plants the same role is proposed to be activated by cytokinins, e.g. [47]. In case we accept this conception, it is easy to understand that *Spcdc25* transformation induced changes in cell division manifested by altered morphological characteristics that mimic the cytokinin application. Moreover, our previous results demonstrated a cytokinin-like effect of fission yeast *Spcdc25* transformation on de novo organ formation in tobacco stem segments manifested by earlier and more abundant shoot formation and restricted root induction [37]. Taken together, our results achieved either on organ or on cellular level are consistent with the model of cell cycle control proposing the cytokinin regulation of CDK activatory dephosphorylation through so far unknown protein action.

3.6. Transgenic cultures showed changes in carbohydrate accumulation; increased starch and soluble sugar levels with higher sucrose proportion in the sugar spectrum. When the cell characteristics were followed we noticed the enhanced presence of small objects in transformed cells that by histochemical tests proved to be starch bodies (*figure 5A, B and D*). The biochemical quantification supported the differences between starch amounts of control and transgenics (*figure 6*) and motivated us to compare the levels of endogenous soluble carbohydrates as the carbohydrate metabolism functions as a network of negative and positive feedback signalling pathways precisely regulating the levels of individual carbohydrates, in particular the balance between soluble carbohydrates and starch levels, e.g. [20]. The observed change in sucrose: hexoses ratio (*figure 7A*) further pointed to the carbohydrate metabolism disturbance resulting from *Spcdc25* transformation.

3.7. BAP application to WT cells caused shift in carbohydrate levels towards those found in Spcdc25 transformants. It is well known that there exists mutual relationship between

cytokinin levels and carbohydrate status of a plant [4, 7, 8]. For cytokinin-independent BY-2 cell cultures it has been published that cytokinin application as well as absence of auxin in the medium results in amyloplast accumulation [18, 19]. Cytokinin application enhanced the expression of plasma membrane hexose uptake carriers in *Chenopodium rubrum* cell suspension cultures thus improving carbohydrate supply to the cells [1]. Therefore, the increase in starch deposition as well as higher soluble carbohydrate levels after cytokinin application (*figure 5C, 6 and 7B*) seems to be in accordance with literature data. In contrast, the question arises how to explain the similar changes induced by *Spcdc25* transformation.

3.8. The Spcdc25 transformation resulted in a decrease of endogenous cytokinin levels.

When discussing the results on growth and cellular characteristics presented here as well as those on de novo organ formation [37] we pointed to the fact that in all cases we observed a cytokinin–like effect of *Spcdc25* transformation. We based our explanation on the idea of Spcdc25 acting as mitotic inducer simulating cytokinin activation of plant cdc25-like phosphatase, and thus having impact on cell-division-dependent processes resembling cytokinin application. As *Spcdc25* transformation operates downstream the cytokinin action, we proposed that constitutive *Spcdc25* expression could be sensed by the plant as high cytokinin availability and in consequence a compensatory decrease in cytokinin levels could be expected [37]. This assumption was later supported by the results obtained with *Spcdc25* transformed BY-2 cells [24]. However, when we searched for the explanation of morphological changes together with the observed changes in carbohydrate metabolism, it appeared that the question of *Spcdc25* influence on the cytokinin levels in plants had to be reconsidered. Nevertheless, the measurement of cytokinin levels revealed a marked decrease in total cytokinins resulting from *cdc25* transformation (*figure 8A*). The transformants had significantly lower levels of *cis*-zeatin derivatives. Minor elevation of dihydrozeatin-type

cytokinins in transformant was fully compensated by elevated content of isopentenyladenine-type cytokinins in WT (*figure 8B*). Thus, the results verified the original hypothesis [37].

3.9. If there is no increase in cytokinin levels, how to explain cytokinin-like changes in carbohydrate metabolism induced by Spcdc25 expression? It seems that there must operate other mechanism responsible for *Spcdc25*-induced changes as regards carbohydrate status besides that proposed for changes in cell morphology. It is now well documented that sugar levels contribute to the decision of the cell to continue in cell cycle (e.g. via positive modulation of D cyclin(s) levels, and the negative regulation of inhibitor levels, e.g. [10, 26, 28]. We propose that the relationship between carbohydrate metabolism and cell cycle is not only unidirectional i.e. sugar level is a component of a complex system controlling cell cycle progression, but instead the relationship is bidirectional. That means that also the decision to continue in cell cycle and especially to enter mitosis generates a signal aimed to prepare the cell for subsequent highly C and energy demanding cell division and therefore, besides others, it changes carbohydrate status. Hence, we propose that higher proportion of active CDK resulting from *Spcdc25* transformation emanate the signal to metabolic pathways including carbohydrate metabolism. The question remains whether some of the enzymes/proteins/compounds, involved in regulation of carbohydrate balance, could be the direct substrate of CDK or whether the control is more indirect. To support this hypothesis the detail study of downstream CDK phosphorylation pathway would be necessary. The unique study of CDK substrates in yeast showed that there exist proteins involved in saccharide biosynthesis and transport that are regulated by CDK activity [40]. So, it is tempting to speculate whether some of the published data on the influence of cytokinins on carbohydrate metabolism do not refer to cytokinin actions mediated by some components of cell cycle regulation.

3.10. Conclusion. Although a lot of work is needed to answer all the arising questions precisely, we would like to propose some possible regulatory pathways indicated by the results achieved with *Spcdc25* transformants. The constitutive expression of *Spcdc25* probably leads to higher proportion of active mitotic CDK compared to the wild type. Consequently, signalling pathways downstream CDK are more active as well, and influence the processes directly dependent on cell division. This status might be sensed by the cell or whole plant as increased cytokinin availability, which results in compensatory decrease in cytokinin levels. In addition we propose that enhanced activity of CDK(s) at G_2/M might generate a signal modifying carbohydrate metabolism to support requirements of forthcoming cell division. Our results bring more insight to the plant cell cycle regulation and open new questions about complexity and interconnection of regulatory networks between the cell cycle and carbohydrate metabolism in plants that need further complex investigations.

4. Methods

4.1. Plant material: Cell suspension cultures derived from internode stem segments of *Nicotiana tabacum*, cv. Samsun, wild type (WT) and three independent lines transformed with *cdc25* cDNA from *Schizosaccharomyces pombe* (*Spcdc25*) under the 35S CaMV promotor (lines A, C and F) [2].

4.2. Cultivation:

4.2.1. Cultivation medium: macro- and micronutrients [11], Fe chelate according to [21], vitamins [45]**,** enriched with 30 $g.l^{-1}$ sucrose, 100 $mg.l^{-1}$ inositol, 1 $g.l^{-1}$ casein hydrolysate, 1 $mg.l^{-1}$ α-naphthylacetic acid (NAA) and 1 $mg.l^{-1}$ 2,4-dichlorphenoxyacetic acid (2,4-D)**;**

4.2.2. Cultivation conditions: orbital shaker 125 rpm, 25°C, 16h photoperiod, irradiance 25 $\mu mol.m^{-2}.s^{-1}$. Subcultivation interval: 3 weeks**.**

4.2.3. Experimental variants: basic medium without cytokinin or supplemented with 0,1, 1 and 2 $mg.l^{-1}$ 6-benzylaminopurine (BAP), cells sampled in the 12^{th} or 14^{th} day of cultivation (exponential phase).

4.3. Cytometry: Sampled cells were stained by Hoechst 33258 dye and mitotic cells were microphotographed (Olympus BX51, Digital Camera Apogee U4000) and cell size and shape measured using image analysis (Lucia G version 4.82). Cell size was determined as a cell area documented in the picture; cell shape was quantified using the parameter of circularity (4π*area /perimeter*perimeter) and elongation (max feret /min feret).

4.4. Growth parameters: dry weight was determined and relative growth rates ((dry weight of sample - dry weight of inoculum) / dry weight of inoculum) were quantified. Inoculum dry weight quantification was based on dry weight / fresh weight ratio in parallel samples.

4.5. Non-structural soluble saccharide (NSS) content determination: The samples were freeze-dried, then boiled with 80% methanol (75 °C, 15 min), the solvent evaporated, and the residue dissolved in Milli-Q ultrapure water (Millipore, Bedford, MA, USA). Then the

samples were purified by centrifugation and filtration. The content of soluble NSS was detected using high-pressure liquid chromatography (HPLC) with refractometric detection (Spectra Physics, refractometer Shodex RI-71), pre-column: Hema-Bio 1000 Q+SB; column: IEX Pb form (Watrex, Czech Republic). For details see [39].

4.6. Starch content determination: Starch granules were histochemically detected using Iodine solution, for photodocumentation see above Cytometry. For biochemical determination, the starch was enzymatically hydrolysed by α-amylase and amyloglucosidase and the glucose content was measured by the HPLC. For details see [36].

4.7. Cytokinin content determination: The procedure used for cytokinin analysis was a modification of the method described by Novák *et al*. [22]. Frozen plant material (~ 2.5 g fresh weight) was extracted overnight in Bieleski buffer. Deuterium-labelled CK internal standards (Olchemim Ltd., Czech Republic) were added, each at 5 pmol per sample to check the recovery during purification and to validate the determination. The extracts were purified using combined cation (SCX-cartridge), anion [DEAE-Sephadex-C18-cartridge] exchanger and immunoaffinity chromatography (IAC) based on wide-range specific monoclonal antibodies against cytokinins [6]. This resulted in three fractions: (1) the free bases, ribosides and N-glycosides (fraction B), (2) a nucleotide fraction (NT) and (3) an O-glucoside fraction (OG). The metabolic eluates from the IAC columns were evaporated to dryness and stored at -20^{o}C until further analyses. CK fractions were quantified by ultra performance liquid chromatography (UPLC) (Acquity UPLC^{TM}; Waters, Milford, MA, USA) coupled to a Quatro *micro* API (Waters, Milford, MA, USA) triple quadrupole mass spectrometer equipped with an electrospray interface. The purified samples were injected onto a C18 reversed-phase column (BEH C18; 1.7 μm; 2.1 x 50 mm; Waters) and eluted with a linear gradient (0 min, 10% B; 0-8 min, 50% B; flow-rate of 0.25 ml.min^{-1}) of 15mM ammonium formate (pH 4.0, A) and methanol (B). Quantitation was obtained by multiple reaction monitoring (MRM) of

$[M+H]^+$ and the appropriate product ion. In MRM mode, the limit of detection (LOD) for most of cytokinins was below 5.0 fmol and the linear range was at least five orders of magnitude.

4.8. Statistical evaluation: For statistical evaluation the NCSS 6.0. software was employed, analysis of variance (one-way ANOVA), Kruskal-Wallis multiple Comparison Z-value and Tukey-Kramer test, at the reliability level α=0,05 or 0,01.

Acknowledgements: The authors wish to thank to Ivana Macháčková, Radomíra Vaňková and Tomáš Mašek for fruitful discussions and Petra Amakorová for skilful technical assistance during cytokinin analysis. This work was supported by the Ministry of Education, Youth and Sports of the Czech Republic (MSM 0021620858 and MSM 6198959216) and by the Grant Agency of Charles University (GAUK 207/2005).

References:

[1] Balibrea L., M. E., Gonzales G.M.C., Fatima T., Ehness R., Lee T.K., Proels R., Tanner W., Roitsch T., Extracellular invertase is an essential component of cytokinin-mediated delay of senescence, Plant Cell 16 (2004) 1276-1287.

[2] Bell M.H., Halford N.G., Ormrod J.C., Francis D., Tobacco Plants Transformed with Cdc25, a Mitotic Inducer Gene from Fission Yeast, Plant Molecular Biology 23 (1993) 445-451.

[3] Boudolf V., Inze D., De Veylder L., What if higher plants lack a CDC25 phosphatase?, Trends Plant Sci 11 (2006) 474-479.

[4] Brenner W.G., Romanov G.A., Kollmer I., Burkle L., Schmulling T., Immediate-early and delayed cytokinin response genes of Arabidopsis thaliana identified by genome-wide expression profiling reveal novel cytokinin-sensitive processes and suggest cytokinin action through transcriptional cascades, Plant J 44 (2005) 314-333.

[5] De Veylder L., Joubes J., Inze D., Plant cell cycle transitions, Curr Opin Plant Biol 6 (2003) 536-543.

[6] Faiss M., Zalubilova J., Strnad M., Schmulling T., Conditional transgenic expression of the ipt gene indicates a function for cytokinins in paracrine signaling in whole tobacco plants, Plant J 12 (1997) 401-415.

[7] Franco-Zorrilla J.M., Martin A.C., Leyva A., Par-Ares J.P., Interaction between phosphate-starvation, sugar, and cytokinin signaling in arabidopsis and the roles of cytokinin receptors CRE1/AHK4 and AHK3, Plant Physiol 138 (2005) 847-857.

[8] Gibson S.I., Sugar and phytohormone response pathways: navigating a signalling network, J Exp Bot 55 (2004) 253-264.

[9] Gonzalez N., Hernould M., Delmas F., Gevaudant F., Duffe P., Causse M., Mouras A., Chevalier C., Molecular characterization of a WEE1 gene homologue in tomato (Lycopersicon esculentum Mill.), Plant Mol Biol 56 (2004) 849-861.

[10] Healy J.M., Menges M., Doonan J.H., Murray J.A., The Arabidopsis D-type cyclins CycD2 and CycD3 both interact in vivo with the PSTAIRE cyclin-dependent kinase Cdc2a but are differentially controlled, J Biol Chem 276 (2001) 7041-7047.

[11] Heller R., Researches on the mineral nutrition of plant tissues, Ann Sci Nat Bot et Biol Vég, 11th Ser. 14 (1953) 1-233.

[12] Hush J., Wu L., John P.C., Hepler L.H., Hepler P.K., Plant mitosis promoting factor disassembles the microtubule preprophase band and accelerates prophase progression in Tradescantia, Cell Biol Int 20 (1996) 275-287.

[13] Inze D., Green light for the cell cycle, Embo J 24 (2005) 657-662.

[14] Khadaroo B., Robbens S., Ferraz C., Derelle E., Eychenie S., Cooke R., Peaucellier G., Delseny M., Demaille J., Van de Peer Y., Picard A., Moreau H., The first green lineage cdc25 dual-specificity phosphatase, Cell Cycle 3 (2004) 513-518.

[15] Landrieu I., da Costa M., De Veylder L., Dewitte F., Vandepoele K., Hassan S., Wieruszeski J.M., Corellou F., Faure J.D., Van Montagu M., Inze D., Lippens G., A small CDC25 dual-specificity tyrosine-phosphatase isoform in Arabidopsis thaliana, Proc Natl Acad Sci U S A 101 (2004) 13380-13385.

[16] Laureys F., Dewitte W., Witters E., Van Montagu M., Inze D., Van Onckelen H., Zeatin is indispensable for the G2-M transition in tobacco BY-2 cells, FEBS Lett 426 (1998) 29-32.

[17] McKibbin R.S., Halford N.G., Francis D., Expression of fission yeast cdc25 alters the frequency of lateral root formation in transgenic tobacco, Plant Molecular Biology 36 (1998) 601-612.

[18] Miyazawa Y., Kato H., Muranaka T., Yoshida S., Amyloplast formation in cultured tobacco BY-2 cells requires a high cytokinin content, Plant Cell Physiol 43 (2002) 1534-1541.
[19] Miyazawa Y., Sakai A., Miyagishima S., Takano H., Kawano S., Kuroiwa T., Auxin and cytokinin have opposite effects on amyloplast development and the expression of starch synthesis genes in cultured Bright Yellow-2 tobacco cells, Plant Physiol 121 (1999) 461-469.
[20] Munoz F.J., Zorzano M.T.M., Alonso-Casajus N., Baroja-Fernandez E., Etxeberria E., Pozueta-Romero J., New enzymes, new pathways and an alternative view on starch biosynthesis in both photosynthetic and heterotrophic tissues of plants, Biocatal Biotransfor 24 (2006) 63-76.
[21] Murashige T., Skoog F., A Revised Medium for Rapid Growth and Bio Assays with Tobacco Tissue Cultures, Physiologia Plantarum 15 (1962) 473-497.
[22] Novak O., Tarkowski P., Tarkowska D., Dolezal K., Lenobel R., Strnad M., Quantitative analysis of cytokinins in plants by liquid chromatography-single-quadrupole mass spectrometry, Anal Chim Acta 480 (2003) 207-218.
[23] O'Farrell P.H., Triggering the all-or-nothing switch into mitosis, Trends Cell Biol 11 (2001) 512-519.
[24] Orchard C.B., Siciliano I., Sorrell D.A., Marchbank A., Rogers H.J., Francis D., Herbert R.J., Suchomelova P., Lipavska H., Azmi A., Van Onckelen H., Tobacco BY-2 cells expressing fission yeast cdc25 bypass a G2/M block on the cell cycle, Plant J 44 (2005) 290-299.
[25] Petrasek J., Fytohormones and Plant Cell Cycle Regulation: Characterization of Cell Division and Growth Rates in Relation to the Cytoskeleton Structure and Function in Tobacco Line WBI-0., Master Degree Thesis (in czech), Department of Plant Physiology, Charles University in Prague, Prague, 1995, pp. 1-67.
[26] Richard C., Lescot M., Inzé D., De Veylder L., Effect of auxin, cytokinin, and sucrose on cell cycle gene expression in Arabidopsis thaliana cell suspension cultures, Plant Cell, Tissue and Organ Culture 69 (2002) 167-176.
[27] Riou-Khamlichi C., Huntley R., Jacqmard A., Murray J.A., Cytokinin activation of Arabidopsis cell division through a D-type cyclin, Science 283 (1999) 1541-1544.
[28] Riou-Khamlichi C., Menges M., Healy J.M., Murray J.A., Sugar control of the plant cell cycle: differential regulation of Arabidopsis D-type cyclin gene expression, Mol Cell Biol 20 (2000) 4513-4521.
[29] Russell P., Nurse P., Cdc25+ Functions as an Inducer in the Mitotic Control of Fission Yeast, Cell 45 (1986) 145-153.
[30] Shibaoka H., Plant Hormone-Induced Changes in the Orientation of Cortical Microtubules - Alterations in the Cross-Linking between Microtubules and the Plasma-Membrane, Annu Rev Plant Phys 45 (1994) 527-544.
[31] Schuppler U., He P.H., John P.C., Munns R., Effect of water stress on cell division and cell-division-cycle 2-like cell-cycle kinase activity in wheat leaves, Plant Physiol 117 (1998) 667-678.
[32] Sipiczki M., Yamaguchi M., Grallert A., Takeo K., Zilahi E., Bozsik A., Miklos I., Role of cell shape in determination of the division plane in Schizosaccharomyces pombe: Random orientation of septa in spherical cells, J Bacteriol 182 (2000) 1693-1701.
[33] Sorrell D.A., Combettes B., Chaubet-Gigot N., Gigot C., Murray J.A., Distinct cyclin D genes show mitotic accumulation or constant levels of transcripts in tobacco bright yellow-2 cells, Plant Physiol 119 (1999) 343-352.
[34] Sorrell D.A., Chrimes D., Dickinson J.R., Rogers H.J., Francis D., The Arabidopsis CDC25 induces a short cell length when overexpressed in fission yeast: evidence for cell cycle function, New Phytol. 165 (2005) 425-428.

[35] Sorrell D.A., Marchbank A., McMahon K., Dickinson J.R., Rogers H.J., Francis D., A WEE1 homologue from Arabidopsis thaliana, Planta 215 (2002) 518-522.
[36] Steinbachova-Vojtiskova L., Tylova E., Soukup A., Novicka H., Votrubova O., Lipavska H., Cizkova H., Influence of nutrient supply on growth, carbohydrate, and nitrogen metabolic relations in Typha angustifolia, Environ Exp Bot 57 (2006) 246-257.
[37] Suchomelova P., Velgova D., Masek T., Francis D., Rogers H.J., Marchbank A.M., Lipavska H., Expression of the fission yeast cell cycle regulator cdc25 induces de novo shoot formation in tobacco: evidence of a cytokinin-like effect by this mitotic activator, Plant Physiology and Biochemistry 42 (2004) 49-55.
[38] Sun Y., Dilkes B.P., Zhang C., Dante R.A., Carneiro N.P., Lowe K.S., Jung R., Gordon-Kamm W.J., Larkins B.A., Characterization of maize (Zea mays L.) Wee1 and its activity in developing endosperm, Proc Natl Acad Sci U S A 96 (1999) 4180-4185.
[39] Svobodova H., Lipavska H., Albrechtova J., Non-structural carbohydrate status in Norway spruce buds in the context of annual bud structural development as affected by acidic pollution, Environ Exp Bot 43 (2000) 253-265.
[40] Ubersax J.A., Woodbury E.L., Quang P.N., Paraz M., Blethrow J.D., Shah K., Shokat K.M., Morgan D.O., Targets of the cyclin-dependent kinase Cdk1, Nature 425 (2003) 859-864.
[41] Vandepoele K., Raes J., De Veylder L., Rouze P., Rombauts S., Inze D., Genome-wide analysis of core cell cycle genes in Arabidopsis, Plant Cell 14 (2002) 903-916.
[42] Weingartner M., Binarova P., Drykova D., Schweighofer A., David J.P., Heberle-Bors E., Doonan J., Bogre L., Dynamic recruitment of Cdc2 to specific microtubule structures during mitosis, Plant Cell 13 (2001) 1929-1943.
[43] Weingartner M., Pelayo H.R., Binarova P., Zwerger K., Melikant B., de la Torre C., Heberle-Bors E., Bogre L., A plant cyclin B2 is degraded early in mitosis and its ectopic expression shortens G2-phase and alleviates the DNA-damage checkpoint, J Cell Sci 116 (2003) 487-498.
[44] Weingartner M., Criqui M.C., Meszaros T., Binarova P., Schmit A.C., Helfer A., Derevier A., Erhardt M., Bogre L., Genschik P., Expression of a nondegradable cyclin B1 affects plant development and leads to endomitosis by inhibiting the formation of a phragmoplast, Plant Cell 16 (2004) 643-657.
[45] White P.R., A Handbook of Plant Tissue Culture, The Jacques Cattell Press, Lancaster, Pa, 1943.
[46] Wyrzykowska J., Pien S., Shen W.H., Fleming A.J., Manipulation of leaf shape by modulation of cell division, Development 129 (2002) 957-964.
[47] Zhang K., Diederich L., John P.C., The cytokinin requirement for cell division in cultured Nicotiana plumbaginifolia cells can be satisfied by yeast Cdc25 protein tyrosine phosphatase: implications for mechanisms of cytokinin response and plant development, Plant Physiol 137 (2005) 308-316.

Legends to figures:

Figure 1:
Relative growth rates of tobacco cell suspension cultures on media with or without cytokinin addition.
The evaluation of relative growth rates (dry weight mass at sampling time (t) related to calculated inoculum dry weight (0); [dry $mass_t$ / (dry $mass_t$ - dry $mass_0$)]) of control and transgenic lines A, C and F and was performed 14 days (the end of exponential growth phase) after the transfer to the fresh medium (modified liquid Heller medium (1 $mg.l^{-1}$ 2,4-D and 1 $mg.l^{-1}$ NAA) without cytokinin (A) or supplied with 0,1; 1 or 2 $mg.l^{-1}$ BAP (B)). Significant differences between variants are indicated by different letters ($n = 6\text{-}20$; $P < 0,05$).

Figure 2:
Cell area in tobacco cell suspension cultures on media without cytokinin.
Tobacco cells of control and transgenic lines A, C and F cultivated in modified liquid Heller media (1 $mg.l^{-1}$ 2,4-D and 1 $mg.l^{-1}$ NAA). The maximum size of mitotic cells was quantified as cell area using image analysis Lucia G. Significant differences between variants are indicated by different letters ($n = 90\text{-}110$; $P < 0,05$).

Figure 3:
Cell shape in tobacco cell suspension cultures on media without cytokinin.
Tobacco cells of control and transgenic lines A, C and F were cultivated in modified liquid Heller media (1 $mg.l^{-1}$ 2,4-D and 1 $mg.l^{-1}$ NAA). The shape of mitotic cells was quantified as parameter of circularity (A) and elongation (B) using image analysis Lucia G. Significant differences between variants are indicated by different letters ($n = 90\text{-}110$; $P < 0,05$).

Figure 4:
Cell arrangement in tobacco cell suspension cultures.
Tobacco cells of control and transgenic lines A and C were cultivated in modified liquid Heller media (1 $mg.l^{-1}$ 2,4-D and 1 $mg.l^{-1}$ NAA) without cytokinin (A, B and D) or control supplied with 1 $mg.l^{-1}$ BAP (C). The arrangements of cells are documented as microphotographs under UV light in combination with Nomarski differential contrast, bar = 100 μm. In the slit, an alternative cell arrangement of transgenic line A occasionally forming chains of doublets, bar = 100 μm.

Figure 5:
Histochemical detection of starch in tobacco cell suspension cultures.
Tobacco cells of control and transgenic lines A and C were cultivated in modified liquid Heller media (1 $mg.l^{-1}$ 2,4-D and 1 $mg.l^{-1}$ NAA) without cytokinin (A, B and D) or control supplied with 1 $mg.l^{-1}$ BAP (C). The starch was visualised by Lugol solution in native preparates. bar = 100 μm.

Figure 6:
Starch content in tobacco cell suspension cultures.
Tobacco cells of control and transgenic lines A and C were cultivated in modified liquid Heller media (1 $mg.l^{-1}$ 2,4-D and 1 $mg.l^{-1}$ NAA) without cytokinin or supplied with 1 $mg.l^{-1}$ BAP. The analysis was performed 14 days after the transfer to the fresh medium. The amount of starch was quantified as glucose content obtained after enzymatic splitting of starch with α-amylase and amyloglucosidase. Significant differences between variants are indicated by different letters ($n = 6$; $P < 0,05$).

Figure 7:

Non-structural soluble carbohydrate levels in tobacco cell suspension cultures.

Tobacco cells of control and transgenic lines A and C were cultivated in modified liquid Heller media (1 $mg.l^{-1}$ 2,4-D and 1 $mg.l^{-1}$ NAA) without cytokinin (A) or supplied with 1 or 2 $mg.l^{-1}$ BAP (B). The analysis was performed 14 days after the transfer to the fresh medium. Significant differences between variants are indicated by different letters ($n = 9\text{-}10$; $P < 0,05$).

Figure 8:

Cytokinin levels in tobacco cell suspension cultures on media without cytokinin.

The analysis of endogenous cytokinin levels of control and transgenic line C was performed 12 days after the transfer to the fresh media (modified liquid Heller media with 1 $mg.l^{-1}$ 2,4-D and 1 $mg.l^{-1}$ NAA). (A) Total amount of endogenous cytokinins and (B) average amount of individual cytokinins. Significant differences between variants are indicated by different letters ($n = 5$; $P < 0,01$).

Figures 1,2,3,6 and 7

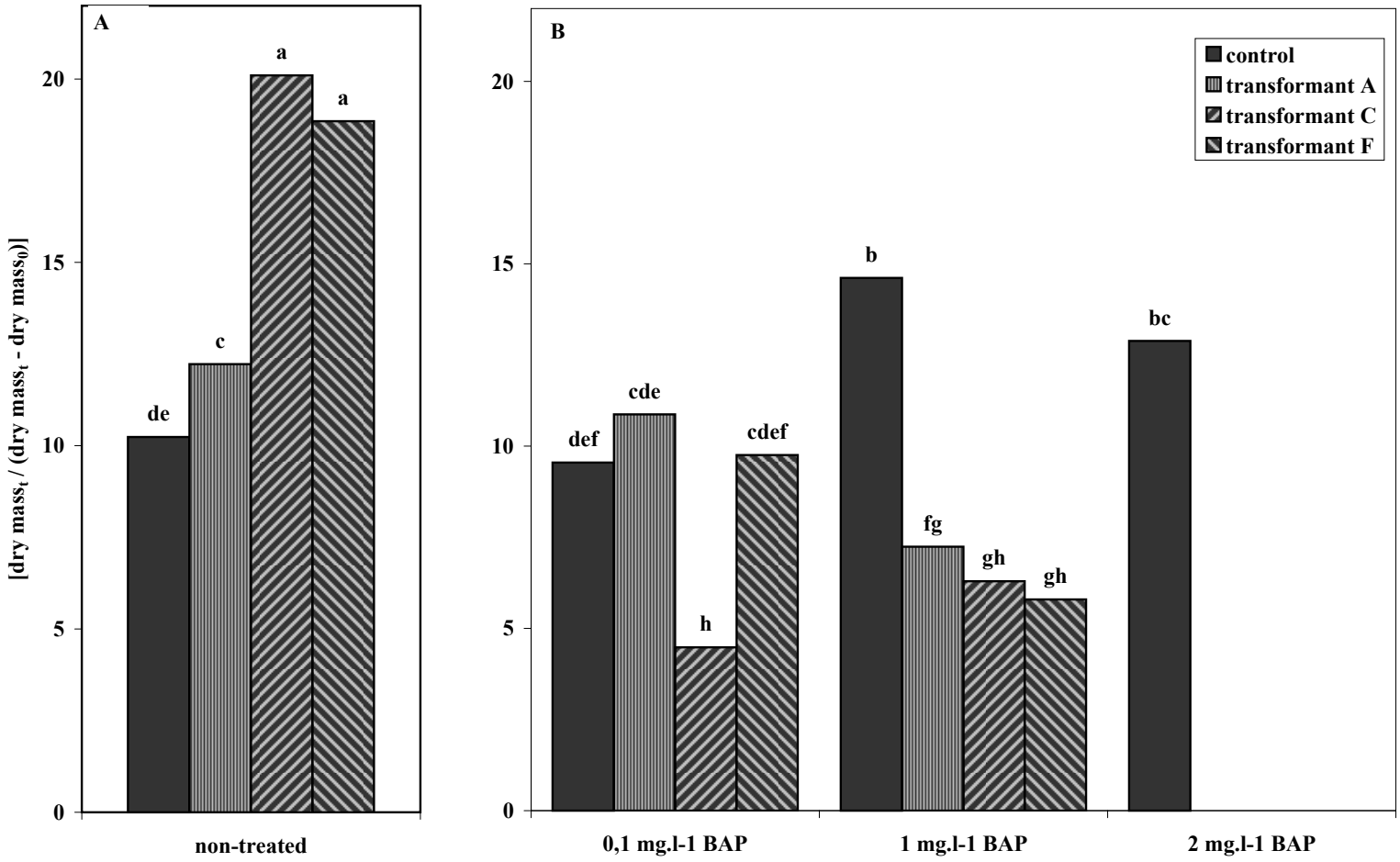

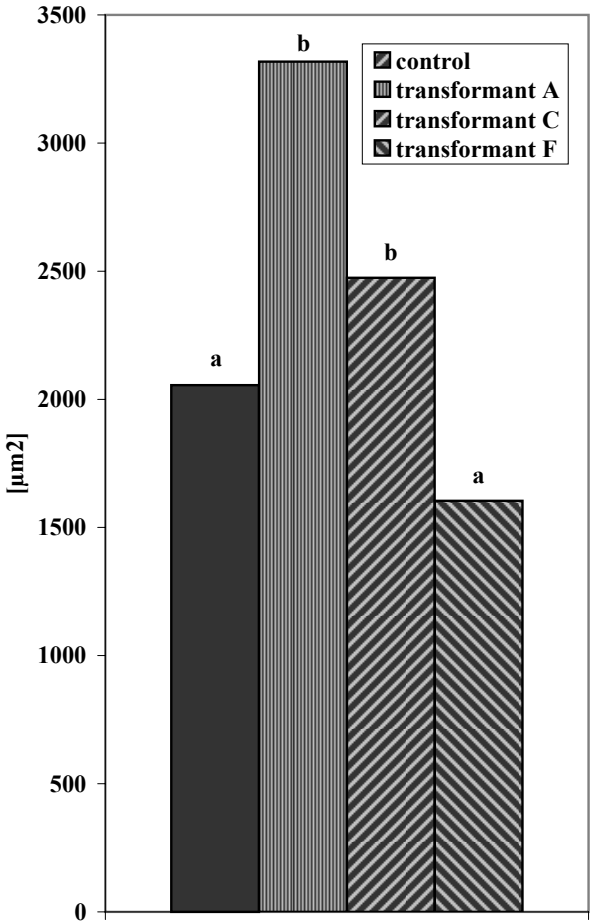
3500
3000
2500
2000
1500
1000
500
0
[µm2]
a
b
b
a
control
transformant A
transformant C
transformant F

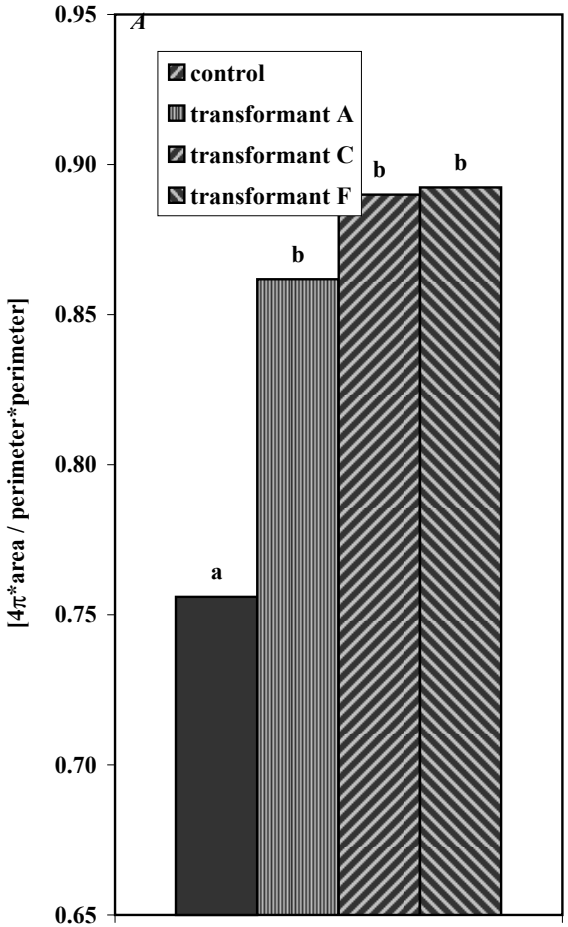
A
control
transformant A
transformant C
transformant F
[4π*area / perimeter*perimeter]
0.95
0.90
0.85
0.80
0.75
0.70
0.65
a
b
b
b

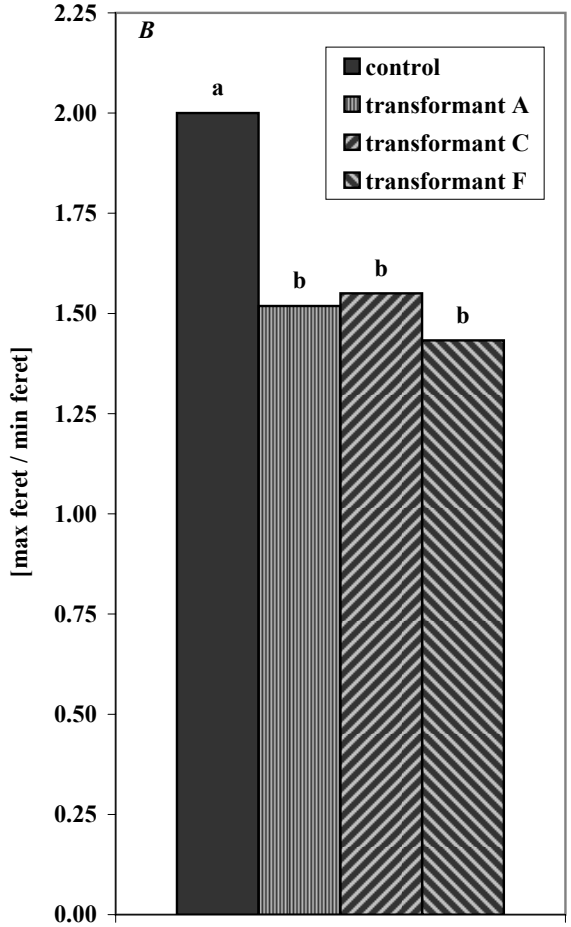
B
control
transformant A
transformant C
transformant F
[max feret / min feret]
2.25
2.00
1.75
1.50
1.25
1.00
0.75
0.50
0.25
0.00
a
b
b
b

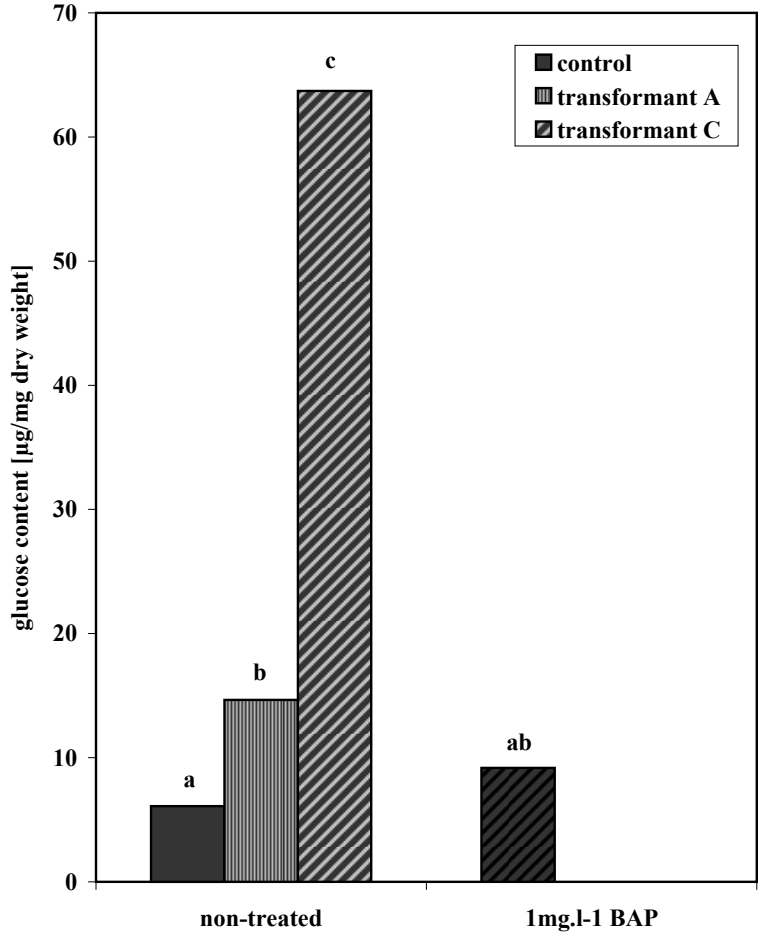
70
60
50
40
30
20
10
0
glucose content [µg/mg dry weight]
control
transformant A
transformant C
a
b
c
ab
non-treated
1mg.l-1 BAP

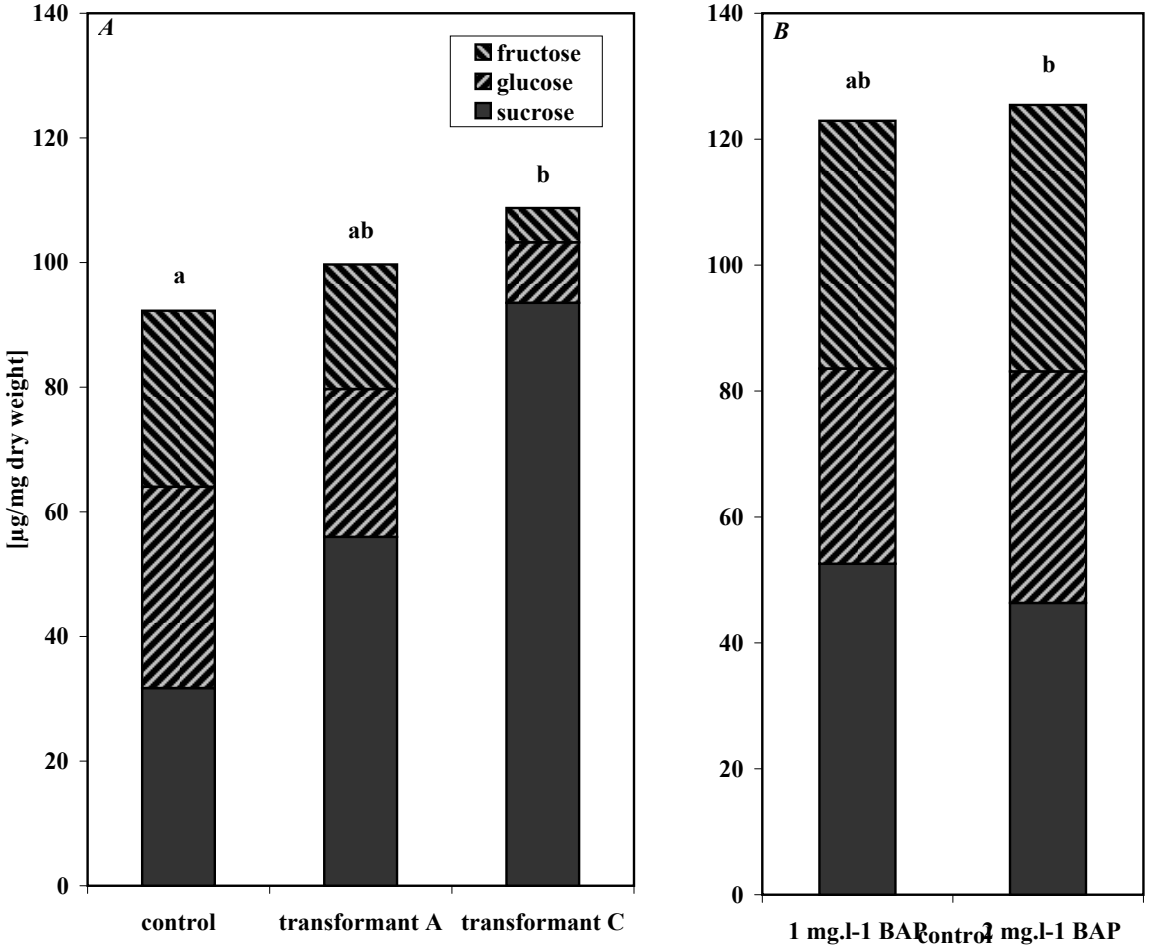
A
fructose
glucose
sucrose
[µg/mg dry weight]
140
120
100
80
60
40
20
0
a
ab
b
control
transformant A
transformant C
B
ab
b
control
1 mg.l-1 BAP
2 mg.l-1 BAP

Figure 4

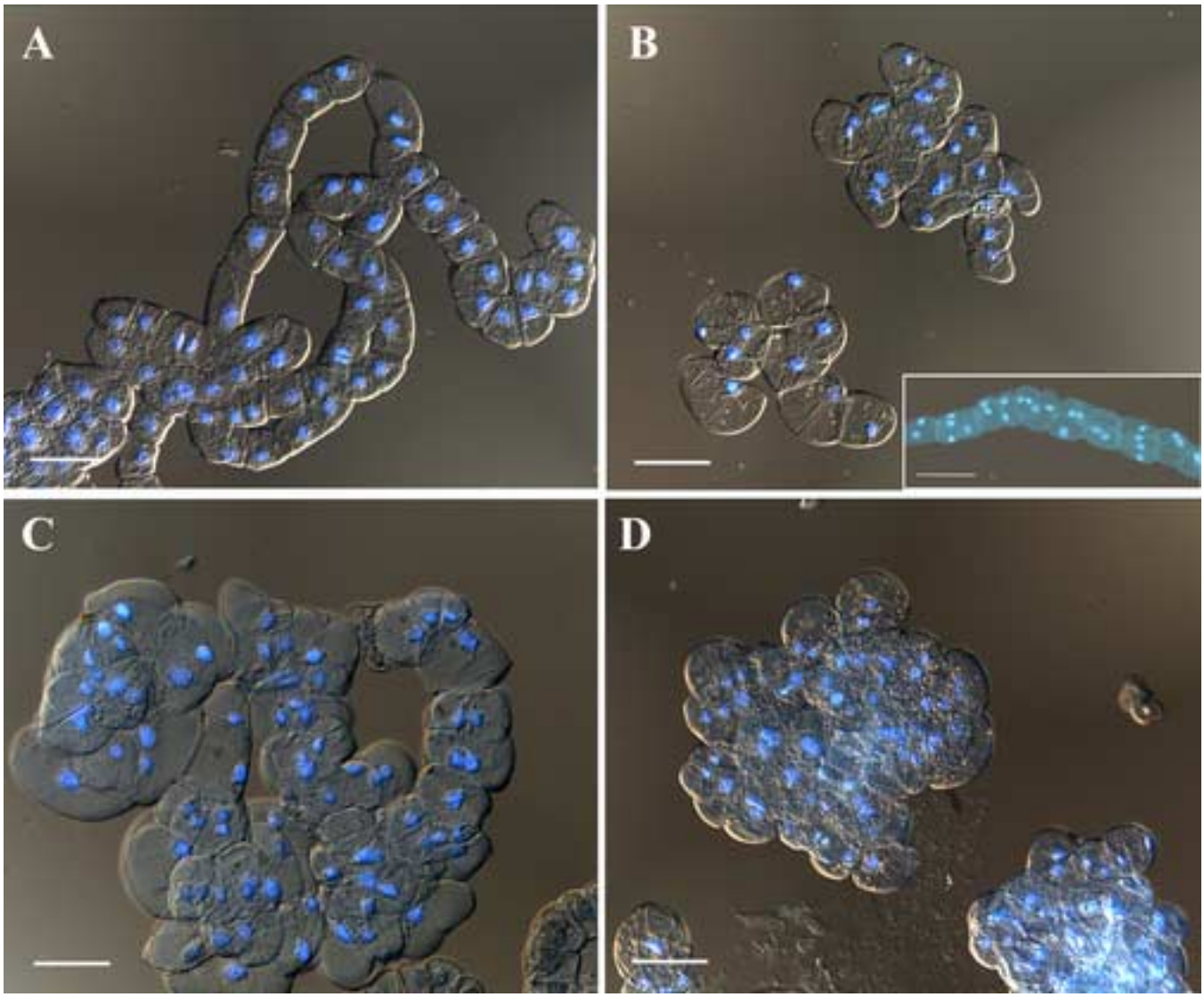

Figure 5

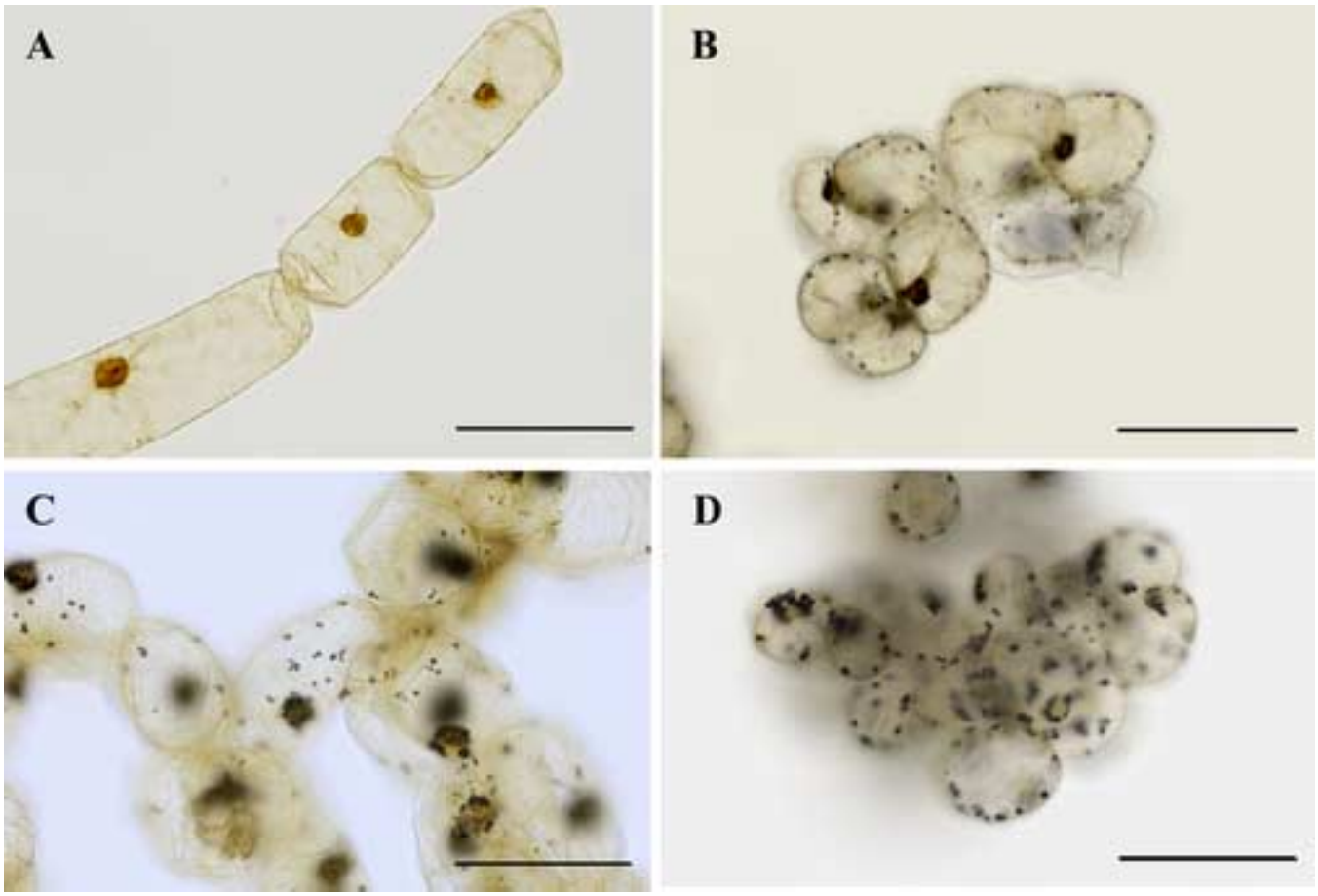

Figure 8

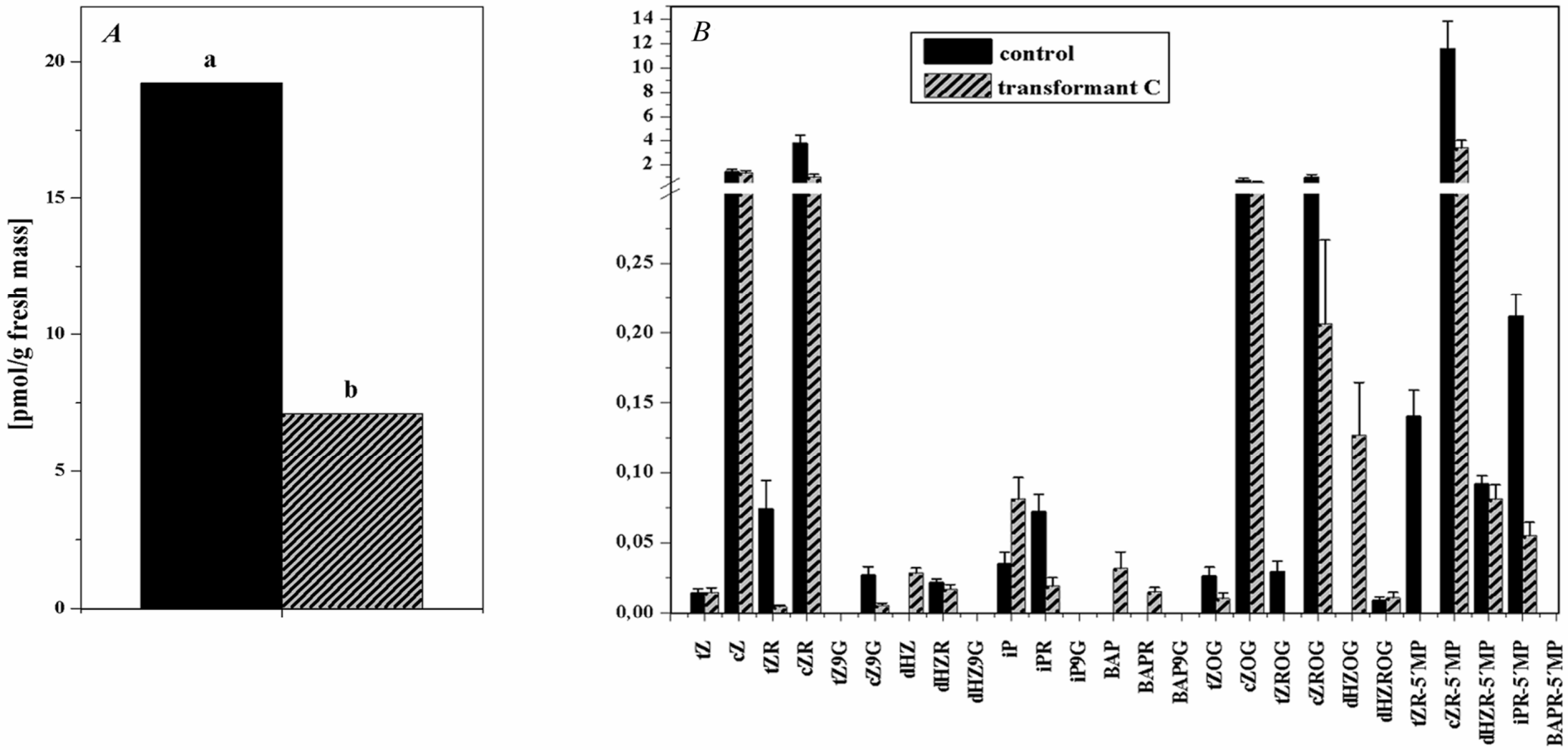
A
a
b
[pmol/g fresh mass]
0
5
10
15
20
B
control
transformant C
0,00
0,05
0,10
0,15
0,20
0,25
2
4
6
8
10
12
14
tZ
cZ
tZR
cZR
tZ9G
cZ9G
dHZ
dHZR
dHZ9G
iP
iPR
iP9G
BAP
BAPR
BAP9G
tZOG
cZOG
tZROG
cZROG
dHZOG
dHZROG
tZR-5'MP
cZR-5'MP
dHZR-5'MP
iPR-5'MP
BAPR-5'MP